

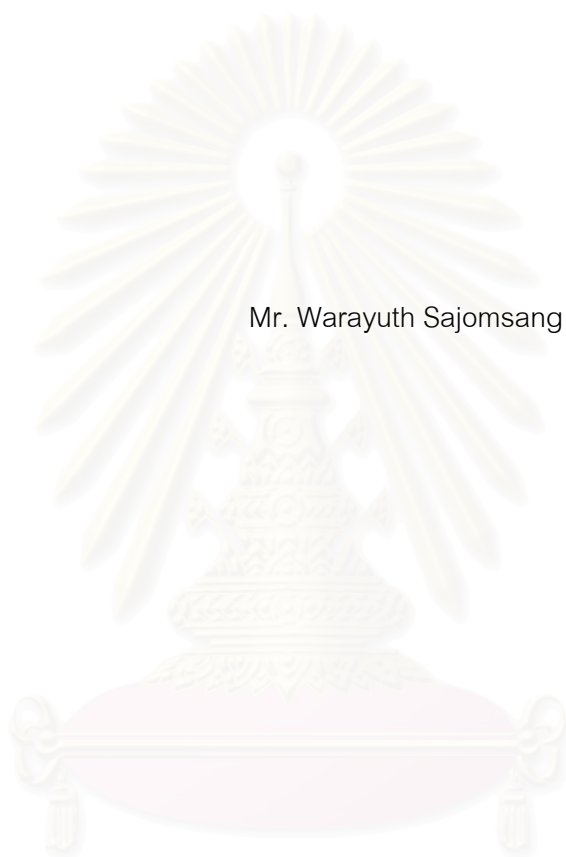
การสังเคราะห์และฤทธิ์ยับยั้งเชื้อแบคทีเรียของควอเทอร์นารีแอมโมเนียมไคโตซานที่มีส่วนของแอโรแมติก



นายวรายุทธ สะใจมแสง

สถาบันวิทยบริการ
วิทยานิพนธ์นี้เป็นส่วนหนึ่งของการศึกษาตามหลักสูตรปริญญาวิทยาศาสตรดุษฎีบัณฑิต
จุฬาลงกรณ์มหาวิทยาลัย
สาขาวิชาเคมี ภาควิชาเคมี
คณะวิทยาศาสตร์ จุฬาลงกรณ์มหาวิทยาลัย
ปีการศึกษา 2549
ลิขสิทธิ์ของจุฬาลงกรณ์มหาวิทยาลัย

SYNTHESIS AND ANTIBACTERIAL ACTIVITIES OF QUATERNARY AMMONIUM CHITOSAN
CONTAINING AROMATIC MOIETIES



Mr. Warayuth Sajomsang

A Dissertation Submitted in Partial Fulfillment of the Requirements
for the Degree of Doctor of Philosophy Program in Chemistry

Department of Chemistry

Faculty of Science

Chulalongkorn University

Academic year 2006

Copyright of Chulalongkorn University

วรายุทธ สะใจมแสง : การสังเคราะห์และฤทธิ์ยับยั้งเชื้อแบคทีเรียของควอเทอร์นารีแอมโมเนียมไคโตซานที่มีส่วนของแอสโรแมติก (SYNTHESIS AND ANTIBACTERIAL ACTIVITIES OF QUATERNARY AMMONIUM CHITOSAN CONTAINING AROMATIC MOIETIES) อ. ที่ปรึกษา : รศ.ดร.ศุภวรรณ ตันตยานนท์, อ. ที่ปรึกษาร่วม : Professor William H. Daly และ ผศ.ดร.วราวุฒิ ตั้งพลสุธาตล; 130 หน้า.

ได้สังเคราะห์เอ็น-ออกทิลและเอ็น-เบนซิลไคโตซานที่มีหมู่เกลือควอเทอร์นารีแอมโมเนียมจำนวน 52 ชนิดสำเร็จ โดยทำเอ็น-แอลคิลเลชันหรือเอ็น-เบนซิลเลชันของไคโตซาน แล้วจึงทำควอเทอร์ไนเซชัน ระดับการแทนที่ที่เอ็น (อีเอส) ขึ้นอยู่กับอัตราส่วนโมลของแอลดีไฮด์กับหมู่เอมิโนของไคโตซาน เวลาที่ใช้ในการเกิดปฏิกิริยา และหมู่แทนที่ที่อยู่บนวงแหวนเบนซีน ได้ทำควอเทอร์ไนเซชันโดยใช้ไอโอดิเมเทน หรือ 3-คลอโร-2-ไฮดรอกซีโพรพิลไตรเมทิลแอมโมเนียมคลอไรด์ (ควอต-188) ได้ดีกรีของควอเทอร์ไนเซชันของไคโตซานต่ำจากการทำปฏิกิริยากับไอโอดิเมเทนหนึ่งครั้ง การทำเมทิลเลชันซ้ำด้วยไอโอดิเมเทนจะเพิ่มดีกรีของควอเทอร์ไนเซชันแต่ทำให้ดีกรีของโอเมทิลเลชันที่หมู่ไฮดรอกซีตำแหน่งที่ 3 และตำแหน่งที่ 6 ของไคโตซานเพิ่มขึ้นด้วย สำหรับการทำควอเทอร์ไนเซชันด้วยควอต-188 พบว่าไม่เกิดโอเมทิลเลชัน เมื่อระดับการแทนที่ที่เอ็นเพิ่มขึ้นดีกรีของควอเทอร์ไนเซชันจะลดลง เนื่องจากหมู่เอมิโนอิสระของไคโตซานมีจำนวนน้อยลงที่จะทำปฏิกิริยากับควอต-188 นอกจากนี้แล้วดีกรีของควอเทอร์ไนเซชันของเอ็น-เบนซิลไคโตซานที่ใช้ควอต-188 จะมีค่าสูงกว่าการใช้ไอโอดิเมเทนเสมอที่ระดับการแทนที่ที่เอ็นเท่ากัน เกลือควอเทอร์นารีของไคโตซานโดยใช้ควอต-188ทั้งหมด สามารถละลายน้ำได้ดีมากที่พีเอชเป็นกลาง การศึกษาความเข้มข้นต่ำสุดที่สามารถยับยั้งเชื้อแบคทีเรีย (เอ็มไอซี) ของเกลือควอเทอร์นารีเหล่านี้ได้ทำโดยใช้ไอโคไล (แกรม-เน็กกาทีฟ) และเอสแอสเรียส (แกรม-โพซิทีฟ) แบคทีเรียอนุพันธ์ควอเทอร์ไนซ์ไคโตซานทั้งหมดแสดงค่าเอ็มไอซีในช่วง 8-128 ไมโครกรัมต่อมิลลิลิตร ในการยับยั้งเชื้อแบคทีเรียทั้งสองชนิด ได้ทำควอเทอร์ไนเซชันของไคโตซานโดยใช้ไอโอดิเมเทน หรือ ควอต-188 ด้วยเพื่อใช้ในการเปรียบเทียบ

ภาควิชา... เคมี..... ลายมือชื่อนิสิต..... *Darys S. M.*
 สาขาวิชา... เคมี..... ลายมือชื่ออาจารย์ที่ปรึกษา..... *Prof. Dr. S. S.*
 ปีการศึกษา... 2549..... ลายมือชื่ออาจารย์ที่ปรึกษาร่วม..... *W. H. Daly*

4573834723 : MAJOR CHEMISTRY

KEY WORD: CHITOSAN / N-BENZYLATION / ANTIBACTERIAL ACTIVITY / QUATERNARY AMMONIUM SALT / SCHIFF BASE

WARAYUTH SAJOMSANG: SYNTHESIS AND ANTIBACTERIAL ACTIVITIES OF QUATERNARY AMMONIUM CHITOSAN CONTAINING AROMATIC MOIETIES. DISSERTATION ADVISOR : ASSOC. PROF. SUPAWAN TANTAYANON, Ph. D. DISSERTATION CO-ADVISOR : PROF. WILLIAM H. DALY, Ph. D. ASSIST.PROF.VARAWUT TANGPASUTHADOL, Ph. D. 130 pp.

The 52 *N*-octyl and *N*-benzyl chitosans bearing quaternary ammonium salts were successfully synthesized by either *N*-alkylation or *N*-benzylation of chitosan and then quaternization. The extent of *N*-substitution (ES) was influenced by the molar ratio of the aldehyde to amino group of chitosan, the reaction time and the substituent on the benzene ring. Quaternization was carried out by using either iodomethane or 3-chloro-2-hydroxypropyl trimethylammonium chloride (Quat-188). The low degree of quaternization (DQ_{Ch}) of chitosan was obtained with single treatment using iodomethane. The repeated methylation with iodomethane would increase not only DQ_{Ch} but also degree of *O*-methylation at 3-hydroxy and 6-hydroxy groups of chitosan. For quaternization using Quat-188, *O*-alkylation was not observed. When ES increased, DQ_{Ch} decreased obviously due to less free amino group of chitosan reacting with Quat-188. Moreover, the DQ_{Ch} of *N*-benzyl chitosans using Quat-188 was always higher than using iodomethane at the same level of ES. All quaternary ammonium salts of chitosan using Quat-188 were highly water soluble at neutral pH. Minimum inhibitory concentration (MIC) antibacterial studies of these materials were carried out on *E. coli* (Gram-negative) and *S. aureus* (Gram-positive) bacteria. All quaternized chitosan derivatives showed very low MIC values which was in the range of 8-128 $\mu\text{g/mL}$ against both bacteria. The quaternization of chitosan using either iodomethane or Quat-188 was also performed for comparison.

Department.....Chemistry.....Student's..... Warayuth Sajomsang
 Field of study.....Chemistry.....Advisor's..... Supawan Tantayanon
 Academic year.....2006.....Co-advisor's..... William H. Daly
 Varawut Tangpasuthadol

ACKNOWLEDGEMENTS

First of all, I would like to express my sincere appreciation to my advisor Associate Professor Supawan Tantayanon, who always inspired me through her guidance and encouragement during the entire course of this work. Her advice, patience and support are greatly acknowledged and I would like to thank my co-advisor, Assistant Professor Varawut Tangpasuthadol, for his advice, patience and support are greatly acknowledged.

I would like to thank Professor William H. Daly, Macromolecular Studies Group, Department of Chemistry, Louisiana State University, Baton Rouge, USA, for having great interest in this work. His wealth of information and input has been invaluable to this project and has helped shaping my perception of the current topic and beyond. I would also like to thank two members in Daly's research group, Lokia Champang and Changde Zhang. Working with them has been a very pleasant experience, particularly for their support and friendship. Discussions during the Daly's group meetings were extremely intriguing and provided a unique learning experience in topics related to the present work and beyond. Professor Ioan Negulescu, Dr. Dale Treleave, Dr. Rafael Cueto, Professor Paul Ruso, from Department of Chemistry, Louisiana State University, Baton Rouge, USA, were acknowledged for their advice and assistance about physical properties of chitosan and its derivatives by using TGA, DSC, ^{13}C -, ^1H -NMR and GPC.

I would also like to take this opportunity to thank the Thailand Research Fund for the financial supports under the Golden Jubilee PHD/0185/2545.

I would also like to thank my research group, the fellow graduate students and the administrative staffs of the department for their friendly assistance. And last but not least important, I am grateful to my parents, grandparents and brother for being a tremendous support and motivator during the course of Ph.D program. Their encouragement and patience is greatly acknowledged.

CONTENTS

	Page
ABSTRACT IN THAI.....	iv
ABSTRACT IN ENGLISH.....	v
ACKNOWLEDGEMENTS.....	vi
CONTENTS.....	vii
LIST OF TABLES.....	xi
LIST OF FIGURES.....	xii
LIST OF SCHEMES.....	xv
LIST OF ABBREVIATION AND SIGNS.....	xvi
CHAPTER I INTRODUCTION	
1.1 Introduction.....	1
1.2 Objective.....	3
1.3 Scope of research.....	3
CHAPTER II THEORETICAL AND LITERATURE REVIEWS	
2.1 Bacteria.....	4
2.1.1 Morphology and ultrastructure.....	4
2.1.2 Gram staining.....	4
2.1.3 Cell walls of bacteria	5
2.1.3.1 Gram-positive bacteria.....	6
2.1.3.2 Gram-negative bacteria.....	7
2.2 Chitin and chitosan.....	8
2.3 Mode of action of chitosan	10
2.4 Antibacterial property of chitosan and its derivatives	11
2.5 <i>N</i> -Alkylation and <i>N</i> -benzylation of chitosan.....	13
2.6 Quaternization of chitosan using iodomethane as quaternizing agent.....	16
2.7 Quaternization of <i>N</i> -alkyl or <i>N</i> -benzyl chitosans using iodomethane as quaternizing agent.....	18
2.8 Quaternization of chitosan using quaternary ammonium epoxide as quaternizing agent.....	20

CHAPTER III EXPERIMENTAL

3.1 General materials and instruments.....	25
3.1.1 Materials.....	25
3.1.3 Instruments.....	25
PART A SYNTHESIS OF <i>N</i> -SUBSTITUTED CHITOSAN	
DERIVATIVES.....	26
3.2 Synthesis of <i>N</i> - <i>n</i> -octyl chitosan.....	26
3.2 Synthesis of <i>N</i> -benzyl chitosans	27
PART B QUATERNIZATION OF CHITOSAN AND <i>N</i> -SUBSTITUTED CHITOSANS.....	
3.3 Quaternization of chitosan and <i>N</i> -substituted chitosans using iodomethane.....	33
3.3.1 Regenerated chitosan and <i>N</i> -substituted chitosans.....	33
3.3.2 Isolation and purification.....	33
3.3.3 <i>N,N,N</i> -Trimethylammonium chitosan chloride	33
3.3.4 High degree of quaternization of <i>N,N,N</i> -trimethylammonium chitosan chloride	35
3.3.5 Quaternized <i>N</i> -(4-methylbenzyl)chitosan, quaternized <i>N</i> -(4- <i>N,N</i> -dimethylaminobenzyl)chitosan and quaternized <i>N</i> -(4-pyridylmethyl)chitosan.....	35
3.4 Quaternization of <i>N</i> -substituted chitosans using 3-chloro-2-hydroxypropyl trimethylammonium chloride.....	37
3.4.1 Chitosan Quat-188.....	37
3.4.2 <i>N</i> -substituted chitosans Quat-188.....	38
3.4.3 Characterization of chitosan and its derivatives.....	43
3.4.3.1 FT-IR spectroscopy.....	43
3.4.3.2 ¹ H-NMR spectroscopy.....	43
3.4.3.3 Determination of molecular weight.....	44
3.4.3.4 Determination of degree of quaternization.....	44

	Page
PART C ANTIBACTERIAL ACTIVITY OF QUATERNIZED	
CHITOSAN AND <i>N</i>-SUBSTITUTED CHITOSANS..... 45	
3.5 Antibacterial assessment	45
3.5.1 Phosphate buffer saline	45
3.5.2 Cell solution preparation.....	45
3.5.3 96-well plate preparation.....	46
 CHAPTER IV RESULTS AND DISCUSSION	
PART A SYNTHESIS OF <i>N</i>-SUBSTITUTED	
CHITOSAN DERIVATIVES..... 48	
4.1 Synthesis of <i>N</i> - <i>n</i> -octyl chitosan	48
4.2 Synthesis of <i>N</i> -benzyl chitosans	49
4.3 Interpretation of <i>N</i> -benzyl chitosans spectra	50
4.4 Impact of <i>N</i> -benzyl substituents on the extent of chitosan substitution ...	56
4.5 Thermal properties of <i>N</i> -benzyl chitosans	63
4.6 Solubility of <i>N</i> -benzyl chitosans	67
PART B QUATERNIZATION OF CHITOSAN AND <i>N</i>-SUBSTITUTED	
CHITOSAN DERIVATIVES..... 69	
4.7 Quaternization of chitosan and <i>N</i> -substituted chitosans using iodomethane.....	69
4.7.1 <i>N,N,N</i> -trimethylammonium chitosan chloride and its high degree of quaternization.....	69
4.7.2 Quaternized <i>N</i> -(4-methylbenzyl)chitosan.....	73
4.7.3 Quaternized <i>N</i> -(4- <i>N,N</i> -dimethylaminobenzyl) chitosan and quaternized <i>N</i> -(4-pyridylmethyl)chitosan.....	74
4.7.4 Chemoselective methylation of <i>N</i> -(4- <i>N,N</i> -dimethylaminobenzyl)chitosan and <i>N</i> -(4-pyridylmethyl)chitosan.....	78
4.8 Quaternization of chitosan and <i>N</i> -substituted chitosans using 3-chloro-2-hydroxypropyl trimethylammonium chloride	81
4.9 Reduction in molecular weight of chitosan during derivatization.....	90

	Page
PART C ANTIBACTERIAL ACTIVITY OF QUATERNIZED CHITOSAN AND N-SUBSTITUTED CHITOSANS.....	94
4.10 Antibacterial activity of quaternized chitosan and <i>N</i> -substituted chitosans using iodomethane.....	95
4.11 Antibacterial activity of quaternized chitosan and <i>N</i> -substituted chitosans using Quat-188.....	96
 CHAPTER V CONCLUSIONS AND FURTHER DIRECTION	
5.1 Conclusion.....	100
5.2 Further direction.....	102
 REFERENCES.....	105
APPENDICES	
APPENDIX A FT-IR SPECTRA	112
APPENDIX B NMR SPECTRA.....	119
APPENDIX C GPC CHROMATOGRAMS.....	124
VITAE.....	129

LIST OF TABLES

	Page
Table 2.1: MIC of native chitosan against fungi.....	12
Table 2.2: MIC of native chitosan against bacteria.....	13
Table 4.1: <i>N</i> -Alkylation and <i>N</i> -benzylation of chitosan.....	59
Table 4.2: DSC and TGA datas of chitosan and selected chitosan derivatives.....	65
Table 4.3: Solubility of chitosan and selected chitosan derivatives in various solvents.....	69
Table 4.4: Quaternization of chitosan and <i>N</i> -benzyl chitosans using iodomethane.....	78
Table 4.5: Quaternization of chitosan and <i>N</i> -benzyl chitosans using Quat-188.....	91
Table 4.6: Determination of the increment of refractive index, the molecular weight and the radius of gyration from chitosan and its derivatives	92
Table 4.7: Antibacterial activity of quaternized of chitosan and <i>N</i> -benzyl chitosans using iodomethane.....	95
Table 4.8: Antibacterial activity of quaternized of chitosan and <i>N</i> -benzyl chitosans using Quat-188.....	98

LIST OF FIGURES

	Page
Figure 2.1: Determination of type of bacteria based on Gram staining reaction.....	4
Figure 2.2: The cross sections of Gram-positive and Gram-negative bacteria cell walls.....	5
Figure 2.3: Cell wall structures of Gram-positive (i.e., <i>Staphylococcus aureus</i>) and Gram-negative (i.e., <i>Escherichia coli</i>).....	5
Figure 2.4: The arrangement of the cell envelope of Gram-positive bacteria.....	6
Figure 2.5: The arrangement of the cell envelope of Gram-negative bacteria.....	7
Figure 2.6: Chemical structures of chitin and chitosan.....	9
Figure 3.1: Schematics of a 96-well plate used in antibacterial assessment.....	46
Figure 4.1: FT-IR (KBr) spectra of chitosan and selected chitosan derivatives with various ES's.....	50
Figure 4.2: ¹ H-NMR spectra of chitosan and selected chitosan derivatives with various ES's in D ₂ O/CF ₃ COOD.....	51
Figure 4.3: ¹ H-NMR spectrum of <i>N</i> -(4- <i>N,N</i> -dimethylaminobenzyl)chitosan with ES 17.5% in D ₂ O/CF ₃ COOD.....	52
Figure 4.4: ¹ H-NMR spectra of <i>N</i> -(4-pyridylmethyl)chitosan with different ES's in D ₂ O/CF ₃ COOD.....	53
Figure 4.5: ¹ H-NMR spectrum of <i>N</i> -(4-thiophenylmethyl)chitosan with ES 13.3% in D ₂ O/CF ₃ COOD.....	54
Figure 4.6: ¹³ C-NMR spectrum of <i>N</i> -benzyl chitosan with ES 18.5% in D ₂ O/CF ₃ COOD.....	55
Figure 4.7: ¹³ C-NMR spectrum of <i>N</i> -(4-nitrobenzyl)chitosan with ES 24.7% in D ₂ O/CF ₃ COOD.....	55
Figure 4.8: ¹ H-NMR spectra of <i>N</i> -(4-methylbenzyl)chitosans with various ES's in D ₂ O/CF ₃ COOD.....	57
Figure 4.9: Substitution control in the synthesis of selected chitosan derivatives bearing either an electron donating or electron withdrawing substituents.....	62
Figure 4.10: DSC thermograms of chitosan and selected <i>N</i> -benzyl chitosans.....	63
Figure 4.11: TGA thermograms of chitosan and selected chitosan derivatives.....	66

Figure 4.12: FT-IR (KBr) spectra of <i>N,N,N</i> -trimethylammonium chitosan and its analog having high degree of quaternization.....	70
Figure 4.13: ¹ H-NMR spectra of chitosan (D ₂ O/CF ₃ COOD) and quaternized chitosan (D ₂ O) respectively, using iodomethane as a quaternizing agent.....	71
Figure 4.14: ¹ H-NMR spectrum of quaternized <i>N</i> -(4-methylbenzyl)chitosan with ES 11.0% in CF ₃ COOD/D ₂ O using 15% (w/v) NaOH.....	73
Figure 4.15: FT-IR (KBr) spectra of quaternized <i>N</i> -(4- <i>N,N</i> -dimethylaminobenzyl)chitosan and quaternized <i>N</i> -(4-pyridylmethyl)chitosan.....	75
Figure 4.16: ¹ H-NMR spectrum of quaternized <i>N</i> -(4- <i>N,N</i> -dimethylaminobenzyl)chitosan with ES 2.7% in D ₂ O using 15% (w/v) NaOH.....	76
Figure 4.17: ¹ H-NMR spectrum of quaternized <i>N</i> -(4-pyridylmethyl)chitosan with ES 12.5% in D ₂ O using 15% (w/v) NaOH.....	76
Figure 4.18: ¹³ C-NMR spectrum of quaternized <i>N</i> -(4- <i>N,N</i> -dimethylaminobenzyl)chitosan with ES 17.5% in D ₂ O using 5% (w/v) NaOH.....	77
Figure 4.19: ¹ H-NMR spectra of <i>N</i> -(4- <i>N,N</i> -dimethylaminobenzyl) chitosan (D ₂ O/CF ₃ COOD) and quaternized <i>N</i> -(4- <i>N,N</i> -dimethylaminobenzyl)chitosan (D ₂ O) with ES 17.5% using 15% (w/v) NaOH.....	79
Figure 4.20: ¹ H-NMR spectra of quaternized <i>N</i> -(4- <i>N,N</i> -dimethylaminobenzyl)chitosan (D ₂ O) with ES 17.5% using 5% and 15% (w/v) of NaOH	80
Figure 4.21: FT-IR (KBr) spectrum of chitosan Quat-188.....	83
Figure 4.22: ¹ H-NMR spectrum of chitosan Quat-188 in D ₂ O.....	83
Figure 4.23: ¹³ C-NMR spectrum of chitosan Quat-188 in D ₂ O.....	84
Figure 4.24: ¹ H-NMR spectrum of <i>N</i> -n-octyl chitosan Quat-188 with ES 4.7% in D ₂ O.....	85
Figure 4.25: ¹ H-NMR spectra of selected <i>N</i> -benzyl chitosans Quat-188 in D ₂ O.....	86

Figure 4.26: ^{13}C -NMR spectrum of <i>N</i> -benzyl chitosan Quat-188 with ES 11.4% in D_2O	87
Figure 4.27: ^1H -NMR spectrum of <i>N</i> -(2-thiophenylmethyl)chitosan Quat-188 with ES 9.6% in D_2O	87
Figure 4.28: Examples of differential distribution of molar mass obtained by GPC on a quaternized <i>N</i> -(4- <i>N,N</i> -dimethylaminobenzyl)chitosan with ES 17.5% using iodomethane when 5% (w/v) was used.....	91
Figure 4.29: Radius of gyration (RMS) expressed in nm plotted as a function of the molar mass (g/mol) on a quaternized <i>N</i> -(4- <i>N,N</i> -dimethylaminobenzyl)chitosan with ES 17.5% using iodomethane when 5% (w/v) was used.....	91

LIST OF SCHEMES

	Page
Scheme 2.1: Preparation of chitosan from chitin.....	9
Scheme 2.2: Synthetic pathway of <i>N</i> -alkyl chitosan with alkyl halides.....	14
Scheme 2.3: Synthetic pathway of <i>N</i> -alkyl or <i>N</i> -benzyl chitosan with aldehydes or ketones.....	14
Scheme 2.4: Synthetic pathway of <i>N</i> -alkyl and <i>N</i> -benzyl chitosan with an aldehydes.....	15
Scheme 2.5: Quaternization of chitosan using iodomethane as quaternizing agent.....	16
Scheme 2.6: Quaternization of <i>N</i> -alkyl chitosans using iodomethane as quaternizing agent.....	19
Scheme 2.7: Quaternization of chitosan using glycidyltrimethylammonium chloride as quaternizing agent.....	21
Scheme 2.8: Quaternization of chitosan using 3-chloro-2-hydroxypropyl trimethylammonium chloride as quaternizing agent.....	21
Scheme 2.9: Synthetic pathway of glycidyltrimethylammonium chloride.....	23
Scheme 3.1: Synthetic pathway of <i>N</i> -n-octyl chitosan.....	27
Scheme 3.2: Synthetic pathway of <i>N</i> -benzyl chitosans.....	28
Scheme 3.3: Synthetic pathway of <i>N,N,N</i> -trimethylammonium chitosan chloride.....	34
Scheme 3.4: Synthetic pathway of chitosan Quat-188.....	38
Scheme 4.1: Synthetic pathway of <i>N</i> -n-octyl chitosan.....	48
Scheme 4.2: Synthetic pathway of <i>N</i> -benzyl chitosans.....	49
Scheme 4.3: Synthetic pathway of chitosan Quat-188.....	81

LIST OF ABBREVIATION AND SIGNS

GluNAc	β -(1 \rightarrow 4)-2-Acetamido-2-deoxy- <i>D</i> -glucopyranose
GluN	β -(1 \rightarrow 4)-2-Amino-2-deoxy- <i>D</i> -glucopyranose
BzCh	<i>N</i> -Benzyl chitosan
BzChQ	<i>N</i> -Benzyl chitosan Quat-188
br	Broad (NMR)
3Br-BzCh	<i>N</i> -(3-Bromobenzyl)chitosan
4Br-BzCh	<i>N</i> -(4-Bromobenzyl)chitosan
3Br-BzChQ	<i>N</i> -(3-Bromobenzyl)chitosan Quat-188
4Br-BzChQ	<i>N</i> -(4-Bromobenzyl)chitosan Quat-188
COOH-BzCh	<i>N</i> -(4-Carboxybenzyl)chitosan
COOH-BzChQ	<i>N</i> -(4-Carboxybenzyl)chitosan Quat-188
ChOS	Chito-oligosaccharide
δ	Chemical shift
Cl-BzCh	<i>N</i> -(4-Chlorobenzyl)chitosan
Cl-BzChQ	<i>N</i> -(4-Chlorobenzyl)chitosan Quat-188
Quat-188	3-Chloro-2-hydroxypropyl trimethylammonium chloride
$^{\circ}\text{C}$	Degree celsius
DDA	Degree of deacetylation
DOM	Degree of <i>O</i> -methylation
DQ _{Ch}	Degree of quaternization of GlcN of chitosan
DI	Deionized water
KDO	3-Deoxy- <i>D</i> -manno-octulosonic acid
DEMChC	<i>N,N,N</i> -Diethylmethyl chitosan chloride
DSC	Differential scanning calorimetry
34OMe-BzCh	<i>N</i> -(3,4-Dimethoxybenzyl)chitosan
34OMe-BzChQ	<i>N</i> -(3,4-Dimethoxybenzyl)chitosan Quat-188
N(CH ₃) ₂ -BCh	<i>N</i> -(4- <i>N,N</i> -Dimethylaminobenzyl)chitosan
N(CH ₃) ₂ -BChQ	<i>N</i> -(4- <i>N,N</i> -Dimethylaminobenzyl)chitosan Quat-188
DMF	<i>N,N</i> -Dimethylformamide
DMSO	<i>N,N</i> -Dimethylsulfoxide
dd	Doublet of doublets (NMR)

<i>E.coli</i>	<i>Escherichia coli</i>
ES	Extent of <i>N</i> -substitution
F-BzCh	<i>N</i> -(4-Fluorobenzyl)chitosan
F-BzChQ	<i>N</i> -(4-Fluorobenzyl)chitosan Quat-188
GPC	Gel permeation chromatography
GTMAC	Glycidyl trimethylammonium chloride
HLB	Hydrophilic/lipophilic balance
OH-BzCh	<i>N</i> -(4-Hydroxybenzyl)chitosan
OH-BzChQ	<i>N</i> -(4-Hydroxybenzyl)chitosan Quat-188
HPTChOSC	<i>N</i> -(2-hydroxy)propyl-3-trimethylammonium chito- oligosaccharide chloride
HPTChC	<i>N</i> -(2-Hydroxy)propyl-3-trimethylammonium chitosan chloride
2OMe-BzCh	<i>N</i> -(2-Methoxybenzyl)chitosan
4OMe-BzCh	<i>N</i> -(4-Methoxybenzyl)chitosan
2OMe-BzChQ	<i>N</i> -(2-Methoxybenzyl)chitosan Quat-188
4OMe-BzChQ	<i>N</i> -(4-Methoxybenzyl)chitosan Quat-188
Me-BzCh	<i>N</i> -(4-Methylbenzyl)chitosan
Me-BzChQ	<i>N</i> -(4-Methylbenzyl)chitosan Quat-188
NMP	<i>N</i> -Methyl-2-pyrrolidone
mL	Mililiter
mmol	Millimole
MBC	Minimum bactericidal concentration
MIC	Minimum inhibitory concentration
M	Molar
NO ₂ -BzCh	<i>N</i> -(4-Nitrobenzyl)chitosan
NO ₂ -BzChQ	<i>N</i> -(4-Nitrobenzyl)chitosan Quat-188
NMR	Nuclear magnetic resonance
M_n	Number average molecular weight
OctCh	<i>N</i> -n-Octyl chitosan
OctChQ	<i>N</i> -n-Octyl chitosan Quat-188
PBS	Phosphate buffer saline
Poly quats	Polymeric quaternary ammonium
M_w/M_n	Polydispersity index

PyMeCh	<i>N</i> -(4-Pyridylmethyl)chitosan
PyMeChQ	<i>N</i> -(4-Pyridylmethyl)chitosan Quat-188
QN(CH ₃) ₂ -BzCh	Quaternized <i>N</i> -(4- <i>N,N</i> -dimethylaminobenzyl)chitosan
QPyMeCh	Quaternized <i>N</i> -(4-pyridylmethyl)chitosan
R _g	Radius of gyration
s	Singlet (NMR)
SEC	Size exclusion chromatography
<i>S.aureus</i>	<i>Staphylococcus aureus</i>
NB	Sterile nutrient broth
TGA	Thermal gravimetric analysis
2ThMeCh	<i>N</i> -(2-Thiophenylmethyl)chitosan
2ThMeChQ	<i>N</i> -(2-Thiophenylmethyl)chitosan Quat-188
CF ₃ -BzCh	<i>N</i> -(4-Trifluoromethylbenzyl)chitosan
CF ₃ -BzChQ	<i>N</i> -(4-Trifluoromethylbenzyl)chitosan Quat-188
TMChC	<i>N,N,N</i> -Trimethylammonium chitosan chloride
TMChI	<i>N,N,N</i> -Trimethylammonium chitosan iodide
DQ _T	Total degree of quaternization
cm ⁻¹	Unit of wavelength
M _w	Weight Average Molecular Weight

สถาบันวิทยบริการ
จุฬาลงกรณ์มหาวิทยาลัย

CHAPTER I

INTRODUCTION

1.1 Introduction

There are different classes of synthetic and modified natural polymers exhibiting antibacterial activity [1]. Biocidal polymers have been divided into five classes such as quaternary ammonium polymers, phosphonium polymers, halogenated poly(styrene-divinylbenzene)sulfonamides, and *N*-halamine polymers [2]. These polymers have numerous potential applications in water treatments, health care and hygienic applications such as coatings, textiles, disinfections of air and gas, and preservatives.

The quaternary nitrogen functionality is an essential component in many biologically active compounds and plays an important role in living processes. Long chain quaternary ammonium compounds exert antibacterial activity against both Gram-positive and Gram-negative bacteria, as well as against some pathogenic species of fungi and protozoa [2]. However, these quaternary ammonium compounds, in general, have toxic effects toward mammalian cells [3]. In humans and animals they are considered too toxic for systemic applications, but acceptable for topical applications. Quaternary ammonium polymers are generally more active than their corresponding monomers, particularly against Gram-positive bacteria [2]. Antimicrobial activity increases as the content of the quaternary ammonium moiety increases, providing that the proper hydrophilic/lipophilic balance (HLB) is maintained [3]. Polymeric quaternary ammonium materials (poly quats) having a higher molecular weight and multiple quaternary nitrogens exhibit increased activity as the charge density increases the attraction to the negatively charged cell membrane. Furthermore, the polyquats tend to be less toxic than their monomeric counterparts. In the present, a number of polyquats having been developed that can be incorporated into cellulose and other materials which should provide significant advances in the biomedical field.

Therefore, investigation of the potential antibacterial activity of quaternary ammonium polysaccharides is warranted. Chitosan is a polysaccharide obtained by deacetylating chitin, the major constituent of the exoskeleton of crustaceans [4]. Chitosan is a biodegradable, non-toxic, biocompatible and renewable polymer, and as a result there has been much interest invested in past few decades in the macromolecule and its derivatives, aimed at exploring new applications. Interestingly, some antibacterial and antifungal activities have been described with chitosan and modified chitosans [5]. Moreover, chitosan has several advantages over other types of disinfectants because it possesses a higher antibacterial activity, a broader spectrum of activity, a higher killing rate, and a lower toxicity toward mammalian cells [5,6]. Although the exact mechanism of antibacterial of chitosan is still debated, disruption of the cell membrane appears to be the most viable candidate. Interaction between positively charged chitosan molecules and negatively charged bacterial cell membranes leads to the leakage of proteinaceous and other intracellular constituents [7-11].

However, chitosan showed its biological activity only in acetic medium because of its poor solubility in water [6]. Many attempts have thus been made in the synthesis of chitosan derivatives to overcome the solubility problem [12,13]. To increase the solubility in water, the quaternary ammonium moiety in chitosan is required [14,15]. In addition, a permanent positive charges may provide an impetus for antibacterial activity. Because of the amphiphilic nature of the bacterial cell wall, an increase in interaction between the bacterial cell wall and the chitosan derivative could be favored when the macromolecule itself contained hydrophobic residues. As a result, chitosan derivatives containing quaternary ammonium functionality in addition to different hydrophobic substituents were synthesized using different levels of reagents and their antibacterial activity was consequently assessed. A systematic study, exploring the effects of different substituents with varying degrees of hydrophobicity, structural rigidity of the macromolecule and its molecular weight on the antibacterial activity was investigated.

1.2 Objective

The aim of this study was to synthesize and characterize *N*-benzyl chitosans and *N*-benzyl chitosans containing quaternary ammonium functionality and to assess their antibacterial activities.

1.3 Scope of research

- 1) To synthesize and characterize *N*-alkyl and *N*-benzyl chitosans prepared by reacting chitosan with corresponding aldehydes in acidic condition.
- 2) To synthesize and characterize *N*-alkyl and *N*-benzyl chitosans containing quaternary ammonium functionality prepared by reacting *N*-alkyl and *N*-benzyl chitosans with either iodomethane or 3-chloro-2-hydroxypropyl trimethylammonium chloride (Quat-188).
- 3) To assess the antibacterial activity of these quaternized chitosans against two bacteria; *Escherichia coli* (Gram-negative bacteria) and *Staphylococcus aureus* (Gram-positive bacteria).
- 4) To study the degradation of chitosan under the synthesis conditions.

CHAPTER II

THEORETICAL AND LITERATURE REVIEWS

2.1 Bacteria

2.1.1 Morphology and ultrastructure

The size, shape and arrangement of bacteria and other microbes is the result of their genes and is defining characteristic called morphology. Bacteria come in a bewildering and exciting variety of size and shapes. The most common bacterial shapes are rods (bacilli) and spheres (cocci). Within each of these groups is hundreds of unique variations. Rods may be long, short, thick, or thin and have rounded or pointed ends, thicker at one end than the other, etc. Cocci may be large, small, or oval shaped to various degrees. Spiral shaped bacteria may be fat, thin, loose spirals or very tight spirals [16].

2.1.2 Gram staining

Bacteria can be classified to two major groups, Gram-positive and Gram-negative, based on the Gram staining reaction shown in Figure 2.1. Differences in cell wall structure and composition account for the differential Gram reaction.

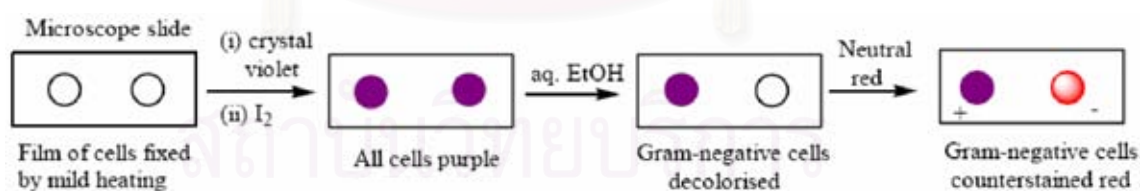


Figure 2.1: Determination of type of bacteria based on Gram staining reaction [16]

2.1.3 Cell walls of bacteria

The fundamental differences in ultrastructure of the cell wall are responsible for the reaction (+ or -) of bacteria towards the Gram stain. In both types of cells, the cytoplasmic membrane is surrounded and supported by a cell wall, which provides strength, rigidity and shape. The cross sections of these structures are shown in Figure 2.2.

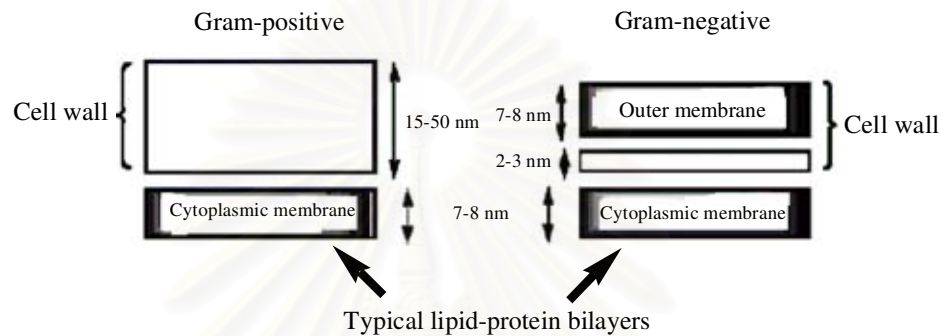


Figure 2.2: The cross sections of Gram-positive and Gram-negative bacteria cell walls [16]

In this study, Gram-positive (i.e., *Staphylococcus aureus*) and Gram-negative (i.e., *Escherichia coli*) were used. Gram-positive bacteria tend to have a loose cell wall, while Gram-negative bacteria have an outer membrane structure in the cell wall forming an additional barrier for foreign molecules as shown in Figure 2.3.

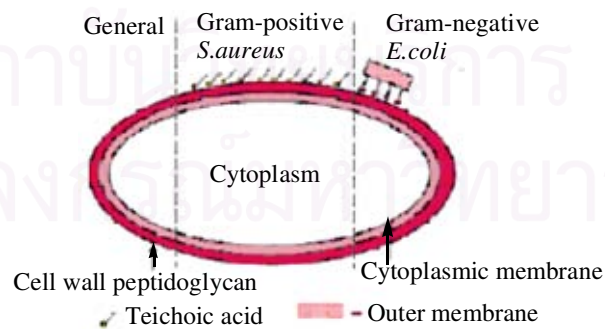


Figure 2.3: Cell wall structures of Gram-positive (i.e., *Staphylococcus aureus*) and Gram-negative (i.e., *Escherichia coli*) [17]

2.1.3.1 Gram-positive bacteria

The wall, which lines outside the cytoplasmic membrane, is usually between 15 and 50 nm thick. The major part of the Gram-positive wall is a large polymer comprising two covalently linked components. One of these components, forming at least 50% of the wall mass, is peptidoglycan. Its cross-linked structure provides a tough, fibrous fabric giving strength and shape to the cell and enabling it to withstand a high internal osmotic pressure. Attached to the peptidoglycan is an acidic polymer, such as teichoic acid, lipo teichoic acid and teichuronic acid, which differs from species to species. The acidic character of the polymer attached to the peptidoglycan ensures that the cell surface is strongly polar and carries a negative charge. This may influence the passage of ions, particularly magnesium ion and possible ionized drugs, into the cell. Other components are protein often present to the extent of 5-10%, and protein of *Staphylococcus aureus* is apparently linked covalently to peptidoglycan [18]. The structure of cell wall Gram-positive bacteria is shown in Figure 2.4.

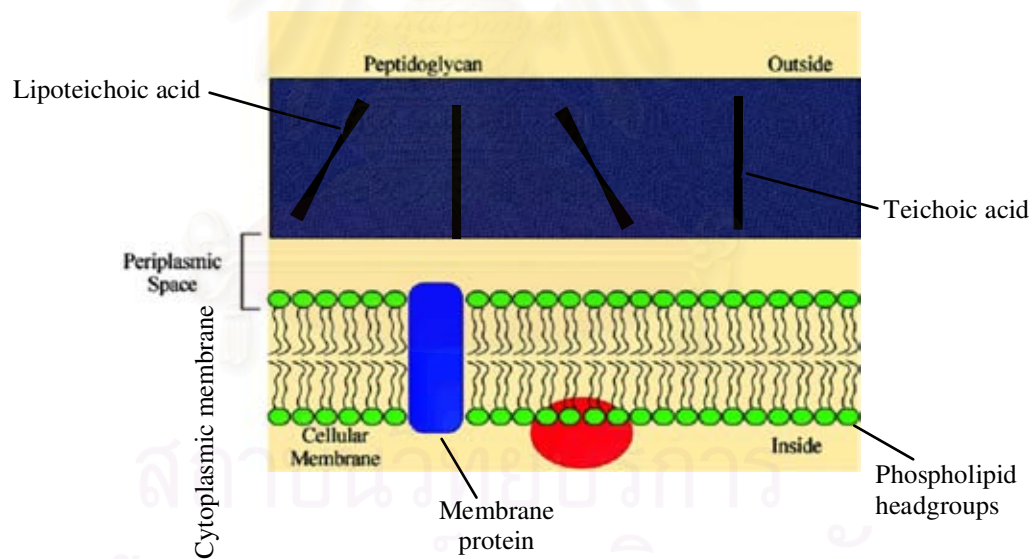


Figure 2.4: The arrangement of the cell envelope of Gram-positive bacteria [19]

2.1.3.2 Gram-negative bacteria

The Gram-negative wall is far more complex. Wide-ranging studies of its structure have been concentrated on *Escherichia coli* in particular. The diagram in Figure 2.5

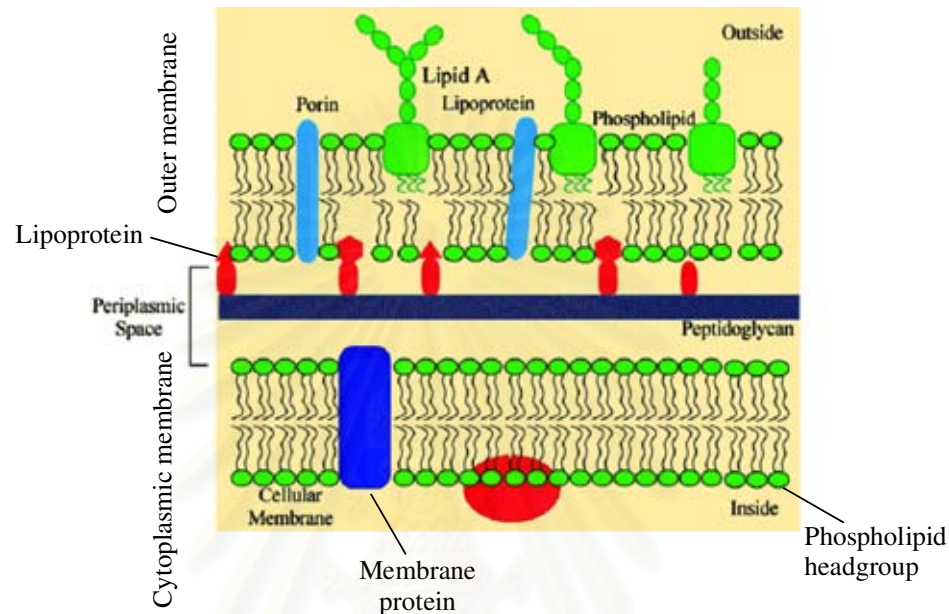


Figure 2.5: The arrangement of the cell envelope of Gram-negative bacteria [19]

illustrates the general arrangement of the components of the Gram-negative cell envelope, which includes the cytoplasmic membrane as well as the cell wall. When cells of *Escherichia coli* are fixed, stained with suitable metal salts, sectioned and examined by electron microscopy, the cytoplasmic membrane is readily identified by its 'sandwich' appearance of two electron-dense layers separated by a lighter space. The electron-dense layer, about 2 nm thick, immediately outside the periplasm represents the peptidoglycan component of the wall. It is much thinner than in Gram-positive bacteria and may constitute only 5 to 10% of the wall mass [18].

The outer regions of the Gram-negative cell wall have been the most difficult to characterize. The various components together form a structure 6-10 nm thick, called the outer membrane. Like the cytoplasmic membrane it is basically a lipid bilayer (giving rise to the two outer most electron-dense bands), hydrophobic in the interior with hydrophilic groups at the outer surfaces. It also has protein components

which penetrate the layer partly or completely and form the membrane. Despite these broad structural similarities, the outer membrane differs widely in composition and function from the cytoplasmic membrane. Its main constituents are lipopolysaccharide, phospholipids, fatty acids and proteins. The phospholipids, mainly phosphatidylethanolamine and phosphatidylglycerol, resemble those in the cytoplasmic membrane. The structure of the lipopolysaccharide is complex and varies considerably from one bacterial strain to another. The molecule has three parts. The core is built from 3-deoxy-*D*-manno-octulosonic acid (KDO), hexoses, heptoses, ethanolamine and phosphoric acid as structural components. The three KDO residues contribute a structural unit which strongly binds the divalent ions of magnesium and calcium, an important feature stabilizing the membrane. Removal of these ions by chelating agents leads to release of some of the lipopolysaccharide into the medium; at the same time the membrane becomes permeable to compounds that would otherwise be excluded. The core polysaccharide is linked to the antigenic side chain, a polysaccharide which can vary greatly from one strain to another even within the same bacterial species. Usually it comprises about 30 sugar units, although these can vary both in number and in structure. It forms the outer most layer of the cell and is the main source of its antigenic characteristics. At the opposite end, the core of the lipopolysaccharide is attached to a moiety known as lipid A which can be hydrolysed to glucosamine, long-chain fatty acids, phosphate and ethanolamine. The fatty acid chains of lipid A, along with those of the phospholipids, align themselves to form the hydrophobic interior of the membrane. The outer membrane is therefore asymmetric, with lipopolysaccharide exclusively on the outer surface and phospholipid mainly on the inner surface [18].

2.2 Chitin and chitosan

Chitin, one of the most abundant natural polysaccharides and generally found in the composition of crustacean shells, insects, molluscan organs, and fungi, consists of β -(1 \rightarrow 4)-2-acetamido-2-deoxy-*D*-glucopyranose (GlcNAc) as a repeating unit [4]. Deacetylation of chitin yields chitosan, which is actually a copolymer of GlcNAc and β -(1 \rightarrow 4)-2-amino-2-deoxy-*D*-glucopyranose (GlcN) with GlcN content greater than 50% [4]. The chemical structures of chitin and chitosan were shown in Figure 2.6.

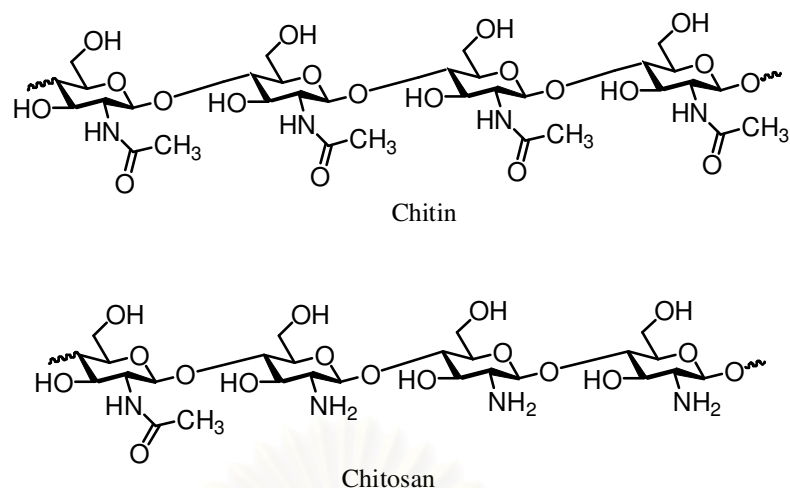
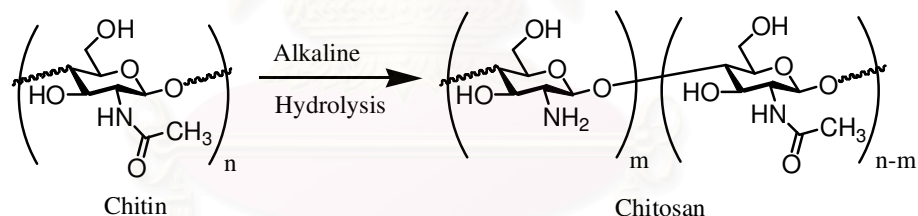


Figure 2.6: Chemical structures of chitin and chitosan

Chitosan is a polysaccharide obtained from chitin by alkaline hydrolysis; the process essentially hydrolyzes *N*-acetyl groups at random within the polymer backbone (Scheme 2.1). However, most commercially available samples of chitosan are not 100% deacetylated and thus the polysaccharide is often represented by the degree of deacetylation (DDA) in addition to the molecular weight.



Scheme 2.1: Preparation of chitosan from chitin

Chitin and chitosan have gained increasing attention due to their properties as non-toxic, biocompatible and biodegradable polymers. Chitosan is insoluble in water and almost all organic solvents, but it is soluble in dilute organic acid solutions such as acetic, formic, succinic, and lactic acids at pH below 6.5. The synthetic modification of chitosan is a widely studied area [12,20]. Such modifications have resulted into several derivatives of chitosan with distinct properties and applications [21-23]. The presence of multiple nucleophilic groups within the chitosan backbone requires following suitable synthetic protocol in order to obtain the desired selectively. The synthetic transformation steps performed are often relatively simple, exploiting the

differences in the nucleophilicities of primary amino group (at C-2) versus the two hydroxy groups (at C-3 and C-6) position. However, the extent of *N*-substitution (ES) varies greatly upon the reaction condition.

2.3 Mode of action of chitosan

Native chitosan exhibits much more pronounced activity compared to chitin [24]. This is due to the greater availability of primary amino groups in chitosan. Under mildly acidic conditions ($\text{pH} < 6.5$), the primary amino groups of chitosan acquire a positive charge, which is usually associated with the demonstrated activity. The exact mechanism of the antimicrobial action of chitin, chitosan, and their derivatives is still debated, disruption of the cell membrane appears to be the most viable candidate. Interaction between positively charged chitosan molecules and negatively charged microbial cell membranes leads to the leakage of proteinaceous and other intracellular constituents [7-11]. Chitosan acts mainly on the outer surface polycationic chitosan probably due to the negatively charged bacterial surface to cause agglutination, while at higher concentrations, the larger number of positive charges may have imparted a net positive charge to the bacterial surfaces to keep them in suspension [25].

Quaternary ammonium polymers have previously been considered bacteriostatic, not bactericidal, because they require long contact times to kill microorganisms, and generally they do not have a broad spectrum activity. Some of these polymers have been reported to have antimicrobial activity [26]. The antimicrobial action is believed to occur when the compounds permeated the lipid cell membrane and caused death through the loss of essential cell materials. In addition, these derivatives of chitosan are generally more active against Gram-positive bacteria than their corresponding monomers particularly. This effect is believed to be due to adsorption of the polymers onto the bacterial cell surface and membrane with subsequent disruption of membrane integrity. Antimicrobial activity generally increases as the content of the quaternary ammonium moiety increases. It was unexpectedly discovered that HPTChC and related chitosan derivatives exhibit antimicrobial activity at concentrations as low as 10-20 $\mu\text{g}/\text{mL}$ [26]. The other is one order of magnitude lower than the concentration at which any previous chitosan

derivative has been reported to exhibit antimicrobial activity. These chitosan derivatives may be included in formulations, where it is desirable to minimize bacterial attack [27].

The antibacterial activities of quaternary ammonium chitosan salts were evaluated against *S.aureus* and *E. coli*, Gram-positive and Gram-negative bacteria, respectively. It was found that the antibacterial activity increased with increasing chain length of the alkyl substituent, and this was attributed to the contribution of the increased hydrophobic properties of the derivatives [28]. These results clearly demonstrated that hydrophobicity and cationic charge of the introduced substituent strongly affected the antibacterial activity of quaternary ammonium chitosan derivatives. Furthermore, the antibacterial activities of quaternary ammonium chitosan salts in acetic medium was stronger than that in water [29]. Their antibacterial activity increased as the concentration of acetic acid was increased.

2.4 Antibacterial property of chitosan and its derivatives

Chitosan and several of its derivatives showed good to excellent antimicrobial (antibacterial and antifungal) properties [5,7,26,28,30]. However, the antimicrobial action is influenced by intrinsic factors such as the type of chitosan, the degree of chitosan polymerization, the host, the natural nutrient constituency, the chemical or nutrient composition of the substrates, and the environmental conditions such as substrate water activity or moisture [5]. Although both native chitosan and its derivatives are effective as antimicrobial agents, there is a clear difference between them. Chitosan has been shown to be fungicidal against several fungi (Table 2.1) [5,31].

Table 2.1: MIC of native chitosan against fungi

Fungi	MIC* (µg/mL)
<i>Botrytis cinerea</i>	10
<i>Fusarium oxysporum</i>	100
<i>Drechstera sorokiana</i>	10
<i>Micronectriella nivalis</i>	10
<i>Piricularia oryzae</i>	5000
<i>Rhizoctonia solani</i>	1000
<i>Trichophyton equinum</i>	2500

*MIC is minimum growth inhibitory concentration.

The antibacterial action is usually rapid and eliminates bacteria as quickly as within few hours. Furthermore, chitosan has several advantages over other types of disinfectants because it possesses a higher antibacterial activity, a broader spectrum of activity, a higher killing rate, and a lower toxicity toward mammalian cells [6]. Chitosan has been studied in terms of bacteriostatic/bactericidal activity to control growth of algae and inhibit viral multiplication [32,33]. Moreover, chitosan inhibits the growth of a wide variety of bacteria (Table 2.2) [5,31]. The antibacterial activity is wide spectrum and includes bacteria of both cell wall types (Gram-positive and Gram-negative bacteria). It is important to note that the monomer of chitosan, 2-amino-2-deoxy-*D*-glucopyranose as its hydrochloride salt, does not exhibit any antibacterial activity against several bacteria, including *Escherichia coli* and *Staphylococcus aureus* [34].

สถาบันวิทยบริการ
จุฬาลงกรณ์มหาวิทยาลัย

Table 2.2: MIC of native chitosan against bacteria

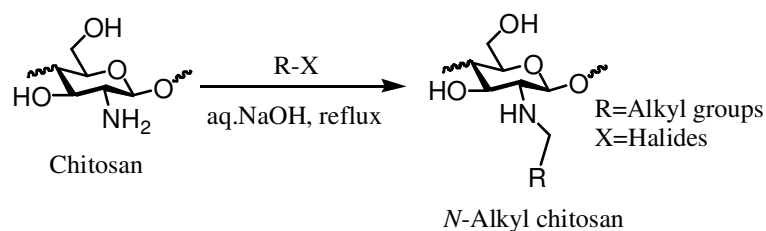
Bacteria	MIC* ($\mu\text{g/mL}$)
<i>Agrobacterium tumefaciens</i>	100
<i>Bacillus cereus</i>	1000
<i>Corinebacterium michiganence</i>	10
<i>Erwinia sp.</i>	500
<i>Erwinia carotovora subsp.</i>	200
<i>Escherichia coli</i>	20?
<i>Klebsiella pneumoniae</i>	700
<i>Micrococcus luteus</i>	20?
<i>Pseudomonas fluorescens</i>	500
<i>Staphylococcus aureus</i>	20?
<i>Xanthomonas campestris</i>	500

*MIC is minimum growth inhibitory concentration.

? is the MIC values reported for *Escherichia coli* and *Staphylococcus aureus* are questionable. It is important to note that these data were obtained at pH 4.5 whereas the data reported in this work was measured at pH 7.0. At the higher pH's, chitosan is insoluble. However, MIC of chitosan are reported in the range 1024-2048 $\mu\text{g/mL}$ by Holappa *et al.* at the neutral pH [35].

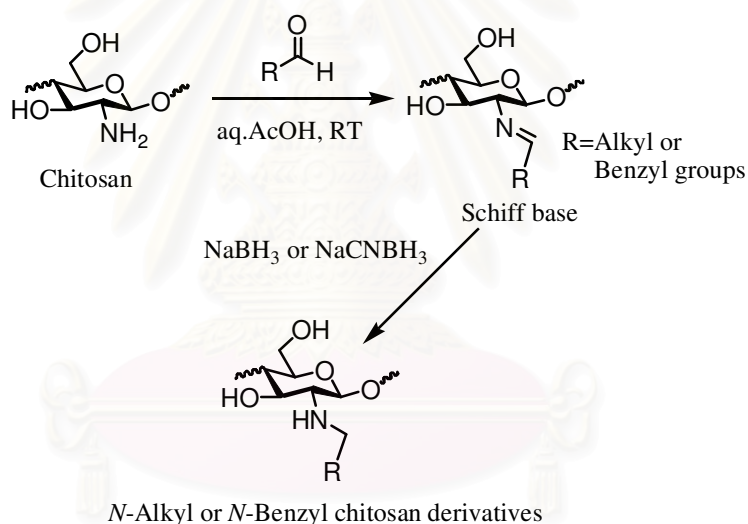
2.5 N-Alkylation and N-benzylation of chitosan

N-Alkylation of chitosan is selectively carried out by using a halogen displacement reaction or by using a reductive amination. The direct N-alkylation of chitosan was carried out by the reaction between the 2-amino group of GlcN of chitosan with alkyl halide under heterogeneous condition in the presence of a strong base (Scheme 2.2). Furthermore, this method were involved the vigorous reaction condition such as high temperature and high concentration of sodium hydroxide as base which resulted in lower degree of substitution and much more degradation of molecular weight in polymer backbone [36].



Scheme 2.2: Synthetic pathway of *N*-alkyl chitosan with alkyl halides

The another selective *N*-alkylation and *N*-benzylation were performed via Schiff bases formed by the reaction between the 2-amino group of GlcN of chitosan with aldehydes or ketones under homogeneous acidic conditions (Scheme 2.3), then followed by reduction of the Schiff base intermediates with sodium borohydride or sodium cyanoborohydride and hence provided for higher ES when desired [37-39].

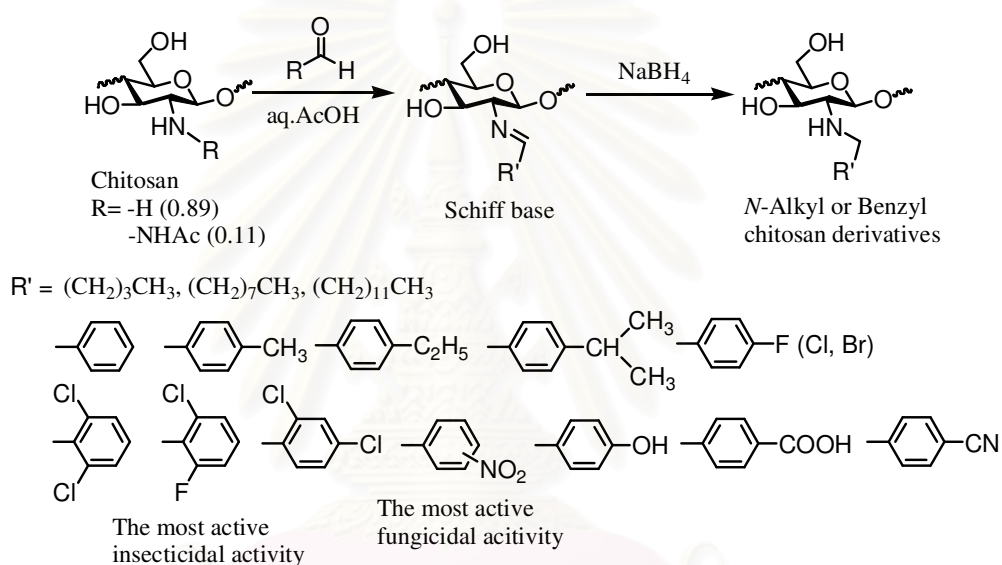


Scheme 2.3: Synthetic pathway of *N*-alkyl or *N*-benzyl chitosan with aldehydes or ketones

N-Alkyl chitosan, one of the most important hydrophobic derivatives of chitosan, has been reported by several research groups [37-41]. Much less attention has been paid on the synthesis of *N*-benzyl chitosans. The reductive benzylation of chitosan with salicylaldehyde has been reported along with its application in metal chelation [42,43]. In 1997, Crini *et al.* synthesized *N*-benzyl sulfonated derivatives of chitosan and reported their one-dimensional and two-dimensional NMR spectra [40].

In 1999, Sashiwa and Shigemasa prepared a series of *N*-benzyl chitosan derivatives, but they only reported their water solubility [44].

Recently, the *N*-alkylated and *N*-benzylated chitosans were prompted by Stevens *et al.* who synthesized the series of 24 *N*-alkyl and *N*-benzyl chitosans with different ES and reported their insecticidal and fungidal activities as shown in Figure 2.4. They found that the insecticidal and fungidal activities of all chitosan derivatives were higher than that of chitosan at the same concentration. Moreover, the functional groups on the benzene ring affected the insecticidal and fungidal activities. [45,46].



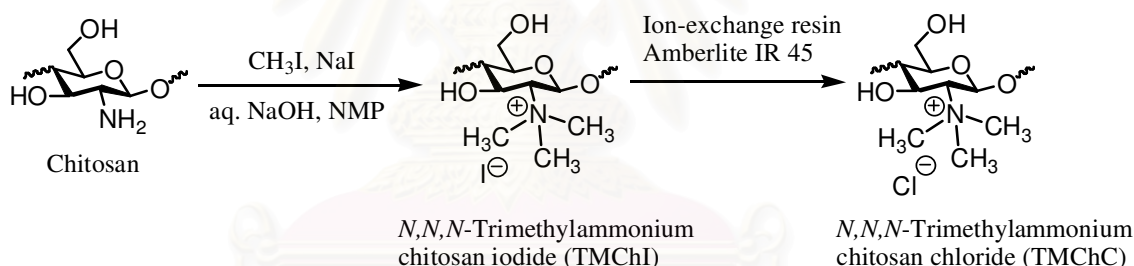
Scheme 2.4: Synthetic pathway of *N*-alkyl and *N*-benzyl chitosan with an aldehydes

However, the impact of the molar aldehyde:GlcN ratio and the effect of substituents on aromatic aldehydes have not been reported. In this study, a series of aromatic aldehydes bearing electron donating and electron withdrawing groups were studied. The influence of the aromatic substituents on the ES is also discussed. Two heterocyclic derivatives, *N*-(4-pyridylmethyl) and *N*-(2-thiophenylmethyl)chitosan are included in the discussion.

2.6 Quaternization of chitosan using iodomethane as quaternizing agent

In 1985, the former approach was earlier used by Muzzarelli *et al.* to prepare *N,N,N*-trimethylammonium chitosan iodide (TMChI) by reacting *N,N*-dimethylated chitosan, which was previously prepared by treating chitosan DDA 60% with formaldehyde followed by reduction with sodium borohydride, with iodomethane in acetonitrile at 35°C for 30 hours. The product was extracted with diethyl ether in a soxhlet apparatus. The high degree of quaternization (DQ_{Ch}) 60% was obtained, but it was not soluble in water [47].

In 1986, Domard *et al.* prepared *N,N,N*-trimethylammonium chitosan chloride (TMChC) by reacting chitosan, which was suspended in *N*-methyl-2-pyrrolidone (NMP), with iodomethane in the presence of sodium hydroxide and sodium iodide at 36°C for 3 hours (Scheme 2.5). After repeated methylation with iodomethane, DQ_{Ch} was 64%.



Scheme 2.5: Quaternization of chitosan using iodomethane as quaternizing agent

Moreover, DQ_{Ch} greater than 25% these polymers are soluble in water [14]. In 1987, the same research group characterized chemical structure and determined various DQ_{Ch} of TMChC by using 1H and ^{13}C -NMR spectroscopic techniques. Moreover, methylation of hydroxy groups of chitosan is demonstrated [48].

In 1994, Dung *et al.* prepared TMChC by single treatment with iodomethane. The procedure was similar to the method used by Domard *et al.*, but they increased sodium hydroxide concentration from 1.4M to 15% (w/v) at 60°C and varied reaction

times from 30-180 minutes. They found that high DQ_{Ch} 53% was obtained without any detectable *O*-methylation [49].

In 1998, Sieval *et al.* applied the method that proposed by Dung *et al.* but their results showed there had been a misinterpretation concerning the 1H -NMR spectrum of TMChC, particularly with respect to the chemical shifts attributed to the protons of *N,N*-dimethylated and *N,N,N*-trimethylated chitosan. Therefore, they proposed new assignments for the above mentioned signals and hence showed that the execution of this single treatment with iodomethane produced a poorly water soluble chitosan derivative with only DQ_{Ch} 10-15%. Furthermore, they concluded that these derivative was mainly a *N,N*-dimethylated chitosan. They also concluded that it was necessary to carry out repeated methylation that DQ_{Ch} close to 60% which was completely water soluble. The repeated methylation by subsequent addition steps resulted in still higher DQ_{Ch} >85%, but it produced a poorly water soluble due to much more *O*-methylation [50].

In 2001, Hamman and Kotze studied effects of type of base, number of methylation on DQ_{Ch} and molecular weight of TMChC. 1H -MNR spectra of TMChCs indicated a major increase in the DQ_{Ch} 21%-59% with an increase in the number of methylation when 15% (w/v) sodium hydroxide was used as the base at 60°C for 45, 15 and 30 minutes, (single, double and triple treatment with iodomethane) respectively. Intrinsic viscosity values exhibited that dimethyl amino pyridine, used as base, did not cause polymer degradation compared to sodium hydroxide, but the DQ_{Ch} stayed low 7.3%–9.6% even when the number of methylation was increased. A combination of the two bases did not reduce polymer degradation, while the DQ_{Ch} was limited to relatively low values DQ_{Ch} 12.5%–34.4% [51].

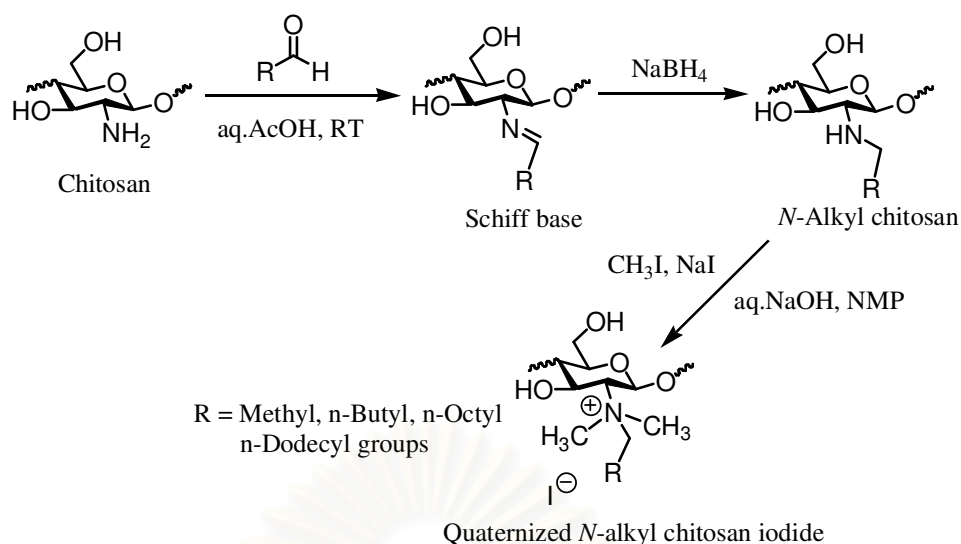
In 2003, Elisabete *et al.* studied the effect of quaternization conditions of chitosan, particularly sodium hydroxide concentration that was added to the medium at room temperature. The average DQ_{Ch} was obtained in the ranged 10.5%-44.8%, and the chemoselectivity of *N*-methylation of chitosan was affected by adding excesses of sodium hydroxide and iodomethane. Therefore, *O*-methylation was favored when the larger excess of these reagents used [52].

In 2004, Polnok *et al.* investigated the effects of the quaternization of chitosan process and types of base. The high DQ_{Ch} with low *O*-methylation was prepared by employing single treatment with iodomethane, single treatment with iodomethane and one subsequent addition, double treatment with iodomethane, double treatment with iodomethane and one subsequent addition steps and controlled alkaline environment of the mixture reaction. However, high $DQ_{Ch}>75\%$ required many reaction steps as resulted high *O*-methylation which would decrease the aqueous solubility of the polymer [53].

2.7 Quaternization of *N*-alkyl or *N*-benzyl chitosans using iodomethane as quaternizing agent

In 1997, Kim *et al.* prepared quaternized *N*-alkyl chitosans containing alkyl substituents of different chain lengths. They reacted chitosan with formaldehyde, butyraldehyde, *n*-octylaldehyde and *n*-dodecylaldehyde and treated the resulting Schiff bases with sodium borohydride. The corresponding quaternary ammonium salt of chitosan was prepared by reacting the *N*-alkyl chitosans with iodomethane in the presence of sodium hydroxide as base (Scheme 2.6). The antibacterial activity in acidic condition of the quaternized chitosan was higher against *Staphylococcus aureus* than that of chitosan, and it increased with increasing chain length of the alkyl substituent [28].

สถาบันวิทยบริการ
จุฬาลงกรณ์มหาวิทยาลัย



Scheme 2.6: Quaternization of *N*-alkyl chitosans using iodomethane as quaternizing agent

In 2001, Jia *et al.* reacted chitosan samples of various molecular weights with propylaldehyde and furfuraldehyde. The resulting Schiff bases were treated with sodium borohydride. Quaternized chitosans were obtained by reaction of *N*-alkyl chitosans with iodomethane. The yields, DQ_{Ch} and water solubility of quaternized chitosans were influenced by the molecular weight of the starting chitosan samples. Antibacterial activities of quaternized chitosan against *Escherchia coli* is related to its molecular weight and in acetic acid medium is stronger than that in water [29].

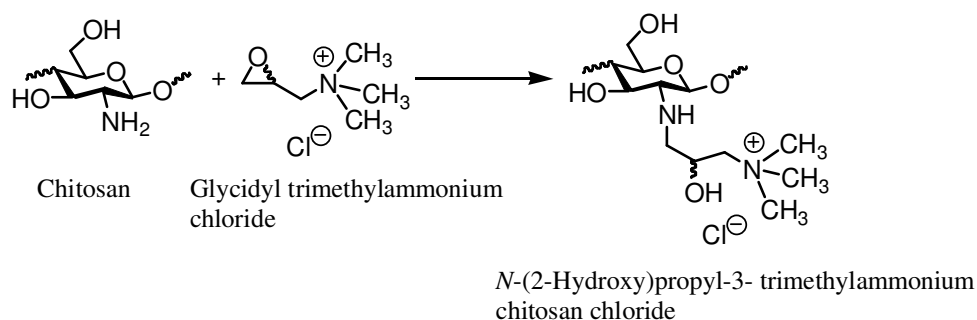
In 2005, Avadi *et al.* prepared *N,N,N*-diethylmethyl chitosan chloride (DEMChC) based on a modified two-step process. *N*-alkyl chitosan has been firstly prepared by introducing a methyl group from formaldehyde into chitosan via Schiff base, followed by reducing with sodium borohydride. Finally, *N*-methyl chitosan reacted with iodoethane to produce DEMChC. The antibacterial activities of chitosan and DEMChC against *Escherchia coli* were evaluated by determination of minimum inhibitory concentration (MIC) and minimum bactericidal concentration (MBC). They found that antibacterial activities in acetic acid medium of DEMChC was higher than that of chitosan [54].

In the literature reviews, it can be concluded that the factors that affected DQ_{Ch} were DDA, type of bases, concentration of base, time, type of quaternizing agent (iodometane or glycidyl trimethylammonium chloride), volume of quaternizing agent, temperature, and the number of methylation [5]. However, higher DQ_{Ch} required more than single treatment with iodomethane. It was noted that the repeated methylation would increase not only DQ_{Ch} but also *O*-methylation. Furthermore, high *O*-methylation from repeated methylation affected the physical properties of quaternized chitosan, lower solubility in water and easier degradation, as well as lower yield [50].

2.8 Quaternization of chitosan using quaternary ammonium epoxide as quaternizing agent

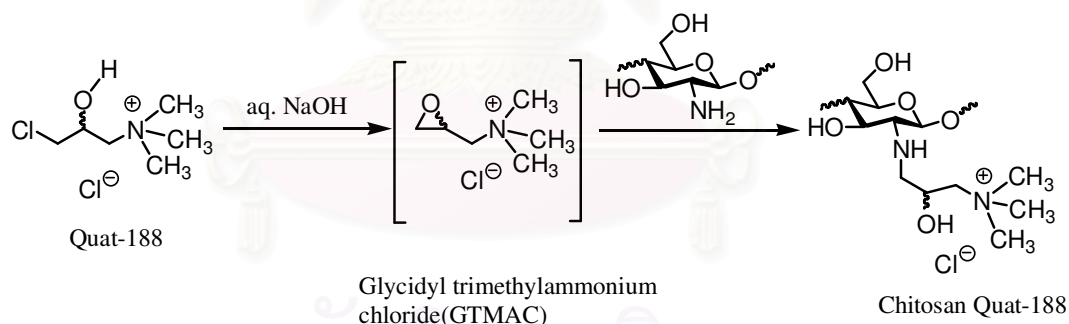
The another alternative for introduction a quaternary ammonium group into chitosan backbone has been reported. Glycidyl trimethylammonium chloride (GTMAC) was selected as quaternizing agent because it has a quaternary ammonium group itself. When a primary amino group at C-2 of chitosan reacted with GTMAC, the chain of quaternary ammonium group obtained was longer than that of TMChC.

In 1990, Lang *et al.* synthesized *N*-(2-hydroxy)propyl-3-trimethylammonium chitosan chloride (HPTChC) by reacting chitosan with GTMAC, but they did not characterize the resulting derivatives [41]. In 1991, Loubaki *et al.* synthesized and characterized GTMAC-modified chitosan (Scheme 2.7). The structure of HPTChC was confirmed using elemental analysis, IR, and NMR spectroscopies. The complete DQ_{Ch} of primary amino groups in chitosan was obtained at a 6:1 ratio (molar ratio of GTMAC:GlcN) in water at 60°C for 15 hours. All results were consistent with *N*-monoalkylation, and a six-fold excess of GTMAC gave rise to almost complete quaternization [15].



Scheme 2.7: Quaternization of chitosan using glycidyl trimethylammonium chloride as quaternizing agent

In 1998, Daly *et al.* have developed a method for synthesis of HPTChC. Chitosan was quaternized using commercially available Quat-188 salt, 3-chloro-2-hydroxypropyl trimethylammonium chloride, (Scheme 2.8) and called these product as chitosan Quat-188. Chitosan Quat-188 exhibited the antimicrobial activity at concentrations as low as 10-20 $\mu\text{g}/\text{mL}$. Furthermore, these compounds may be used as preservatives in cosmetic formulation and as antimicrobial pharmaceutical agents [26,56].



Scheme 2.8: Quaternization of chitosan using 3-chloro-2-hydroxypropyltrimethylammonium chloride as quaternizing agent

In 1999, Nam *et al.* synthesized HPTChC used as antibacterial agent in fibers by blending with polyacrylonitrile (PAN). The complete DQ_{Ch} of primary amino groups in chitosan was obtained at a 4:1 ratio (molar ratio of GTMAC:GlcN) in water and $\text{Zn}(\text{BF}_4)_2$ used as a catalyst at 100°C for 20 hours. The only 0.5% of

HPTChC/PAN blend fibers exhibited nearly 100% reduction of *Staphylococcus aureus* bacteria [57].

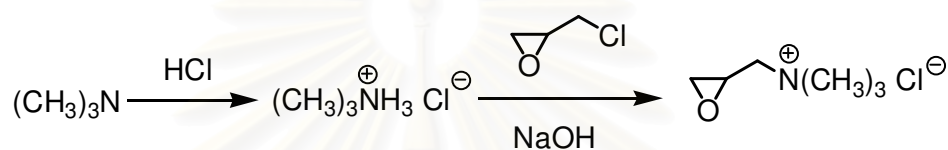
In 2000, Seong *et al.* synthesized *N*-(2-hydroxy)propyl-3-trimethylammonium chito-oligosaccharide chloride (HPTChOSC) as antibacterial agent for cellulosic fibers. The complete DQ_{Ch} 102% of primary amino groups in chito-oligosaccharide (ChOS) was obtained at a 4:1 (molar ratio of GTMAC:GlcN) in acetic acid at 80°C for 18 hours. MIC values of HPTChOSC and ChOS were 50 and 400 µg/mL against *Staphylococcus aureus*, respectively. A cotton fabric treated with 0.2% HPTChOSC and 1.8% ChOS exhibited 100% reduction of bacteria. For durability of laundering, 0.3% HPTChOSC showed 100% bacterial reduction while 2.4% ChOS showed 96% bacterial reduction after the 50th wash cycle [58].

In 2003, Kim *et al.* used a similar procedure of Seong *et al.* for synthesis of HPTChC as antibacterial agent for cotton fabrics, but different reaction conditions. In this case, it was performed in water at 70°C for 24 hours. HPTChC had a lower MIC values against *Staphylococcus aureus*, *Escherichia coli*, and *Klebsiella pneumoniae* compared to chitosan. The bacterial reduction values of the fabrics treated with 8% butanetetracarboxylic acid and 0.1% HPTChC were greater than 90% even after 20 laundering cycles [59].

In 2003, Kim *et al.* used a similar procedure of Ho Kim *et al.* for synthesis HPTChOSC. They found that HPTChOSC exhibited the growth inhibition of above 80% against *Streptococcus mutans* after 5 hours which was higher than that of ChOS [60].

In 2004, Lim *et al.* synthesized HPTChC. The complete DQ_{Ch} of primary amino groups in chitosan was obtained at a 3:1 (molar ratio of GTMAC:GlcN) in water at 85°C, and GTMAC was added in three portions (7.1 mL each) at 2 hour interval for 10 hours. This derivative was further modified by introducing functional (acrylamidomethyl) groups into primary amino groups of chitosan. The fiber-reactive chitosan derivative, *O*-acrylamidomethyl-HPTChC, showed complete bacterial reduction within 20 minutes at the concentration of 10 µg/mL, contacted with *Staphylococcus aureus* and *Escherichia coli* [61].

In 2004, Li *et al.* synthesized HPTChC for potential retention-aids in alkaline papermaking. The complete DQ_{Ch} of primary amino groups in chitosan was obtained at a 6:1 (molar ratio of GTMAC:GlcN) in aqueous sodium hydroxide (pH 9) at 75°C for 8 hours. In this study, the GTMAC was synthesized from trimethylamine and concentrated hydrochloric acid at 4°C and followed by adding epoxy chloropropane at 31°C in a basic condition as shown in Scheme 2.9. It was found that HPTChC was almost completely adsorbed onto the surfaces of calcium carbonate particles at the experiment dosage level, and the calcium carbonate flocculation induced by the adsorption of HPTChC was dominated by a charge patch mechanism [62].



Scheme 2.9: Synthetic pathway of glycidyltrimethylammonium chloride

In 2004, Thatte synthesized derivatives of chitosan consisting of a variety of hydrophobic as well as strongly and weakly acidic organic group. Three synthetic approaches, Bosch reduction, lactone addition and anhydride addition, were studied as means of preparing hydrophobic derivatives. Then Quat-188 was used as a quaternizing agent. Antibacterial studies of these materials were carried out on *Escherichia coli* and *Staphylococcus aureus* by MIC method in order to explore the impact of the substituents on their biological activity. He found that incorporation of aromatic sulfonates as sodium salt (strongly acidic) proved detrimental to the antibacterial activity. This effect was not observed in the presence of weakly acidic groups in the polymer. The presence of hydrophobic groups lowered the MIC values [63].

In this study, chitosan and its derivatives were quaternized by two different methods. The first method was using iodomethane as the quaternizing agent. Single treatment with iodomethane of chitosan and chitosans bearing *N*-methylbenzyl, *N,N*-dimethylaminobenzyl and *N*-pyridylmethyl substituents were subjected. *N*-methylation and *O*-methylation and the influence of sodium hydroxide concentration during methylation on *N*-(4-*N,N*-dimethylaminobenzyl)chitosans and *N*-(4-pyridylmethyl)chitosan were determined. *N*-(4-*N,N*-dimethylaminobenzyl)chitosans was particularly selected as a model for chemoselective methylation. Therefore, *N*-(4-*N,N*-dimethylaminobenzyl)chitosans with different ES were synthesized and then methylated. The second method involved the reaction of chitosan and its derivatives with quaternary ammonium epoxide, generated from 3-chloro-2-hydroxypropyl trimethylammonium chloride (Quat-188) as the quaternizing agent. According to the reviews mentioned earlier, the Quat-188 was more selective in quaternizing at primary amino group than hydroxy group of chitosan. The resulting products tended to be more soluble in water than the ones from methylation method. Antibacterial activity of all quaternized chitosan derivatives were evaluated against *Escherichia coli* (Gram-negative) and *Staphylococcus aureus* (Gram-positive) bacteria by MIC method.



สถาบันวิทยบริการ
จุฬาลงกรณ์มหาวิทยาลัย

CHAPTER III

EXPERIMENTAL SECTION

3.1 General materials and instruments

3.1.1 Materials

Chitosan with molecular weight 227 kDa was purchased from Seafresh Chitosan (lab) Co., Ltd in Thailand. Its DDA was determined to be 94% by $^1\text{H-NMR}$ spectroscopic method. A cellulose membrane dialysis tubing (Aldrich) with molecular weight cut off 12,000-14,000 g/mol was used. Sodium cyanoborohydride (Aldrich), all aldehydes, i.e., n-octyl aldehyde, 4-carboxybenzaldehyde (Aldrich), benzaldehyde and 4-*N,N*-dimethylaminobenzaldehyde (Merck), 4-methylbenzaldehyde, 4-hydroxybenzaldehyde, 4-fluorobenzaldehyde, 4-trifluoromethylbenzaldehyde and 4-nitrobenzaldehyde (Fluka), 4-pyridinecarboxaldehyde and 2-thiophenecarboxaldehyde (Acros) were used. Sodium iodide (Merck), iodomethane (Riedel-deHaen), 1-methyl-2-pyrrolidone, NMP (Fluka), silver nitrate and potassium chromate (Lancaster), nutrient broth (Becton, Dickinson company), potassium phosphate mono and disasic (Merck) were also used. A 65% solution of 3-chloro-2-hydroxypropyl trimethylammonium chloride (Quat-188) was obtained from the Dow Chemical Company. Other organic solvents were distilled before use.

3.1.2 Instruments

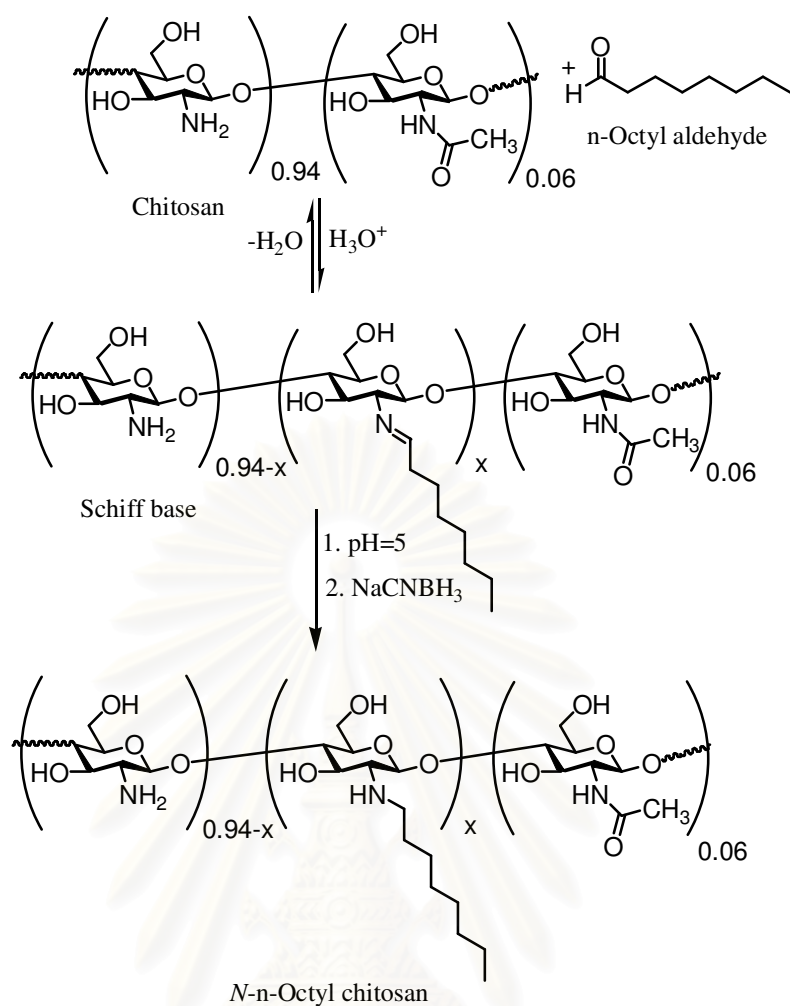
IR spectra were recorded on a Nicolet Impact 410 Fourier Transform Infrared (FT-IR) spectrometer, and all samples were prepared as potassium bromide pellets. The $^1\text{H-NMR}$ and $^{13}\text{C-NMR}$ spectra were measured on a Mercury Varian 400 MHz and Bruker DPX 250 MHz spectrometers, respectively. Differential scanning calorimetry (DSC) 2920 and thermal gravimetric analysis (TGA) 2950 were performed using TA Instruments Inc. Prior to thermal analysis, reabsorption of water was measured by storing the samples in a desiccator at 100% humidity. All samples were prepared by heating at 150°C overnight and then kept in the desiccator for one month. For DSC, the samples were placed into aluminum pans and sealed. An empty pan was used as reference, the sample was heated from 30-300°C at a heating rate of 5°C/min. TGA samples were placed into an open aluminum cup and heated from 30-

600°C at a heating rate of 5°C/min both in the nitrogen and in the air. The molecular weight of chitosan and its derivatives were determined by a gel permeation chromatography/light-scattering (GPC/LS) system consisting of a Agilent 1100 Series generic pump and injector, three Viscotek Columns (ViscoGEL Poly-CAT™) at 20°C, a Wyatt Optilab rEX refractive index detector, and a Wyatt Dawn Heleos light-scattering detector. The mobile phase used was 5% acetic acid (pH 4) at a flow rate of 1 mL/min. The chromatograms were collected by Astra V software and analyzed with the Astra 5.3.1.5 program.

PART A: SYNTHESIS OF *N*-SUBSTITUTED CHITOSAN DERIVATIVES

3.2 Synthesis of *N*-*n*-octyl chitosan

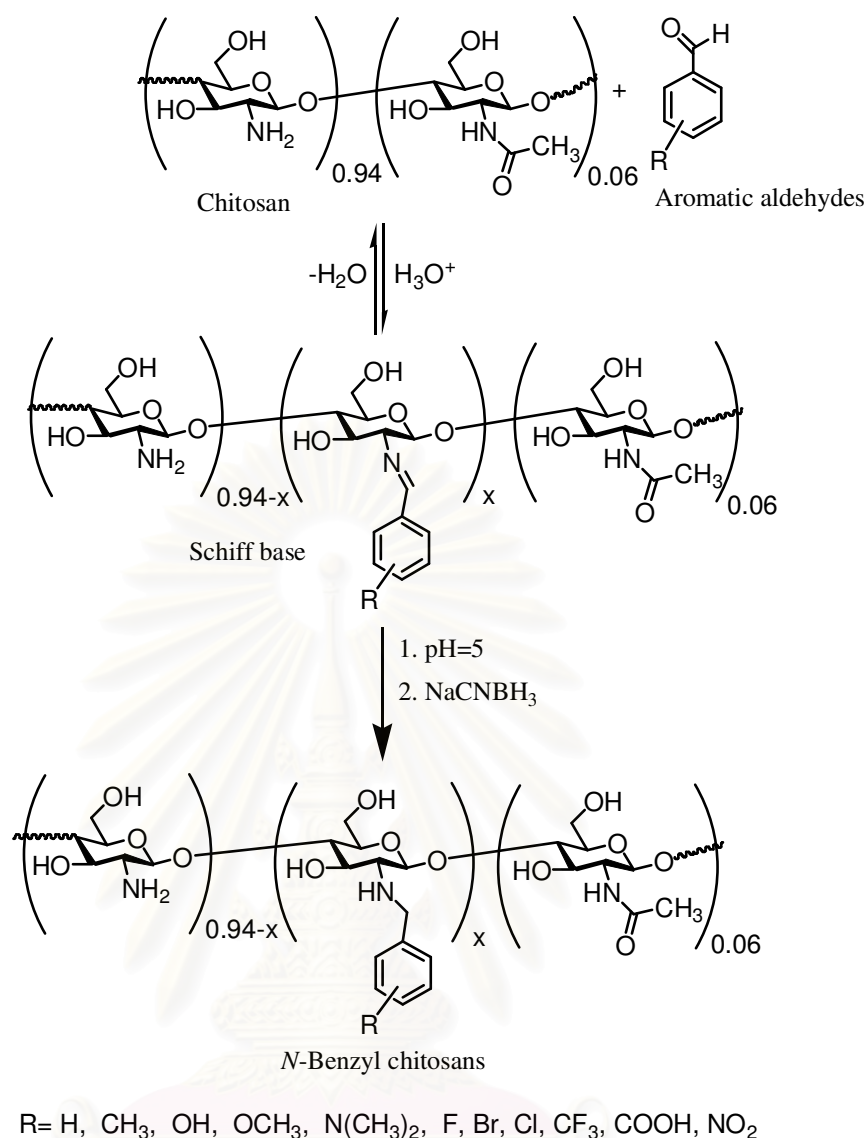
Chitosan (1.00 g, 6.11 meq/GlcN) was dissolved in 0.2M acetic acid (pH 4, 70 mL). The solution was diluted with ethanol (70 mL), and then *n*-octyl aldehyde (0.5 meq/GlcN) was added to the solution. The reaction mixture was stirred at room temperature for 1 hour. At this point the pH of the solution was adjusted to 5 by adding 1M NaOH. Then, NaCNBH₃ (1.54 g, 24.46 meq/GlcN) was added to the resulting solution. The solution was allowed to stir at room temperature for 24 hours, followed by adjusting the pH to 7 with 15% (w/v) NaOH. At higher mole equivalent of aldehyde was used, the solid will be appeared that it was continuously extracted (Soxhlet) with ethanol:ether (1:1 v/v) for 2 days and washed with ethanol several times followed by acetone wash prior to drying at room temperature under nitrogen. On the other hand, at lower mole equivalent of aldehyde was used, the samples was aqueous solution that it was dialyzed in distilled water for 4 days and then freeze-dried (0.93 g, 87.0%, ES 10.3%). The synthetic pathway of *N*-*n*-octyl chitosan is shown in Scheme 3.1. FT-IR (KBr): ν 3430 (O-H and N-H stretching of alcohol and amine), 2979 (C-H stretching of CH₂ of alkane), 1155 (C-O-C asymmetric stretching of GlcN), 1081 and 1033 (C-O stretching of GlcN) cm⁻¹. ¹H-NMR (D₂O/CF₃COOD): δ 3.20-3.92 (m; 7H NHCH₂, H3, H4, H5, H6 and H6'), 3.05 (br. s; 2H H2, H2'), 1.91 (s; 3H NHCOCH₃), 1.56-1.16 (m; 14H (CH₂)₇), 0.75 (s; 3H CH₃) ppm.



Scheme 3.1: Synthetic pathway of *N*-n-octyl chitosan

3.2 Synthesis of *N*-benzyl chitosans

By using the same procedure as described for the synthesis of *N*-n-octyl chitosan, aromatic aldehydes and heterocyclic aromatic aldehydes (0.05-3 meq/GlcN) were used instead of n-octyl aldehyde. In case of 4-nitrobenzaldehyde, the solution was diluted with *N,N*-dimethylformamide (DMF) instead of ethanol (0.82-1.15 g). The synthetic pathway of *N*-benzyl chitosans were shown in Scheme 3.2.



Scheme 3.2: Synthetic pathway of *N*-benzyl chitosans

N-Benzyl chitosan (BzCh). FT-IR (KBr): ν 3430 (O-H and N-H stretching of alcohol and amine), 1514, 1452 (C=C stretching of aromatic), 1155 (C-O-C asymmetric stretching of GlcN), 1081, 1033 (C-O stretching of GlcN), 752, and 704 (C-H bending out of plane of aromatic) cm^{-1} . $^1\text{H-NMR}$ ($\text{D}_2\text{O}/\text{CF}_3\text{COOD}$): δ 7.28 (s; 5H Ph), 4.62-3.48 (br. m; 7H NHCH_2 , H3, H4, H5, H6 and H6'), 2.93 (br. s; 2H H2 and H2'), 1.89 (s; 3H NHCOCH_3) ppm. $^{13}\text{C-NMR}$ ($\text{D}_2\text{O}/\text{CF}_3\text{COOD}$): δ 131.33-130.06 (C-Ph), 97.74 (C1), 77.28 (C40), 75.05 (C5), 69.92 (C3), 61.13 (C6), 52.89 (C2), 51.26 (NHCH_2) ppm.

N-(4-Methylbenzyl)chitosan (Me-BzCh). FT-IR (KBr): ν 3430 (O-H and N-H stretching of alcohol and amine), 1514, 1452, (C=C stretching of aromatic), 1155, (C-O-C asymmetric stretching of GlcN), 1081 1033 (C-O stretching of GlcN), and 807 (C-H bending out of plane of aromatic) cm^{-1} . $^1\text{H-NMR}$ ($\text{D}_2\text{O}/\text{CF}_3\text{COOD}$): δ 7.18 (s; 4H Ph), 4.48-3.51 (br. m; 7H NHCH_2 , H3, H4, H5 H6 and H6'), 2.97 (br. s; 2H H2 and H2'), 2.21 (s; 3H CH_3 Ph), 1.91 (s; 3H NHCOCH_3) ppm. $^{13}\text{C-NMR}$ ($\text{D}_2\text{O}/\text{CF}_3\text{COOD}$): δ 145.03, 140.20, 130.56, 119.03 (C-Ph), 97.96 (C1), 76.64 (C4), 75.06 (C5), 70.50 (C3), 60.19(C2), 56.15(C6), 50.53 (NHCH_2), 35.54 (CH_3 Ph) ppm.

N-(4-Hydroxybenzyl)chitosan (OH-BzCh). FT-IR (KBr): ν 3430 (O-H and N-H stretching of alcohol and amine), 1514, 1452 (C=C stretching of aromatic), 1155 (C-O-C asymmetric stretching of GlcN), 1081, 1033 (C-O stretching of GlcN), and 829 (C-H bending out of plane of aromatic) cm^{-1} . $^1\text{H-NMR}$ ($\text{D}_2\text{O}/\text{CF}_3\text{COOD}$): δ 7.24-6.78 (dd; 4H Ph), 4.34-3.42 (br. m; 7H NHCH_2 , H3, H4, H5, H6 and H6'), 2.96 (br. s; 2H H2 and H2'), 1.93 (s; 3H NHCOCH_3) ppm.

N-(2-Methoxybenzyl)chitosan (2OMe-BzCh). FT-IR (KBr): ν 3430 (O-H and N-H stretching of alcohol and amine), 1494 (C=C stretching of aromatic), 1155 (C-O-C asymmetric stretching of GlcN), 1081, 1033 (C-O stretching of GlcN), and 759 (C-H bending out of plane of aromatic) cm^{-1} . $^1\text{H-NMR}$ ($\text{D}_2\text{O}/\text{CF}_3\text{COOD}$): δ 7.03-7.00 (m; 4H Ph), 4.48-3.75 (br. m; 10H NHCH_2 , H3, H4, H5, H6 and H6', and OCH_3), 2.97 (br. s; 2H H2 and H2'), 1.91 (s; 3H NHCOCH_3) ppm.

N-(4-Methoxybenzyl)chitosan (4OMe-BzCh). $^1\text{H-NMR}$ ($\text{D}_2\text{O}/\text{CF}_3\text{COOD}$): δ 7.31-6.91 (m; 4H Ph), 4.48-3.75 (br. m; 10H NHCH_2 , H3, H4, H5, H6 and H6', and OCH_3), 2.97 (br. s; 2H H2 and H2'), 1.91 (s; 3H NHCOCH_3) ppm.

N-(3,4-Dimethoxybenzyl)chitosan (34OMe-BzCh). FT-IR (KBr): ν 3430 (O-H and N-H stretching of alcohol and amine), 1553, 1515 (C=C stretching of aromatic), 1155 (C-O-C asymmetric stretching of GlcN), 1081, 1033 (C-O stretching of GlcN), 836, and 804 (C-H bending out of plane of aromatic) cm^{-1} . $^1\text{H-NMR}$ ($\text{D}_2\text{O}/\text{CF}_3\text{COOD}$): δ 7.01 (s; 3H Ph), 4.48-3.78 (br. m; 13H NHCH_2 , H3, H4, H5, H6 and H6', and (OCH_3)₂), 3.08 (br. s; 2H H2 and H2'), 1.98 (s; 3H NHCOCH_3) ppm.

N-(4-*N,N*-Dimethylaminobenzyl)chitosan (N(CH₃)₂-BzCh). FT-IR (KBr): ν 3430 (O-H and N-H stretching of alcohol and amine), 1602, 1526 (C=C stretching of aromatic), 1155 (C-O-C asymmetric stretching of GlcN), 1081, 1033 (C-O stretching of GlcN), and 811 (C-H bending out of plane of aromatic) cm⁻¹. ¹H-NMR (D₂O/CF₃COOD): δ 7.52 (s; 4H Ph), 4.93 (s; 1H H1), 4.42-3.53 (br. m; 7H NHCH₂, H3, H4, H5, H6 and H6'), 3.12 (s; 6H N(CH₃)₂ Ph), 2.97 (br. s; 2H H2 and H2'), 1.91 (s; 3H NHCOCH₃) ppm.

N-(4-Fluorobenzyl)chitosan (F-BzCh). FT-IR (KBr): ν 3430 (O-H and N-H stretching of alcohol and amine), 1514 (C=C stretching of aromatic), 1155 (C-O-C asymmetric stretching of GlcN), 1081, 1033 (C-O stretching of GlcN), and 829 (C-H bending out of plane of aromatic) cm⁻¹. ¹H-NMR (D₂O/CF₃COOD): δ 7.32-7.05 (dd; 4H Ph), 4.48-3.51 (br. m; 7H NHCH₂, H3, H4, H5, H6 and H6'), 2.97 (br. s; 2H H2 and H2'), 1.91 (s; 3H NHCOCH₃) ppm.

N-(3-Bromobenzyl)chitosan (3Br-BzCh). FT-IR (KBr): ν 3430 (O-H and N-H stretching of alcohol and amine), 1470 (C=C stretching of aromatic), 1155 (C-O-C asymmetric stretching of GlcN), 1081, 1033 (C-O stretching of GlcN), 836, and 782 (C-H bending out of plane of aromatic) cm⁻¹. ¹H-NMR (D₂O/CF₃COOD): δ 7.53-7.29 (m; 4H Ph), 4.43-3.49 (br. m; 7H NHCH₂, H3, H4, H5, H6 and H6'), 3.10 (br. s; 2H H2 and H2'), 1.93 (s; 3H NHCOCH₃) ppm.

N-(4-Bromobenzyl)chitosan (4Br-BzCh). FT-IR (KBr): ν 3430 (O-H and N-H stretching of alcohol and amine), 1478 (C=C stretching of aromatic), 1155 (C-O-C asymmetric stretching of GlcN), 1081, 1033 (C-O stretching of GlcN), and 801 (C-H bending out of plane of aromatic) cm⁻¹. ¹H-NMR (D₂O/CF₃COOD): δ 7.53-7.25 (dd; 4H Ph), 4.48-3.58 (br. m; 7H NHCH₂, H3, H4, H5, H6 and H6'), 3.03 (br. s; 2H H2 and H2'), 1.93 (s; 3H NHCOCH₃) ppm.

N-(4-Chlorobenzyl)chitosan (Cl-BzCh). FT-IR (KBr): ν 3430 (O-H and N-H stretching of alcohol and amine), 1470 (C=C stretching of aromatic), 1155 (C-O-C asymmetric stretching of GlcN), 1081, 1033 (C-O stretching of GlcN), and 834 (C-H bending out of plane of aromatic) cm⁻¹. ¹H-NMR (D₂O/CF₃COOD): δ 7.36-7.30 (dd;

4H Ph), 4.43-3.58 (br. m; 7H NHCH_2 , H3, H4, H5, H6 and H6'), 3.03 (br. s; 2H H2 and H2'), 1.91 (s; 3H NHCOCH_3) ppm.

N-(4-Trifluoromethylbenzyl)chitosan ($\text{CF}_3\text{-BzCh}$). FT-IR (KBr): ν 3430 (O-H and N-H stretching of alcohol and amine), 1514 (C=C stretching of aromatic), 1155 (C-O-C asymmetric stretching of GlcN), 1081, 1033 (C-O stretching of GlcN), and 836 (C-H bending out of plane of aromatic) cm^{-1} . $^1\text{H-NMR}$ ($\text{D}_2\text{O}/\text{CF}_3\text{COOD}$): δ 7.72-7.54 (dd; 4H Ph), 4.43-3.55 (br. m; 7H NHCH_2 , H3, H4, H5, H6 and H6'), 2.98 (br. s; 2H H2 and H2'), 1.91 (s; 3H NHCOCH_3) ppm.

N-(4-Nitrobenzyl)chitosan ($\text{NO}_2\text{-BzCh}$). FT-IR (KBr): ν 3430 (O-H and N-H stretching of alcohol and amine), 1602, 1519 (C=C stretching of aromatic), 1155 (C-O-C asymmetric stretching of GlcN), 1081, 1033 (C-O stretching of GlcN), and 850 (C-H bending out of plane of aromatic) cm^{-1} . $^1\text{H-NMR}$ ($\text{D}_2\text{O}/\text{CF}_3\text{COOD}$): δ 8.14-7.57 (dd; 4H Ph), 4.42-3.53 (br. m; 7H NHCH_2 , H3, H4, H5 H6, and H6'), 2.99 (br. s; 2H H2 and H2'), 1.91 (s; 3H NHCOCH_3) ppm. $^{13}\text{C-NMR}$ ($\text{D}_2\text{O}/\text{CF}_3\text{COOD}$): δ 148.26, 140.90, 130.99, 124.56 (C-Ph), 97.99 (C1), 76.66 (C4), 75.06 (C5), 70.50 (C3), 60.21(C6), 56.15(C2), 50.53 (NHCH_2) ppm.

N-(4-Carboxybenzyl)chitosan (COOH-BzCh). FT-IR (KBr): ν 3430 (O-H and N-H stretching of alcohol and amine), 1714 (C=O stretching of carboxylic acid), 1556, 1462 (C=C stretching of aromatic), 1155 (C-O-C asymmetric stretching of GlcN), 1081, 1033 (C-O stretching of GlcN), and 818 (C-H bending out of plane of aromatic) cm^{-1} . $^1\text{H-NMR}$ ($\text{D}_2\text{O}/\text{CF}_3\text{COOD}$): δ 7.83-7.40 (dd; 4H Ph), 4.48-3.58 (br. m; 7H NHCH_2 , H3, H4, H5, H6 and H6'), 3.02 (br. s; 2H H2 and H2'), 1.96 (s; 3H NHCOCH_3) ppm.

N-(4-Pyridylmethyl)chitosan (PyMeCh). FT-IR (KBr): ν 3430 (O-H and N-H stretching of alcohol and amine), 1605, 1470 (C=C stretching of aromatic), 1155 (C-O-C asymmetric stretching of GlcN), 1081, 1033 (C-O stretching of GlcN), and 818 (C-H bending out of plane of aromatic) cm^{-1} . $^1\text{H-NMR}$ ($\text{D}_2\text{O}/\text{CF}_3\text{COOD}$): δ 8.58-7.96 (dd; 4H Ph), 6.1 (s; 1H $\text{CH}=\text{NH}$), 3.51-4.48 (br. m; 7H NHCH_2 , H3, H4, H5, H6 and H6'), 2.97 (br. s; 2H H2 and H2'), 1.91 (s; 3H NHCOCH_3) ppm.

N-(2-Thiophenylmethyl)chitosan (2ThMeCh). FT-IR (KBr): ν 3430 (O-H and N-H stretching of alcohol and amine), 1453 (C=C stretching of aromatic), 1155 (C-O-C asymmetric stretching of GlcN), 1081, 1033 (C-O stretching of GlcN), and 834 (C-H bending out of plane of aromatic) cm^{-1} . $^1\text{H-NMR}$ ($\text{D}_2\text{O}/\text{CF}_3\text{COOD}$): δ 7.22-6.95 (m; 3H Ph), 3.51-4.48 (br. m; 7H NHCH_2 , H3, H4, H5, H6 and H6'), 2.97 (br. s; 2H H2 and H2'), 1.91 (s; 3H NHCOCH_3) ppm.



สถาบันวิทยบริการ
จุฬาลงกรณ์มหาวิทยาลัย

PART B: QUATERNIZATION OF CHITOSAN AND *N*-SUBSTITUTED CHITOSANS

3.3 Quaternization of chitosan and *N*-substituted chitosans using iodomethane

3.3.1 Regenerated chitosan and *N*-substituted chitosans

Chitosan and *N*-substituted chitosans (0.50 g) were regenerated by dissolving in 1 % (w/v) aqueous acetic acid (100 mL). This solution was stirred for one hour and was dropped slowly into 2% (w/v) aqueous sodium bicarbonate, (H₂O:MeOH; 40:60 v/v), (100 mL). Methanol was added to help precipitate the chitosan out of the solution. The pH of the solution was adjusted to 9 by the addition 15% (w/v) aqueous sodium hydroxide [62]. The regenerated chitosan and *N*-substituted chitosans were then recovered by filtration and kept while still moist before the next synthesis step.

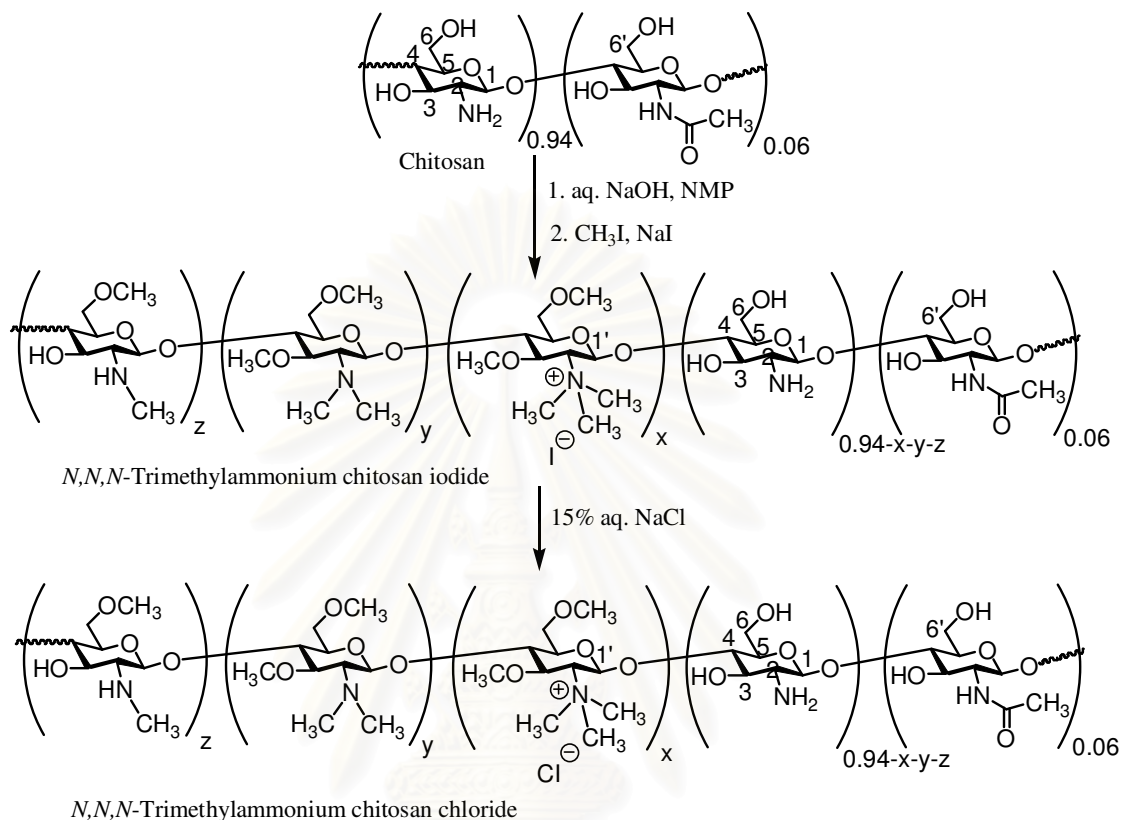
3.3.2 Isolation and purification

After quaternization, quaternized chitosan and its derivatives were precipitated in acetone (300 mL). The precipitate was dissolved in 15% (w/v) aqueous sodium chloride solution in order to replace the iodide ion by chloride ion. The suspension was dialyzed with deionized water for 3 days to remove inorganic materials. The dialysed solution was then concentrated under vacuum on a rotary evaporator. Product precipitated from the concentrated solution was added into acetone (100 mL). The solid thus obtained was then collected and dried overnight at room temperature under a stream of nitrogen.

3.3.3 *N,N,N*-Trimethylammonium chitosan chloride

Regenerated chitosan (about 0.50 g) while still moist was dispersed in *N*-methyl-2-pyrrolidone (NMP) (25 mL) at room temperature for 12 hours. Then sodium iodide (1.5 g, 0.01 mol) and 15% (w/v) aqueous sodium hydroxide (3.0 mL) were added and stirred at 50°C for 15 minutes. Subsequently, iodomethane (1 mL, 0.016 mol) was added every four hour and stirred at 50°C for 12 hours. The reaction mixture appeared yellow and clear [49-52]. The isolation and purification of product was

performed as described above **3.3.2** (0.41 g, 82%, DQ_{Ch} 31%). The synthetic pathway of *N,N,N*-trimethylammonium chitosan chloride (TMChC) is shown in Scheme 3.3. TMChC, FT-IR (KBr): ν 3444 (O-H and N-H stretching of



Scheme 3.3: Synthetic pathway of *N,N,N*-trimethylammonium chitosan chloride

of alcohol and amine), 1475 (C-H symmetric bending of (CH₃)₃N⁺R), 1107, 1071, and 1057 (C-O stretching of GlcN) cm⁻¹. ¹H-NMR (D₂O): δ 5.42 (br. s; 1H H1, H1'), 4.40-3.01 (br. m; 23H -NH-CH₂-, H2, H3, H4, H5, H6 and H6', s; OCH₃, br. s; N⁺(CH₃)₃), 2.71 (br. m; 6H N(CH₃)₂), 2.31 (s; 3H NHCH₃), 1.97 (s; 3H NHCOCH₃) ppm. ¹³C-NMR (D₂O): δ 96.55 (C1), 77.62 (C4), 74.74 (C5), 68.85 (C5), 60.0-55.5 (C2 and C6), 54.43 (N⁺(CH₃)₃), 42.71 (N(CH₃)₂) ppm.

3.3.4 High degree of quaternization of *N,N,N*-trimethylammonium chitosan chloride

N,N,N-trimethylammonium chitosan chloride (about 0.50 g) was dispersed in NMP (25 mL) at room temperature for 12 hours. Then sodium iodide (1.5 g, 0.01 mol) and 15% (w/v) aqueous sodium hydroxide (3.0 mL) were added and stirred at 50°C for 15 minutes. Subsequently, iodomethane (1 mL, 0.016 mol) was added every four hours and stirred at 50°C for 12 hours. An additional iodomethane (1 mL, 0.016 mol) and small amount of sodium hydroxide pellet were added and the stirring was continued for 4 hour [49-52]. The isolation and purification of product was performed as described above **3.3.2** (0.14 g, 28%, DQ_{Ch} 89%). HDQ-TMChC, FT-IR (KBr): ν 3438 (O-H and N-H stretching of alcohol and amine), 1475 (C-H symmetric bending of (CH₃)₃N⁺R), 1107, 1071, and 1057 (C-O stretching of GlcN) cm⁻¹. ¹H-NMR (D₂O): δ 5.59 (br. s; 2H H1, H1'), 4.64-3.13 (br. m; 23H -NH-CH₂-, H2, H3, H4, H5, H6 and H6', s; OCH₃, br. s; N⁺(CH₃)₃), 2.71 (br. m; 6H N(CH₃)₂), 2.31 (s; 3H NHCH₃), 1.97 (s; 3H NHC(O)CH₃) ppm.

3.3.5 Quaternized *N*-(4-methylbenzyl)chitosan, quaternized *N*-(4-*N,N*-dimethylaminobenzyl)chitosan and quaternized *N*-(4-pyridylmethyl) chitosan

Each of regenerated *N*-(4-methylbenzyl)chitosan, *N*-(4-*N,N*-dimethylaminobenzyl) chitosan and *N*-(4-pyridylmethyl)chitosan (about 0.50 g) while still moist was dispersed in NMP (25 mL) at room temperature for 12 hours. Then sodium iodide (1.5 g, 0.01 mol) and 5% or 15% (w/v) aqueous sodium hydroxide (3.0 mL) were added and stirred at 50°C for 15 minutes. Subsequently, iodomethane (1 mL, 0.016 mol) was added every four hours and stirred at 50°C for 12 hours. The reaction mixture appeared yellow and clear [40-52]. The isolation and purification of product was performed as described above **3.3.2** (0.34-0.43 g).

Quaternized *N*-(4-methylbenzyl)chitosan (QMe-BzCh). $^1\text{H-NMR}$ (D_2O): δ 7.36 (br. s; 4H Ph), 5.40, 4.96 (s; 2H H1, H1'), 4.42-3.13 (br. m; 23H -NH-CH₂-, H2, H3, H4, H5, H6 and H6', s; OCH₃, br. s; N⁺(CH₃)₃), 2.71 (br. m; 6H N(CH₃)₂), 2.31 (s; 3H CH₃ Ph), 1.97 (s; 3H NHCOCH₃) ppm.

Quaternized *N*-(4-*N,N*-dimethylaminobenzyl)chitosan (QN(CH₃)₂-BzCh). FT-IR (KBr): ν 3430 (O-H and N-H stretching of alcohol and amine), 1559 (C=C stretching of aromatic), 1475 (C-H symmetric bending of (CH₃)₃N⁺R), 1155 (C-O-C asymmetric stretching of GlcN), 1081, 1033 (C-O stretching of GlcN), and 811 (C-H bending out of plane of aromatic) cm⁻¹. $^1\text{H-NMR}$ (D_2O): δ 7.75-7.50 (dd; 4H Ph), 5.40, 4.96 (s; 2H H1, H1'), 4.42-3.13 (br. m; 32H -NH-CH₂-, H2, H3, H4, H5, H6 and H6', br. s; N⁺(CH₃)₃ Ph, s; OCH₃, br. s; N⁺(CH₃)₃), 2.71 (br. m; 6H N(CH₃)₂), 2.31 (s; 3H NHCH₃), 1.97 (s; 3H NHCOCH₃) ppm. $^{13}\text{C-NMR}$ (D_2O): δ 145.52, 141.53, 130.98, 119.56 (C-Ph), 96.55 (C1), 77.13-58.67 (C2, C3, C4, C5, and C6), 56.98 (N⁺(CH₃)₃ Ph), 53.88 (N⁺(CH₃)₃), 41.77 (N(CH₃)₂), 36.30 (NCH₃) ppm.

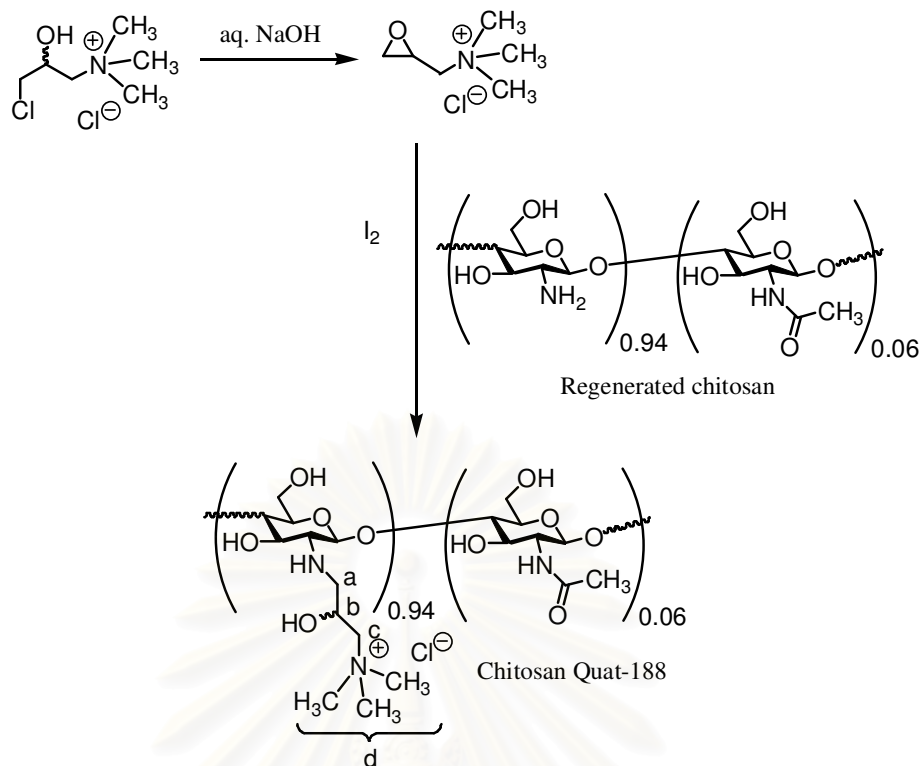
Quaternized *N*-(4-pyridylmethyl)chitosan (QPyMeCh). FT-IR (KBr): ν 3453 (O-H and N-H stretching of alcohol and amine), 1475 (C-H symmetric bending of (CH₃)₃N⁺R), 1155 (C-O-C asymmetric stretching of GlcN), 1081, 1033 (C-O stretching of GlcN) cm⁻¹. $^1\text{H-NMR}$ (D_2O): δ 8.60-7.95 (dd; 4H Ph), 5.36, 4.96 (s; 2H H1, H1'), 4.42-3.15 (br. m; 35H -NH-CH₂-, H2, H3, H4, H5, H6 and H6', s; OCH₃, s; N⁺CH₃ Py, s; N⁺(CH₃)₃), 2.83 (s; 6H N(CH₃)₂), 2.37 (s; 3H NHCH₃), 1.98 (s; 3H NHCOCH₃) ppm. $^{13}\text{C-NMR}$ (D_2O): δ 174.99, 160.69, 144.82, 127.45 (C-Ph), 96.55 (C1), 78.8-60.9 (C2, C3, C4, C5, and C6), 68.31 (N⁺CH₃ Py), 54.43 (N⁺(CH₃)₃), 42.71 (N(CH₃)₂) ppm.

3.4 Quaternization of *N*-substituted chitosans using 3-chloro-2-hydroxypropyl trimethylammonium chloride

3.4.1 Chitosan Quat-188

A 65% (w/w) solution of 3-chloro-2-hydroxypropyl trimethylammonium chloride (Quat-188) (20 mL) was added to the reaction flask, and the pH of the solution was raised to 8 by using 15% (w/v) sodium hydroxide. Then iodide (0.25 g) was added along with regenerated chitosan (about 0.50 g) while still moist. Upon stirring, the solution went from light tan-brown to yellow. The solution was stirred at room for 48 hours, and then water (50 mL) was added and temperature raised to 50°C for stirring another 24 hours. The solution was dialyzed with deionized water for 24 hours, and the deionized water was replaced every 8 hours [62]. The isolation and purification of product was performed as described above **3.3.2** (0.51 g, 57.9%, DQ_{Ch} 91.2%). The synthetic pathway of chitosan Quat-188 is shown in Scheme 3.4. FT-IR (KBr): ν 3430 (O-H and N-H stretching), 1644 and 1369 (C=O and C-O stretching of amide), 1594 (N-H deformation of amino), 1480 cm^{-1} (C-H symmetric bending of $(CH_3)_3N^+R$), 1155 (C-O-C asymmetric stretching of GlcN), 1081 and 1033 cm^{-1} (C-O stretching of GlcN) cm^{-1} . 1H -NMR (D_2O): δ 4.43-3.30 (m; 15H H3, H4, H5, H6 and H6', s; 1H $\underline{C}HOH$ b, s; 2H $\underline{C}H_2N^+(CH_3)_3$ c, s; 9H $N^+(CH_3)_3$ d), 2.87 (br. s; 1H H2), 2.68 (br. s; 2H $\underline{C}H_2NH$, a), 1.94 (s; 3H $NHCO\underline{C}H_3$) ppm. ^{13}C -NMR (D_2O): δ 102.15 (C1), 77.80 (C4), 74.74 (C5), 72.88 (C3), 68.96 ($\underline{C}H_2N^+(CH_3)_3$, c), 65.07, 64.57 ($\underline{C}HOH$, b), 63.80, 62.34 (C2), 60.25 (C6), 54.06 ($N^+(CH_3)_3$, d), 51.66 ($\underline{C}H_2NH$, a) ppm.

สถาบันวิทยบริการ
จุฬาลงกรณ์มหาวิทยาลัย



Scheme 3.4: Synthetic pathway of chitosan Quat-188

3.4.2 *N*-substituted chitosans Quat-188

By using the same procedure as described for the synthesis of chitosan Quat-188, *N*-substituted chitosans were used instead of chitosan (0.5-0.8 g) [62].

N-*n*-Octyl chitosan Quat-188 (OctChQ). FT-IR (KBr): ν 3430 (O-H and N-H stretching), 2979 (C-H stretching of CH₂ of alkane), 1480 (C-H symmetric bending of (CH₃)₃N⁺R), 1155 (C-O-C asymmetric stretching of GlcN), 1081 and 1033 (C-O stretching of GlcN) cm⁻¹. ¹H-NMR (D₂O): δ 4.43-3.30 (m; 15H H₃, H₄, H₅, H₆ and H_{6'}, s; 1H $\underline{\text{C}}\text{HOH}$ b, s; 2H $\underline{\text{C}}\text{H}_2\text{N}^+(\text{CH}_3)_3$ c, s; 9H N⁺($\underline{\text{C}}\text{H}_3$)₃ d), 2.87 (br. s; 1H H₂), 2.68 (br. s; 2H $\underline{\text{C}}\text{H}_2\text{NH}$, a), 1.94 (s; 3H $\text{NHCO}\underline{\text{C}}\text{H}_3$), 1.56-1.16 (m; 14H ($\underline{\text{C}}\text{H}_2$)₇), 0.75 (s; 3H $\underline{\text{C}}\text{H}_3$) ppm.

N-Benzyl chitosan Quat-188 (BzChQ). FT-IR (KBr): ν 3430 (O-H and N-H stretching), 1514 (C=C stretching of aromatic ring), 1480 (C-H symmetric bending of (CH₃)₃N⁺R), 1155 (C-O-C asymmetric stretching of GlcN), 1081 and 1033 (C-O stretching of GlcN), 752, 704 (C-H deformation of the aromatic ring) cm⁻¹. ¹H-NMR (D₂O): δ 7.34 (s; 5H Ph), 4.43-3.30 (m; 15H H₃, H₄, H₅, H₆ and H_{6'}, s; 1H $\underline{\text{C}}\text{HOH}$ b,

s; 2H $\underline{\text{CH}}_2\text{N}^+(\text{CH}_3)_3$ c, s; 9H $\text{N}^+(\underline{\text{CH}}_3)_3$ d), 2.87 (br. s; 1H H2), 2.68 (br. s; 2H $\underline{\text{CH}}_2\text{NH}$, a), 1.94 (s; 3H $\text{NHCO}\underline{\text{CH}}_3$) ppm. ^{13}C -NMR (D_2O): δ 129.4- 128.7 (C-Ph), 102.12, 100.00 (C1), 77.78 (C4), 74.74 (C5), 72.91 (C3), 68.60 ($\underline{\text{CH}}_2\text{N}^+(\text{CH}_3)_3$, c), 65.03, 64.56 ($\underline{\text{C}}\text{HOH}$, b), 63.79, 62.65 (C2), 60.33 (C6), 54.07 ($\text{N}^+(\underline{\text{CH}}_3)_3$, d), 51.65 ($\underline{\text{CH}}_2\text{NH}$, a) ppm.

N-(4-Methylbenzyl)chitosan Quat-188 (Me-BzChQ). FT-IR (KBr): ν 3430 (O-H and N-H stretching), 1514 (C=C stretching of aromatic ring), 1480 (C-H symmetric bending of $(\text{CH}_3)_3\text{N}^+\text{R}$), 1155 (C-O-C asymmetric stretching of GlcN), 1081 and 1033 (C-O stretching of GlcN), 807 (C-H deformation of the aromatic ring) cm^{-1} . ^1H -NMR (D_2O): δ 7.20-7.17 (m; 4H Ph), 4.43-3.30 (m; 15H H3, H4, H5, H6 and H6', s; 1H $\underline{\text{C}}\text{HOH}$ b, s; 2H $\underline{\text{CH}}_2\text{N}^+(\text{CH}_3)_3$ c, s; 9H $\text{N}^+(\underline{\text{CH}}_3)_3$ d), 2.87 (br. s; 1H H2), 2.68 (br. s; 2H $\underline{\text{CH}}_2\text{NH}$, a), 2.21 (s; 3H $\underline{\text{C}}\text{H}_3$ -Ph), 1.94 (s; 3H $\text{NHCO}\underline{\text{C}}\text{H}_3$) ppm.

N-(4-Hydroxybenzyl)chitosan Quat-188 (OH-BzChQ). FT-IR (KBr): ν 3430 (O-H and N-H stretching), 1514, 1452 (C=C stretching of aromatic ring), 1480 (C-H symmetric bending of $(\text{CH}_3)_3\text{N}^+\text{R}$), 1155 (C-O-C asymmetric stretching of GlcN), 1081 and 1033 (C-O stretching of GlcN), 804 (C-H deformation of the aromatic ring) cm^{-1} . ^1H -NMR (D_2O): δ 7.20-7.17 (dd; 4H Ph), 4.43-3.30 (m; 15H H3, H4, H5, H6 and H6', s; 1H $\underline{\text{C}}\text{HOH}$ b, s; 2H $\underline{\text{CH}}_2\text{N}^+(\text{CH}_3)_3$ c, s; 9H $\text{N}^+(\underline{\text{CH}}_3)_3$ d), 2.87 (br. s; 1H H2), 2.68 (br. s; 2H $\underline{\text{CH}}_2\text{NH}$, a), 1.94 (s; 3H $\text{NHCO}\underline{\text{C}}\text{H}_3$) ppm.

N-(2-Methoxybenzyl)chitosan Quat-188 (2OMe-BzChQ). FT-IR (KBr): ν 3430 (O-H and N-H stretching), 1514 (C=C stretching of aromatic ring), 1480 (C-H symmetric bending of $(\text{CH}_3)_3\text{N}^+\text{R}$), 1155 (C-O-C asymmetric stretching of GlcN), 1081 and 1033 (C-O stretching of GlcN), 759 (C-H deformation of the aromatic ring) cm^{-1} . ^1H -NMR (D_2O): δ 7.28-6.93 (m; 4H Ph), 4.43-3.30 (m; 18H H3, H4, H5, H6 and H6', s; 1H $\underline{\text{C}}\text{HOH}$ b, br, s; 3H $\text{O}\underline{\text{C}}\text{H}_3$, s; 2H $\underline{\text{CH}}_2\text{N}^+(\text{CH}_3)_3$ c s; 9H $\text{N}^+(\underline{\text{CH}}_3)_3$ d), 2.89 (br, s; 1H H2), 2.68 (br. s; 2H $\underline{\text{CH}}_2\text{NH}$, a), 1.96 (s; 3H $\text{NHCO}\underline{\text{C}}\text{H}_3$) ppm.

N-(4-Methoxybenzyl) chitosan Quat-188 (4OMe-BzChQ). $^1\text{H-NMR}$ ($\text{D}_2\text{O}/\text{CF}_3\text{COOD}$): δ 7.31-6.91 (dd; 4H Ph), 4.43-3.30 (m; 18H H3, H4, H5, H6 and H6', s; 1H CHOH b, br, s; 3H OCH_3 , s; 2H $\text{CH}_2\text{N}^+(\text{CH}_3)_3$ c s; 9H $\text{N}^+(\text{CH}_3)_3$ d), 2.89 (br, s; 1H H2), 2.68 (br. s; 2H CH_2NH , a), 1.96 (s; 3H NHCOCH_3) ppm.

N-(3,4-Methoxybenzyl)chitosan Quat-188 (34OMe-BzChQ). FT-IR (KBr): ν 3430 (O-H and N-H stretching), 1553, 1515 (C=C stretching of aromatic ring), 1480 (C-H symmetric bending of $(\text{CH}_3)_3\text{N}^+\text{R}$), 1155 (C-O-C asymmetric stretching of GlcN), 1081 and 1033 (C-O stretching of GlcN), 804 (C-H deformation of the aromatic ring) cm^{-1} . $^1\text{H-NMR}$ (D_2O): δ 7.06-6.92 (br. m; 3H Ph), 4.43-3.30 (m; 21H H3, H4, H5, H6 and H6', s; 1H CHOH b, br, s; 6H OCH_3 , s; 2H $\text{CH}_2\text{N}^+(\text{CH}_3)_3$ c s; 9H $\text{N}^+(\text{CH}_3)_3$ d), 2.89 (br, s; 1H H2), 2.68 (br. s; 2H CH_2NH , a), 1.96 (s; 3H NHCOCH_3) ppm.

N-(4-*N,N*-Dimethylaminobenzyl)chitosan Quat-188 ($\text{N}(\text{CH}_3)_2\text{-BzChQ}$). FT-IR (KBr): ν 3430 (O-H and N-H stretching of alcohol and amine), 1602, 1526 (C=C stretching of aromatic), 1480 (C-H symmetric bending of $(\text{CH}_3)_3\text{N}^+\text{R}$), 1155 (C-O-C asymmetric stretching of GlcN), 1081, 1033 (C-O stretching of GlcN), and 811 (C-H bending out of plane of aromatic) cm^{-1} . $^1\text{H-NMR}$ ($\text{D}_2\text{O}/\text{CF}_3\text{COOD}$): δ 7.52 (s; 4H Ph), 4.93 (s; 1H H1), 4.43-3.30 (m; 15H H3, H4, H5, H6 and H6', s; 1H CHOH b, s; 2H $\text{CH}_2\text{N}^+(\text{CH}_3)_3$ c, s; 9H $\text{N}^+(\text{CH}_3)_3$ d), 3.12 (br. s; 6H $\text{N}(\text{CH}_3)_2\text{Ph}$), 2.87 (s; 1H H2), 2.68 (br. s; 2H CH_2NH , a), 1.93 (s; 3H NHCOCH_3) ppm.

N-(4-Fluorobenzyl)chitosan Quat-188 (F-BzChQ). FT-IR (KBr): ν 3430 (O-H and N-H stretching), 1514 (C=C stretching of aromatic ring), 1480 (C-H symmetric bending of $(\text{CH}_3)_3\text{N}^+\text{R}$), 1155 (C-O-C asymmetric stretching of GlcN), 1081 and 1033 (C-O stretching of GlcN), 829 (C-H deformation of the aromatic ring) cm^{-1} . $^1\text{H-NMR}$ (D_2O): δ 7.33-7.05 (dd; 4H Ph), 4.43-3.30 (m; 15H H3, H4, H5, H6 and H6', s; 1H CHOH b, s; 2H $\text{CH}_2\text{N}^+(\text{CH}_3)_3$ c, s; 9H $\text{N}^+(\text{CH}_3)_3$ d), 2.87 (br. s; 1H H2), 2.68 (br. s; 2H CH_2NH , a), 1.94 (s; 3H NHCOCH_3) ppm.

N-(3-Bromobenzyl)chitosan Quat-188 (3Br-BzChQ). FT-IR (KBr): ν 3430 (O-H and N-H stretching), 1470 (C=C stretching of aromatic ring), 1480 (C-H symmetric bending of $(\text{CH}_3)_3\text{N}^+\text{R}$), 1155 (C-O-C asymmetric stretching of GlcN), 1081 and 1033

(C-O stretching of GlcN), 836, and 782 (C-H deformation of the aromatic ring) cm^{-1} . $^1\text{H-NMR}$ (D_2O): δ 7.56-7.34 (m; 4H Ph), 4.43-3.30 (m; 15H H3, H4, H5, H6 and H6', s; 1H CHOH b, s; 2H $\text{CH}_2\text{N}^+(\text{CH}_3)_3$ c, s; 9H $\text{N}^+(\text{CH}_3)_3$ d), 2.87 (br. s; 1H H2), 2.68 (br. s; 2H CH_2NH , a), 1.94 (s; 3H NHCOCH_3) ppm.

N-(4-Bromobenzyl)chitosan Quat-188 (4Br-BzChQ). FT-IR (KBr): ν 3430 (O-H and N-H stretching), 1478 (C=C stretching of aromatic ring), 1480 (C-H symmetric bending of $(\text{CH}_3)_3\text{N}^+\text{R}$), 1155 (C-O-C asymmetric stretching of GlcN), 1081 and 1033 (C-O stretching of GlcN), 801 (C-H deformation of the aromatic ring) cm^{-1} . $^1\text{H-NMR}$ (D_2O): δ 7.75-7.52 (dd; 4H Ph), 4.43-3.30 (m; 15H H3, H4, H5, H6 and H6', s; 1H CHOH b, s; 2H $\text{CH}_2\text{N}^+(\text{CH}_3)_3$ c, s; 9H $\text{N}^+(\text{CH}_3)_3$ d), 2.87 (br. s; 1H H2), 2.68 (br. s; 2H CH_2NH , a), 1.94 (s; 3H NHCOCH_3) ppm.

N-(4-Chlorobenzyl)chitosan Quat-188 (Cl-BzChQ). FT-IR (KBr): ν 3430 (O-H and N-H stretching), 1478 (C=C stretching of aromatic ring), 1480 (C-H symmetric bending of $(\text{CH}_3)_3\text{N}^+\text{R}$), 1155 (C-O-C asymmetric stretching of GlcN), 1081 and 1033 (C-O stretching of GlcN), 834 (C-H deformation of the aromatic ring) cm^{-1} . $^1\text{H-NMR}$ (D_2O): δ 7.30 (br, s; 4H Ph), 4.43-3.30 (m; 15H H3, H4, H5, H6 and H6', s; 1H CHOH b, s; 2H $\text{CH}_2\text{N}^+(\text{CH}_3)_3$ c, s; 9H $\text{N}^+(\text{CH}_3)_3$ d), 2.87 (br. s; 1H H2), 2.68 (br. s; 2H CH_2NH , a), 1.94 (s; 3H NHCOCH_3) ppm.

N-(4-Trifluorobenzyl)chitosan Quat-188 (CF_3 -BzChQ). FT-IR (KBr): ν 3430 (O-H and N-H stretching), 1514 (C=C stretching of aromatic ring), 1480 (C-H symmetric bending of $(\text{CH}_3)_3\text{N}^+\text{R}$), 1155 (C-O-C asymmetric stretching of GlcN), 1081 and 1033 (C-O stretching of GlcN), 836 (C-H deformation of the aromatic ring) cm^{-1} . $^1\text{H-NMR}$ (D_2O): δ 7.62-7.44 (dd; 4H Ph), 4.43-3.30 (m; 15H H3, H4, H5, H6 and H6', s; 1H CHOH b, s; 2H $\text{CH}_2\text{N}^+(\text{CH}_3)_3$ c, s; 9H $\text{N}^+(\text{CH}_3)_3$ d), 2.87 (br. s; 1H H2), 2.68 (br. s; 2H CH_2NH , a), 1.94 (s; 3H NHCOCH_3) ppm.

N-(4-Nitrobenzyl)chitosan Quat-188 (NO_2 -BzChQ). FT-IR (KBr): ν 3430 (O-H and N-H stretching), 1602, 1519 (C=C stretching of aromatic ring), 1480 (C-H symmetric bending of $(\text{CH}_3)_3\text{N}^+\text{R}$), 1155 (C-O-C asymmetric stretching of GlcN), 1081 and 1033

(C-O stretching of GlcN), 850 (C-H deformation of the aromatic ring) cm^{-1} . $^1\text{H-NMR}$ (D_2O): δ 8.15-7.57 (dd; 4H Ph), 4.43-3.30 (m; 15H H3, H4, H5, H6 and H6', s; 1H CHOH b, s; 2H $\text{CH}_2\text{N}^+(\text{CH}_3)_3$ c, s; 9H $\text{N}^+(\text{CH}_3)_3$ d), 2.87 (br. s; 1H H2), 2.68 (br. s; 2H CH_2NH , a), 1.94 (s; 3H NHCOCH_3) ppm.

N-(4-Carboxybenzyl)chitosan Quat-188 (COOH-BzChQ). FT-IR (KBr): ν 3430 (O-H and N-H stretching), 1714 (C=O stretching of carboxylic acid), 1556, 1462 (C=C stretching of aromatic ring), 1480 (C-H symmetric bending of $(\text{CH}_3)_3\text{N}^+\text{R}$), 1155 (C-O-C asymmetric stretching of GlcN), 1081 and 1033 (C-O stretching of GlcN), 818 (C-H deformation of the aromatic ring) cm^{-1} . $^1\text{H-NMR}$ (D_2O): δ 7.75-7.39 (dd; 4H Ph), 4.43-3.30 (m; 15H H3, H4, H5, H6 and H6', s; 1H CHOH b, s; 2H $\text{CH}_2\text{N}^+(\text{CH}_3)_3$ c, s; 9H $\text{N}^+(\text{CH}_3)_3$ d), 2.87 (br. s; 1H H2), 2.68 (br. s; 2H CH_2NH , a), 1.94 (s; 3H NHCOCH_3) ppm.

N-(4-Pyridylmethyl)chitosan Quat-188 (PyMeChQ). FT-IR (KBr): ν 3430 (O-H and N-H stretching), 1605, 1470 (C=C stretching of aromatic ring), 1480 (C-H symmetric bending of $(\text{CH}_3)_3\text{N}^+\text{R}$), 1155 (C-O-C asymmetric stretching of GlcN), 1081 and 1033 (C-O stretching of GlcN), 818 (C-H deformation of the aromatic ring) cm^{-1} . $^1\text{H-NMR}$ (D_2O): δ 7.75-7.39 (dd; 4H Ph), 4.43-3.30 (m; 15H H3, H4, H5, H6 and H6', s; 1H CHOH b, s; 2H $\text{CH}_2\text{N}^+(\text{CH}_3)_3$ c, s; 9H $\text{N}^+(\text{CH}_3)_3$ d), 2.87 (br. s; 1H H2), 2.68 (br. s; 2H CH_2NH , a), 1.94 (s; 3H NHCOCH_3) ppm.

N-(2-Thiophenylmethyl)chitosan Quat-188 (2ThMeChQ). FT-IR (KBr): ν 3430, (O-H and N-H stretching), 1453, (C=C stretching of aromatic ring), 1480 (C-H symmetric bending of $(\text{CH}_3)_3\text{N}^+\text{R}$), 1155, (C-O-C asymmetric stretching of GlcN), 1081, 1033, (C-O stretching of GlcN), 834 (C-H deformation of the aromatic ring) cm^{-1} . $^1\text{H-NMR}$ (D_2O): δ 7.35-6.95 (m; 3H Ph), 4.43-3.30 (m; 15H H3, H4, H5, H6 and H6', s; 1H CHOH b, s; 2H $\text{CH}_2\text{N}^+(\text{CH}_3)_3$ c, s; 9H $\text{N}^+(\text{CH}_3)_3$ d), 2.87 (br. s; 1H H2), 2.68 (br. s; 2H CH_2NH , a), 1.94 (s; 3H NHCOCH_3) ppm. $^{13}\text{C-NMR}$ (D_2O): δ 127.1- 126.4 (C-Ph), 102.12 (C1), 77.78 (C4), 74.74 (C5), 73.07 (C3), 68.95 ($\text{CH}_2\text{N}^+(\text{CH}_3)_3$, c), 66.22, 64.76 (CHOH , b), 63.45, 62.39 (C2), 60.30 (C6), 54.06 ($\text{N}^+(\text{CH}_3)_3$, d), 51.73 (CH_2NH , a) ppm.

3.4.3 Characterization of chitosan and its derivatives

3.4.3.1 FT-IR spectroscopy

IR spectra of chitosan and its derivatives were recorded on a Nicolet Impact 410 Fourier Transform Infrared (FT-IR) spectrometer, and all samples were prepared as potassium bromide pellets.

3.4.3.2 ¹H-NMR spectroscopy

Each of Chitosan and its derivatives (10 mg) was dissolved in 1% (v/v) D₂O/CF₃COOD or D₂O and spectra were recorded at 300 °K, using pulse accumulating of 64 scans and the LB parameter of 0.30 Hz.

3.4.3.3 Determination of molecular weight

The molecular weight of chitosan and its derivatives were determined by a gel permeation chromatography (GPC). Chitosan and its derivatives were dissolved in 5% (w/v) acetic acid and they were injected in GPC column, three Viscotek Columns (ViscoGEL Poly-CATTM), at a flow rate of 1 mL/min 20°C. The GPC chromatograms were collected by Astra V software and analyzed with the Astra 5.3.1.5 program. The weight-average molecular weight (M_w) and the number-average molecular weight (M_n) were determined by comparing the signals from the refractive index detector to that of the light-scattering detector 90° signal time. The increment of refractive index (dn/dc) was determined using a concentration 5 and 25 mg/mL for chitosan, *N*-benzyl chitosans and quaternized chitosans, respectively.

3.4.3.4 Determination of degree of quaternization

The degree of quaternization of chitosan derivatives Quat-188 was determined by titrating with silver nitrate. Silver nitrate (0.722 g, 4.250 mmol) was dissolved in deionized water (250 mL) to make a 0.017M solution. The indicator solution was made by dissolving potassium chromate (0.250 g, 1.287 mmol) in deionized water (20 mL). Chitosan derivatives Quat-188 (0.035 g) was dissolved in deionized water (25

mL) and then 0.064mM potassium chromate was added (0.5 mL). After stirring for 1 mintue, the solution was titrated with 0.017M silver nitrate, until the end-point of the reaction was reached, as evidence by the formation of the red-brown precipitate silver chromate. The same procedure was used to determine the degree of quaternization of *N*-substituted chitosans [48].



สถาบันวิทยบริการ
จุฬาลงกรณ์มหาวิทยาลัย

PART C: ANTIBACTERIAL ACTIVITY OF QUATERNIZED CHITOSAN AND N-SUBSTITUTED CHITOSANS

3.5 Antibacterial assessment

3.5.1 Phosphate buffer saline

Solution A: 0.1M aqueous solution of potassium phosphate monobasic (KH_2PO_4) was prepared in deionized (DI) water (10.88 g/800 mL).

Solution B: 0.1M aqueous solution of potassium phosphate dibasic, anhydrous (K_2HPO_4) was prepared in deionized (DI) water (13.92 g/800 mL).

A 50mM phosphate buffer saline (PBS) of pH 7 was prepared and used currently assessments by mixing together **solution A** (78 mL), **solution B** (122 mL) and deionized (DI) water (400 mL).

3.5.2 Cell solution preparation

These assessments were carried out in 50mM phosphate buffer saline solution at pH 7. Selected bacteria were incubated at 37°C in a culture tube containing sterile nutrient broth, NB, (5 mL) for 12 hours. A portion of the resulting culture (1 mL) was transferred into a culture flask containing sterile nutrient broth (25 mL) and incubated on a shaker at 37°C for 3.5 hours. A part of the resulting bacterial culture (2 mL) was diluted with sterile nutrient broth such that the optical density (absorbance) of the resulting dilute solution was either 0.200 (for *E. coli*) or 0.400 (for *S. aureus*) when compared to sterile nutrient broth as the blank. Finally, this solution (0.8 mL) was further diluted to a volume four times that of the original using sterile nutrient broth. The resulting bacterial solutions appeared clear to the eye and was immediately stored at 0°C prior to used for anti-bacterial assessment against each bacterium. The bacterial cell density in this solution was predetermined to be 4×10^7 cells/mL. This solution was further diluted to 2×10^6 cells/mL in the individual wells during assessments [27,62].

3.5.3 96-well plate preparation

A schematic of the well plate is given in Figure 3.1. The plate was divided in three distinct categories of columns as shown, with each category containing solution as indicated below. A combination of multi-channel (8) pipettor and sterile throughs was used, when appropriate to facilitate the plate preparation. One 96-well plate was used to test 5 different agents at one time. The solution once introduced into the wells appeared clear without the presence of any turbidity. The cell count in each of the cell control and test well was calculated to be 2×10^6 cells/well.

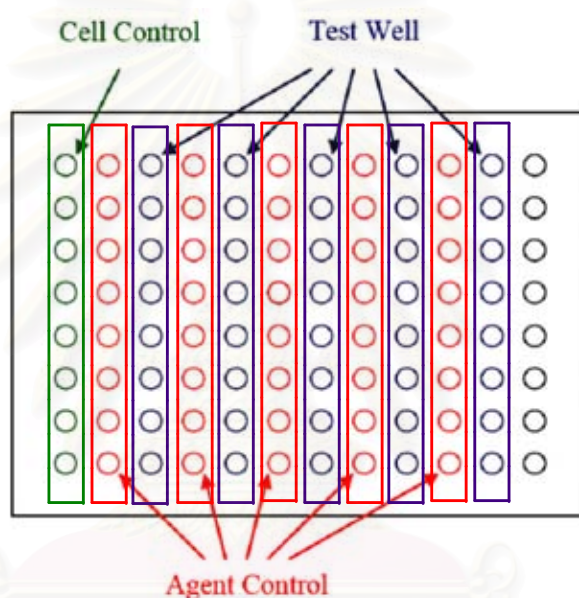


Figure 3.1: Schematic of a 96-well plate used in antibacterial assessment

Cell Control: PBS (50 μ L) + Cell bacterial solution (50 μ L) + DI water (100 μ L)

Agent Control: PBS (50 μ L) + NB (50 μ L) + Antibacterial agent (100 μ L)

Test Well: PBS (50 μ L) + Cell bacterial solution (50 μ L) + Antibacterial agent (100 μ L)

To test the antibacterial activity of the chitosan derived agents, the diluted bacterial culture was incubated at 37°C for 14 hours in a 96-well plate in the presence of each agent with final concentrations ranging from 2 µg/mL to 256 µg/mL in multiples of 2 pieces of the agent in separate wells. After this period, individual results were visually assessed; the wells where bacterial growth occurred turned visibly turbid, indicating no activity against the microorganism growth. MIC values were assigned as the lowest possible concentration of the agent that inhibited growth (identified as the first clear well of the lowest agent concentration along the length of each column). Control tests were simultaneously run to ensure proper bacterial growth within the diluted bacterial culture in absence of any agent (cell control) and indication of no growth in solutions of the agent in absence of any bacterial culture (agent control). Each assessment was performed at least two times to ensure reproducibility of results [27,62].



สถาบันวิทยบริการ
จุฬาลงกรณ์มหาวิทยาลัย

CHAPTER IV

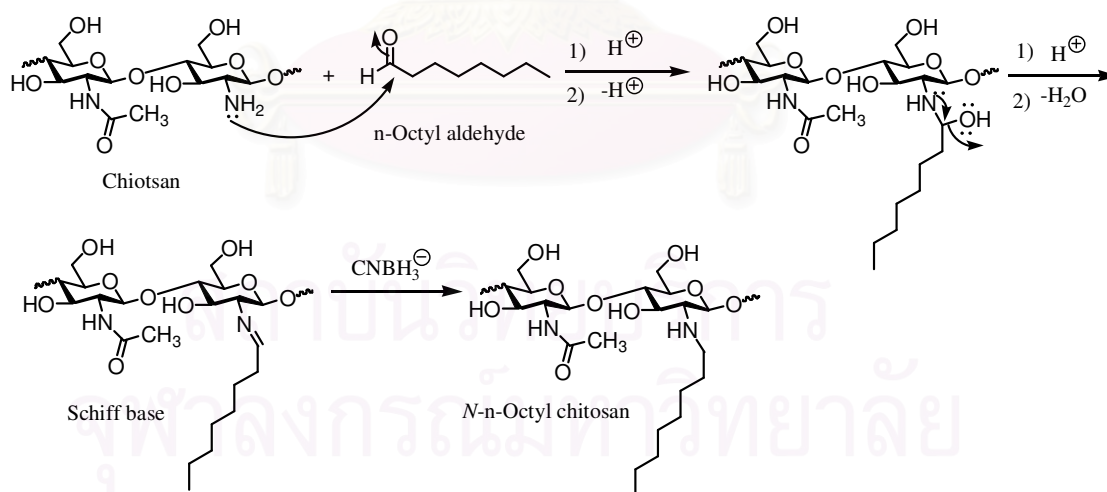
RESULTS AND DISCUSSION

PART A: SYNTHESIS OF *N*-SUBSTITUTED CHITOSAN DERIVATIVES

The *N*-substituted derivatives of chitosan can be synthesized by reductive amination [64]. It is a versatile and specific method for creating a covalent bond between an aldehyde and an amine function at C-2 position of chitosan. There are two distinct steps involved in this process; the formation of Schiff base and then the reduction to amine. In this study, three types of aldehydes were used, an aliphatic aldehyde, aromatic aldehydes, and heterocyclic aromatic aldehydes.

4.1 Synthesis of *N*-*n*-octyl chitosan

The selected aliphatic aldehyde used in derivatizing chitosan was *n*-octyl aldehyde. The formation of *N*-*n*-octyl chitosan (OctCh) occurred via the corresponding Schiff base intermediate as shown in Scheme 4.1. The reduction of the corresponding Schiff base was performed by using NaCNBH₃ which was more reactive and selective than usual reducing agents, such as NaBH₄ and PhSeH. The advantage of this reducing



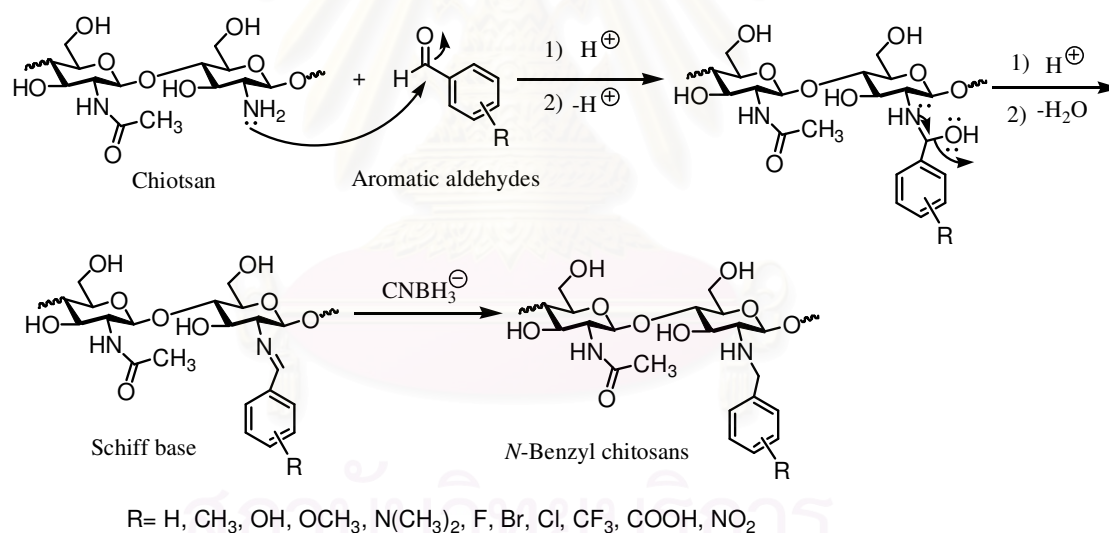
Scheme 4.1: Synthetic pathway of *N*-*n*-octyl chitosan

agent is its stability in acetic acid medium. Moreover, BH₃CN⁻ rapidly reacts with the Schiff base at pH values of 6-7, and thus the reduction of aldehydes or ketones is negligible in this pH range [36]. The FT-IR spectrum of OctCh (Figure 4.1) was

similar to that of chitosan except for the increasing intensity of the absorption band at wavenumber 2975 cm^{-1} due to C-H stretching of the pendant methylene groups [28]. The $^1\text{H-NMR}$ spectrum of OctCh was similar to the one of chitosan except the additional signals of the n-octyl group which appeared as the multiplet and singlet at δ 1.6-1.2 and 0.7 ppm due to methylene and methyl protons, respectively [37]. Accordingly, the final product was confirmed to be *N*-n-octyl chitosan. The extent of *N*-substitution (ES) of OctCh was found to be 10.2%, which was determined by $^1\text{H-NMR}$ as thoroughly discussed in section 4.4.

4.2 Synthesis of *N*-benzyl chitosans

The series of 17 *N*-benzyl chitosans with either electron donating or electron withdrawing substituents were obtained by the same synthetic pathway as described for OctCh which was shown in Scheme 4.2. Moreover, aromatic aldehydes at different

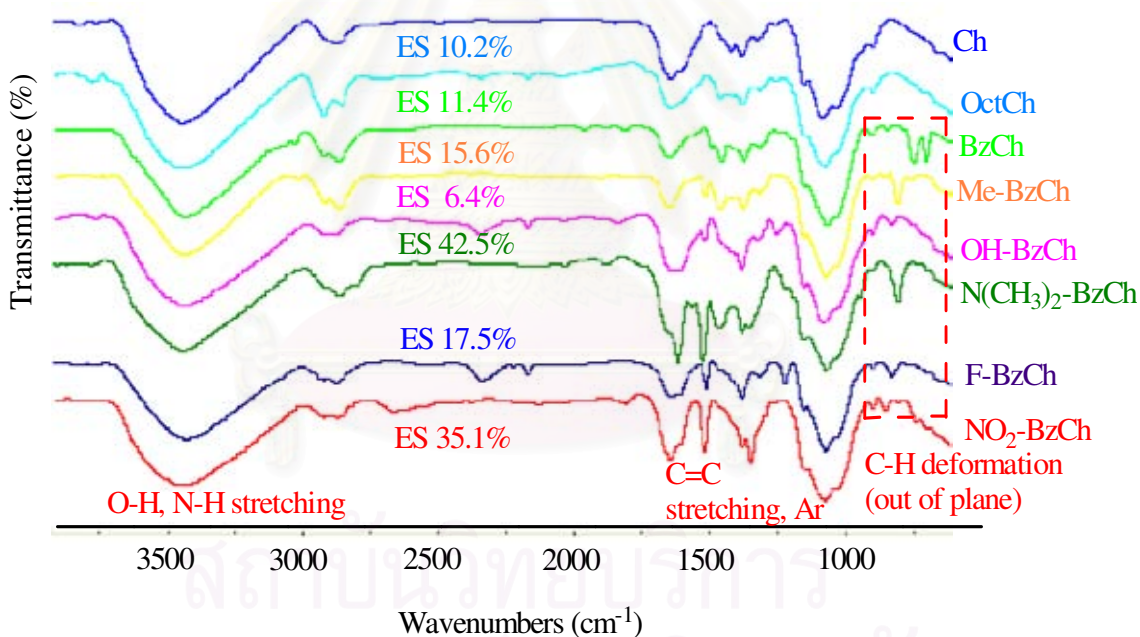


Scheme 4.2: Synthetic pathway of *N*-benzyl chitosans

mole ratios with respect to GlcN of chitosan were used in order to investigate the ES in these reactions (Table 4.1). All these *N*-benzyl chitosans were identified by FT-IR, $^1\text{H-NMR}$ and $^{13}\text{C-NMR}$ spectroscopy which was thoroughly discussed in next section. By varying the substituents on the aromatic aldehydes, the impact of the electronic factors on ES could be ascertained.

4.3 Interpretation of *N*-benzyl chitosans spectra

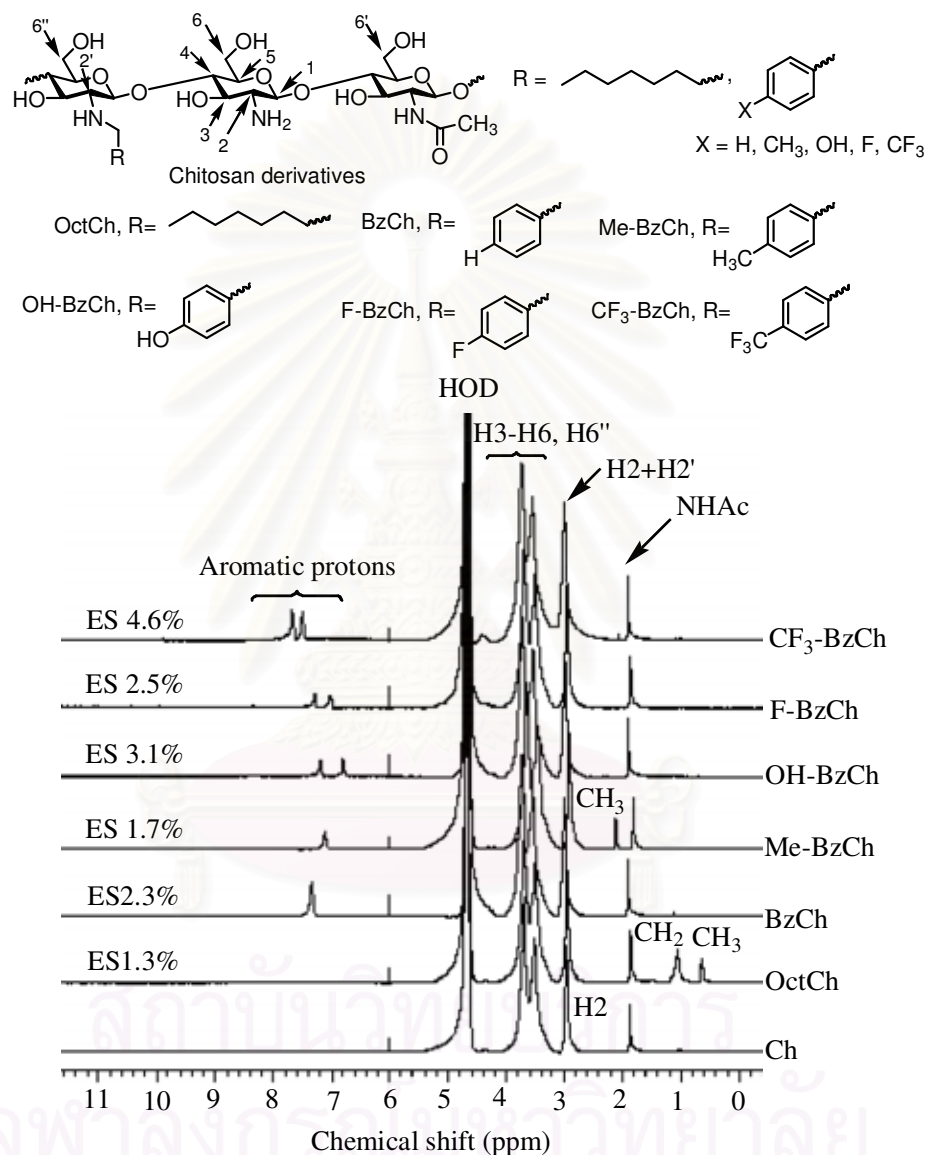
The FT-IR spectra of chitosan and selected *N*-benzyl chitosans with various ES's are shown in Figure 4.1. All spectra had the characteristic FT-IR pattern of chitosan, i.e., the absorption bands at wavenumber 3430 cm^{-1} due to OH and NH_2 groups, 1648 and 1377 cm^{-1} corresponding to the C=O and C-O stretching of amide groups, 1594 cm^{-1} due to N-H deformation of amino groups, 1155 , 1081 and 1033 cm^{-1} corresponding to the symmetric stretching of the C-O-C and involved skeletal vibration of the C-O stretching [65]. The additional absorption bands at 1602 , 1514 and 1470 and 704 - 836 cm^{-1} were assigned to C=C stretching and C-H bending out of plane of the aromatic group, respectively, which were actually absent in the FT-IR spectra of chitosan and OctCh. These absorption bands appeared more intense for those *N*-benzyl chitosans with higher ES's.



Ch, Chitosan; OctCh, *N*-n-Octyl chitosan; BzCh, *N*-Benzyl chitosan; Me-BzCh, *N*-(4-Methylbenzyl)chitosan; OH-BzCh, *N*-(4-Hydroxybenzyl)chitosan; $\text{N}(\text{CH}_3)_2$ -BzCh, *N*-(4-*N,N*-Dimethylaminobenzyl)chitosan; F-BzCh, *N*-(4-Fluorobenzyl)chitosan; NO_2 -BzCh, *N*-(4-Nitrobenzyl)chitosan.

Figure 4.1: FT-IR (KBr) spectra of chitosan and selected chitosan derivatives with various ES's

The $^1\text{H-NMR}$ spectra of chitosan and selected *N*-benzyl chitosans with various ES's are shown in Figure 4.2. All spectra exhibited the characteristic $^1\text{H-NMR}$ pattern of chitosan, i.e., the multiplet at δ 4.4-3.3 ppm from H3, H4, H5, H6 and H6'' protons and two singlets at δ 3.0 and 1.9 ppm due to the H2 proton of GlcN and *N*-acetyl protons of GlcNAc, respectively [66,67].



Ch, Chitosan; OctCh, *N*-n-Octyl chitosan; BzCh, *N*-Benzyl chitosan; Me-BzCh, *N*-(4-Methylbenzyl)chitosan; OH-BzCh, *N*-(4-Hydroxybenzyl)chitosan; F-BzCh, *N*-(4-Fluorobenzyl)chitosan; CF₃-BzCh, *N*-(4-Trifluorobenzyl)chitosan.

Figure 4.2: $^1\text{H-NMR}$ spectra of chitosan and selected chitosan derivatives with various ES's in $\text{D}_2\text{O}/\text{CF}_3\text{COOD}$

For all *N*-benzyl chitosans, their $^1\text{H-NMR}$ spectra exhibited typical signals in the aromatic region, δ 7-8 ppm, and a broad singlet signal at δ 4.3 ppm due to the benzylic protons of *N*-benzyl groups. In case of BzCh and Me-BzCh, one broad singlet at δ 7.3 ppm, due to aromatic protons which were in approximately the same chemical environment, were observed. The additional singlet at δ 2.2 ppm was assigned to the methyl protons at *para*-position of the aromatic ring of Me-BzCh. In the presence of either strong electron donating or electron withdrawing groups on the benzene ring, the aromatic protons clearly appeared as a doublet of doublets as the result of the magnetic anisotropic effect of the substituent at *para*-position. However, the $^1\text{H-NMR}$ spectrum of $\text{N}(\text{CH}_3)_2\text{-BzCh}$ showed the broad singlet, at δ 7.5 ppm, in the aromatic region and another singlet at δ 3.1 ppm assigned to *N,N*-dimethyl protons as shown in Figure 4.3. This indicated that the *N,N*-dimethylamino substituent is not protonated under this condition.

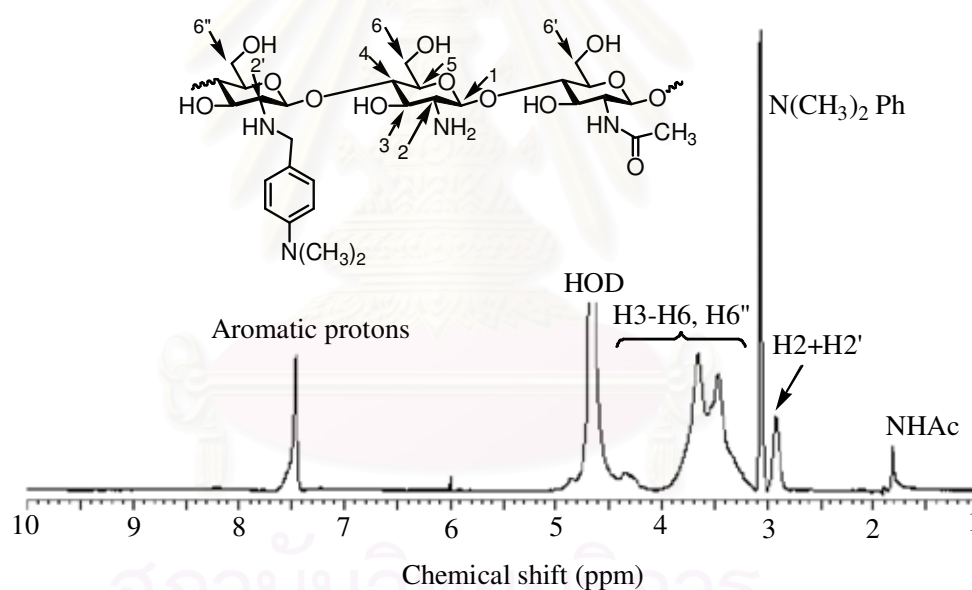


Figure 4.3: $^1\text{H-NMR}$ spectrum of *N*-(4-*N,N*-dimethylaminobenzyl)chitosan with ES 17.5% in $\text{D}_2\text{O}/\text{CF}_3\text{COOD}$

The $^1\text{H-NMR}$ spectrum of *N*-(4-pyridylmethyl)chitosan (PyMeCh) (Figure 4.4), showed a doublet of doublet signals at δ 8.6-8.0 ppm due to the protons of the pyridine ring. It should be noted that at molar ratios of 4-pyridinecarboxaldehyde to GlcN greater than 0.1 which afforded ES 5.2%, a signal near δ 6.0 ppm attributed to the proton of imine was clearly observed. Particularly, it appeared more intense when the ES was higher as 30.4%. Rodrigues *et al.* had also reported the detection of such a

signal and concluded that more reducing agent was required to assure complete reduction of the imine intermediate [68].

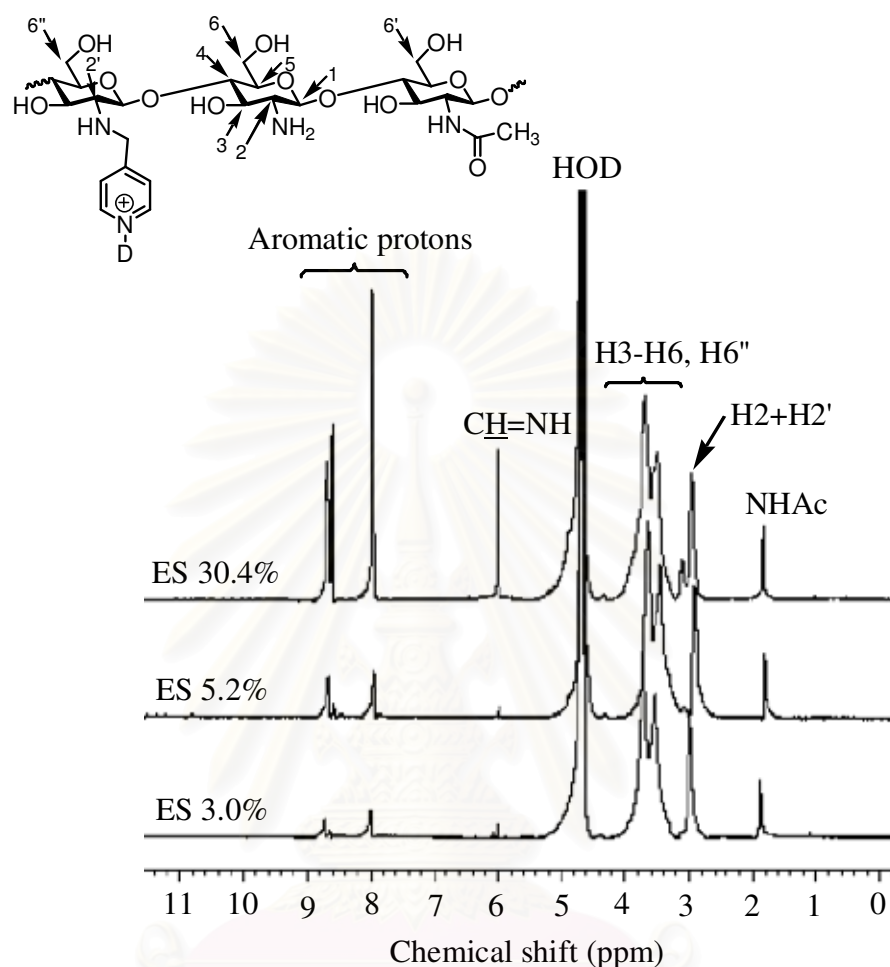


Figure 4.4: $^1\text{H-NMR}$ spectra of *N*-(4-pyridylmethyl)chitosan with different ES's in $\text{D}_2\text{O}/\text{CF}_3\text{COOD}$

The $^1\text{H-NMR}$ spectrum of *N*-(4-thiophenylmethyl)chitosan (2ThMeCh) was similar to that of PyMeCh. The doublet and multiplet at δ 7.3 and 7.1 ppm shown in Figure 4.5 were due to the protons of thiophene ring.

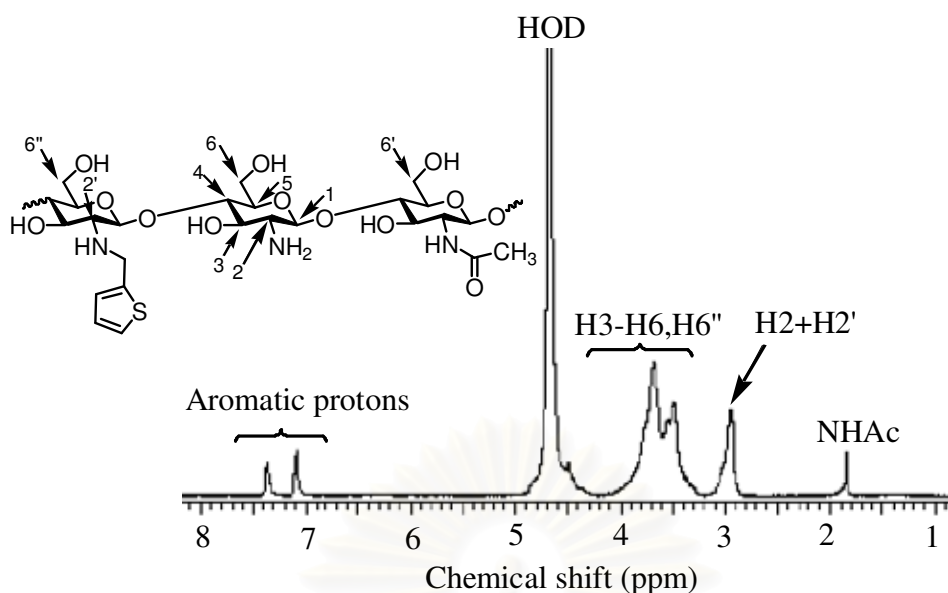


Figure 4.5: ^1H -NMR spectrum of *N*-(4-thiophenylmethyl)chitosan with ES 13.3% in $\text{D}_2\text{O}/\text{CF}_3\text{COOD}$

This observation confirms the synthetic pathway of *N*-benzyl chitosans as shown in Scheme 4.2.

In addition, the ^{13}C -NMR spectra of chitosan and the selected *N*-benzyl chitosans were recorded. Chitosan exhibited signals at δ 98.3, 76.6, 75.3, 70.5, 60.3, and 56.0 ppm which were assigned to C1, C4, C5, C3, C6, and C2 carbons of GlcN, respectively. This was consistent with that reported by Ramos *et al* [69]. BzCh exhibited a new signal at δ 51.0 ppm belonging to $\underline{\text{C}}\text{H}_2\text{NH}$ appearing in the aliphatic region (Figure 4.6). The presence of the aromatic carbons is evidenced by the signals at δ 130-131 ppm.

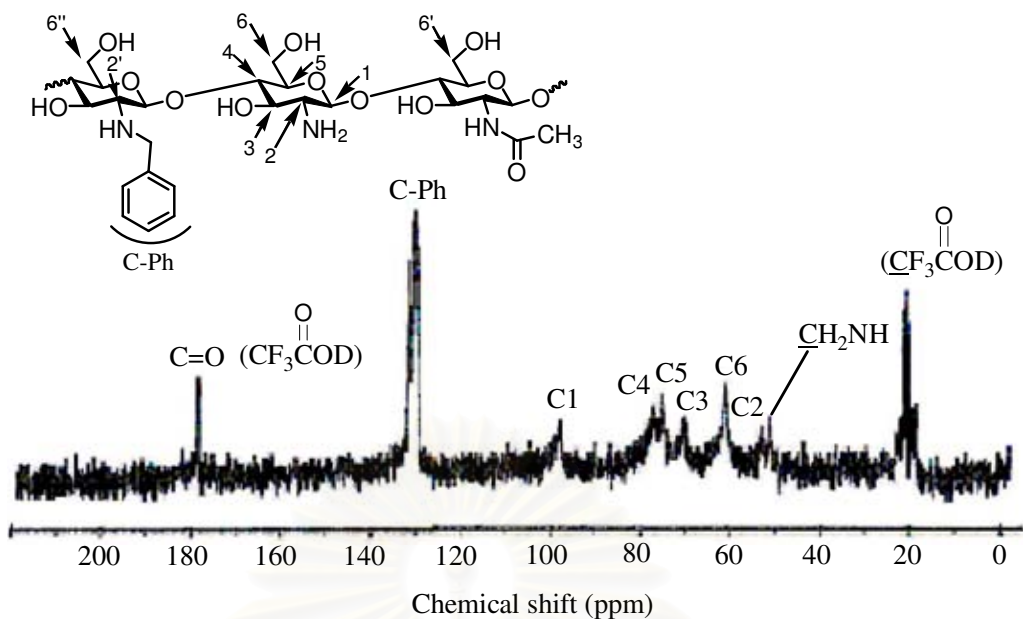


Figure 4.6: ^{13}C -NMR spectrum of *N*-benzyl chitosan with ES 18.5% in $\text{D}_2\text{O}/\text{CF}_3\text{COOD}$

In the spectrum of $\text{NO}_2\text{-BzCh}$ (Figure 4.7), the aromatic signals are clearly resolved which appeared as four peaks at δ 148.3, 140.9, 130.9, and 124.5 ppm indicating the existence of the *para*-substituted benzene ring.

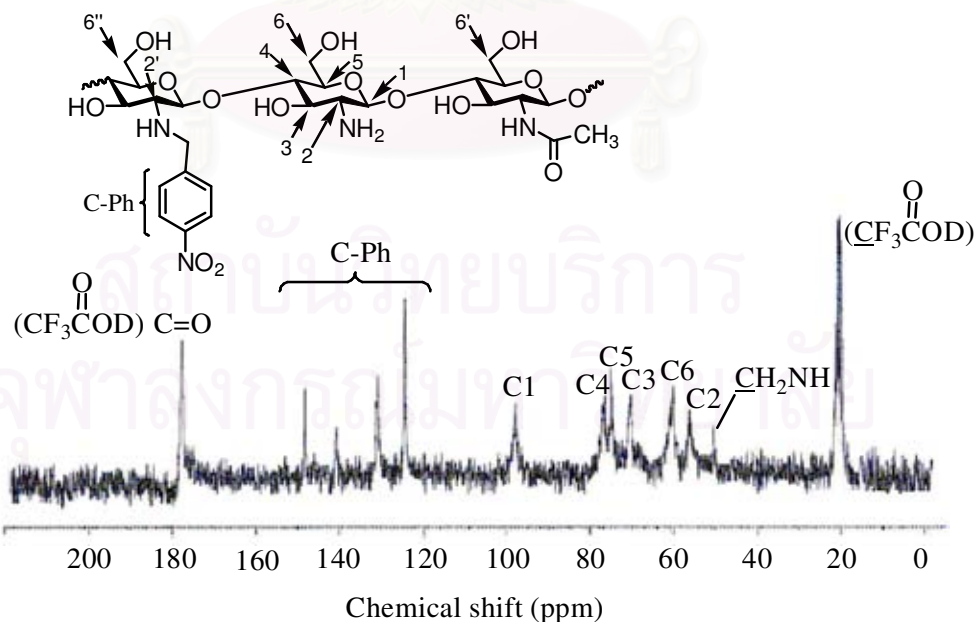


Figure 4.7: ^{13}C -NMR spectrum of *N*-(4-nitrobenzyl)chitosan with ES 24.7% in $\text{D}_2\text{O}/\text{CF}_3\text{COOD}$

4.4 Impact of *N*-benzyl substituents on the extent of chitosan substitution

In order to establish ES and hence calculate the yield of the polymer, it was necessary to determine the DDA of the chitosan sample which was performed by using $^1\text{H-NMR}$ spectroscopy and Equation 4.1 [66,67].

$$\text{DDA (mol\%)} = 1 - \left[\frac{\frac{1(\text{NAc})}{3}}{\frac{1(\text{H2 to H6})}{6}} \right] \times 100 \quad (4.1)$$

Where DDA (mol%) is degree of deacetylation, NAc is integral area of *N*-acetyl glucopyranose of chitosan (GlcNAc) protons, H2 to H6 are the integral area of the protons of glucopyranose of chitosan (GlcN).

In this study, DDA was determined from the relative integral area of *N*-acetyl protons of GlcNAc at δ 1.9 ppm and the combined integral areas of the H2 to H6 of GlcN protons at δ 4.4-3.0 ppm. It was found that DDA of parent chitosan was 94%. In other words, is chitosan comprised GlcN 94% and GlcNAc 6%.

Because the aromatic proton region did not overlap with the proton resonances of GlcN, the aromatic proton signal in $^1\text{H-NMR}$ spectrum of each *N*-benzyl chitosan was used to determine ES. Since the aromatic proton signal appears in the downfield region compared to GlcN protons, it can be integrated with minimal interference leading to greater accuracy. Comparison of the integral area of the H2+H2'+1/3 NAc signals with those of the aromatic protons allows the ES of benzyl group to be calculated by using Equation 4.2 [44]. Using the above approach (Equation 4.2), the ES of each chitosan derivative was thus calculated and recorded as listed in Table 4.1.,

$$\text{ES (mol\%)} = \left[\frac{\frac{\text{Ar}}{n}}{\frac{\text{H2}+\text{H2}'+\frac{1}{3}(\text{NAc})}{3}} \right] \times 100 \quad (4.2)$$

where ES (mol%) is the extent of *N*-substitution of *N*-benzyl group, Ar is the integral area of aromatic protons, n is number of aromatic hydrogen atoms per substituent, H2 and H2' are integral areas of the protons at C-2 carbon of GlcN both with and without substitution, and NAc is integral area of GlcNAc protons.

Figure 4.8 exhibits the $^1\text{H-NMR}$ spectra of Me-BzCh with various ES's in $\text{D}_2\text{O}/\text{CF}_3\text{COOD}$. It showed that the reasonable correlation of ES and the molar ratio of aldehyde to GlcN. When the mole equivalent amount of an aldehyde was increased, the ES was also increased as revealed by the relative increase of the aromatic proton signals. Most of these *N*-benzyl chitosans were obtained with high yield over 80%.

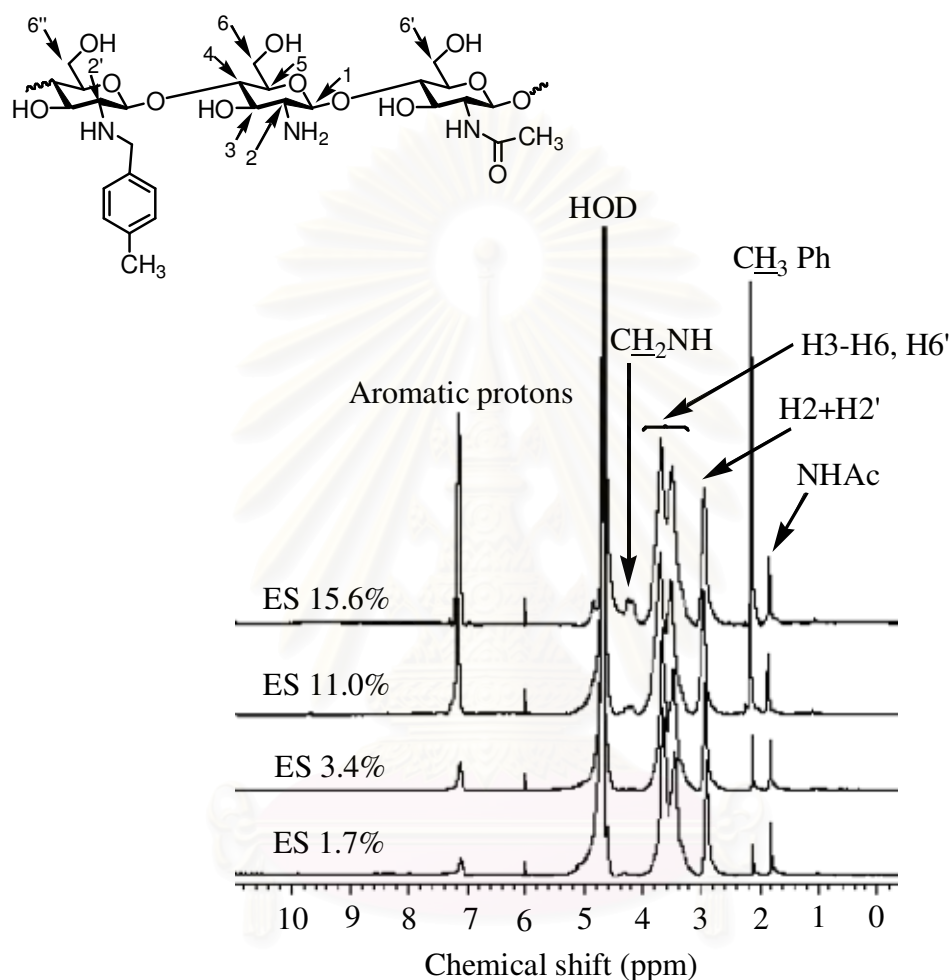


Figure 4.8: $^1\text{H-NMR}$ spectra of *N*-(4-methylbenzyl)chitosans with various ES's in $\text{D}_2\text{O}/\text{CF}_3\text{COOD}$

In addition, Thatte reported that changing the solvent composition from only diluted acetic acid solution to 60%DMF in dilute acetic acid solution produced a more homogeneous reaction medium which enhanced the ES [63]. In this study, $\text{NO}_2\text{-BzCh}$ had a high ES when the reaction was carried out in 50%DMF in diluted acetic acid solution. However, the complete removal of DMF from the reaction mixture was unsuccessful, although soxhlet extraction or dialysis were lasted for as long as 5 days. Ethanol (EtOH) was then used instead of DMF. 50%EtOH in diluted acetic acid

solution was finally used as the reaction medium for synthesis of all *N*-benzyl chitosans except for NO₂-BzCh, because it dissolves in EtOH.

Table 4.1 summarizes the results of chitosan modification with various aromatic aldehydes. *N*-benzylation of chitosan by benzaldehyde afforded higher ES's than *N*-alkylation by n-octyl aldehyde at every molar ratio of aldehyde to GlcN.



สถาบันวิทยบริการ
จุฬาลงกรณ์มหาวิทยาลัย

Table 4.1: *N*-Alkylation and *N*-benzylation of chitosan

Samples	Molar ratio (aldehyde:GlcN)	Targeted ES (%)	Obtained ES (%)	FW	Yield (%)
OctCh	1:1	100	>10.3	ND	ND
	0.5:1	50	10.3	175.1	87
	0.3:1	30	4.7	168.8	86
	0.1:1	10	1.8	165.5	91
	0.05:1	5	1.3	165.0	88
BzCh	1:1	100	>18.5	ND	ND
	0.5:1	50	18.5	180.2	94
	0.3:1	30	11.4	173.8	92
	0.1:1	10	3.6	166.8	84
	0.05:1	5	2.3	165.6	85
Me-BzCh	1:1	100	>15.6	ND	ND
	0.5:1	50	15.6	178.3	82
	0.3:1	30	11.0	175.0	85
	0.1:1	10	3.4	167.1	83
	0.05:1	5	1.7	165.3	87
OH-BzCh	1:1	100	>12.1	ND	ND
	0.5:1	50	12.1	176.4	90
	0.3:1	30	6.4	170.2	86
	0.1:1	10	3.1	165.0	90
	0.05:1	5	NR	NR	NR
	0.05:1	5*	trace	ND	ND
2OMe-BzCh	0.3:1	30	6.0	170.7	91
4OMe-BzCh	0.3:1	30	8.0	173.1	86
34OMe-BzCh	0.3:1	30	7.8	175.2	88
N(CH ₃) ₂ -BzCh	3:1	300	42.2	219.6	74
	1:1	100	17.5	186.8	75
	0.5:1	50	10.0	176.8	80
	0.3:1	30	5.9	171.4	79
	0.1:1	10	2.7	167.1	80
	0.05:1	5	NR	NR	NR

Table 4.1: *N*-Alkylation and *N*-benzylation of chitosan (cont.)

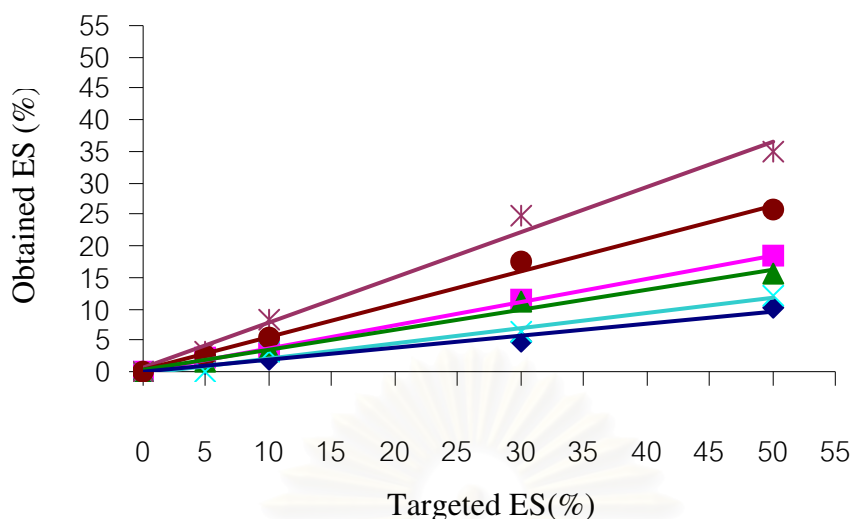
Samples	Molar ratio (aldehyde:GlcN)	Targeted ES (%)	Obtained ES (%)	FW	Yield (%)
F-BzCh	1:1	100	>25.7	ND	ND
	0.5:1	50	25.7	191.3	93
	0.3:1	30	17.5	182.4	92
	0.1:1	10	5.5	169.5	88
	0.05:1	5	2.5	166.2	91
4Br-BzCh	0.3:1	30	11.2	182.4	85
3Br-BzCh	0.3:1	30	12.5	184.6	81
Cl-BzCh	0.3:1	30	10.0	176.0	77
CF ₃ -BzCh	1:1	100	>35.8	ND	ND
	0.5:1	50	35.8	220.1	82
	0.1:1	10	6.7	174.1	90
	0.05:1	5	4.6	170.8	86
NO ₂ -BzCh	1:1	100	>35.1	ND	ND
	0.5:1	50	35.1	220.0	86
	0.3:1	30	24.7	203.3	87
	0.1:1	10	8.3	176.9	88
	0.05:1	5	3.3	168.8	88
COOH-BzCh	0.2:1	20	12.5	180.3	86
	0.1:1	10	6.8	172.6	84
PyMeCh	0.5:1	50	30.4	191.2	86
	0.3:1	30	20.3	182.0	83
	0.2:1	20	12.5	174.9	89
	0.1:1	10	5.2	168.2	88
	0.05:1	5	3.0	166.2	86
2ThMeCh	0.5:1	50	13.3	176.3	81
	0.3:1	30	9.6	172.7	80
	0.1:1	10	3.2	166.6	86

*24hrs; NR is no reaction as revealed by ¹H-NMR; ND is non detectable; > is expected to be higher ES but could not be determined by ¹H-NMR due to its insolubility in D₂O/CF₃COOD; FW is a formula weight of the repeating unit = 12.2 + (FW of *N*-benzyl GlcN × ES) + [163.5 × (0.94-ES)]; ES is the extent of *N*-substitution determined by ¹H-NMR; Yield (%) = [(weight of *N*-benzyl chitosan derivatives (g) × 163.5) / [weight of chitosan (g) × calculated FW of *N*-benzyl GlcN)] × 100.

According to Table 4.1, at the highest molar ratio of aldehyde to GlcN, 0.5:1, n-octyl aldehyde gave ES 10% while benzaldehyde afforded ES 18%. This indicated that n-octyl aldehyde was less reactive than benzaldehyde in this reaction. Another reason can be attributed to the relative stability of the Schiff base intermediate. In the case of benzaldehyde, the Schiff base is stabilized by the resonance with the aromatic ring. Similar observations had been reported by Desbrieres *et al.* [37].

The polarity of the aldehydic carbonyl group must play the important role in the formation of Schiff base intermediate. Under the reaction conditions employed, aldehydes with electron donating substituents were less active than the aldehydes with the electron withdrawing substituents. Strong electron donating substituents such as *para*-hydroxy and 4-*N,N*-dimethylaminobenzaldehyde failed to react at low molar ratios, i.e., 0.05. The *N,N*-dimethylamino group is not protonated in the mild acid medium, so it is a powerful electron donor. The extent of electron donation of *para*-hydroxybenzaldehyde could be moderated by esterifying the hydroxyl group, but the *para*-acetoxy derivative still exhibited low reactivity [63]. The carbonyl carbon of the aromatic aldehyde containing an electron donating group is less electrophilic as a result of the mesomeric effect of the electron rich hetero atom at the *para*-position. This polarization impacts negatively the intermediate Schiff base equilibrium leading to lower substitution levels.

In contrast, the extent of reaction of aldehydes with electron withdrawing substituents was closely correlated with the initial aldehyde to GlcN ratios. 4-Nitro, 4-carboxy, 4-trifluoromethyl and 4-fluorobenzaldehyde exhibited a linear relationship between the targeted ES and obtained ES as shown in Figure 4.9.



OctCh, *N*-n-Octyl chitosan (◆); BzCh, *N*-Benzyl chitosan (■); Me-BzCh, *N*-(4-Methylbenzyl) chitosan (▲); OH-BzCh, *N*-(4-Hydroxybenzyl)chitosan (×); F-BzCh, *N*-(4-Fluorobenzyl) chitosan (●); NO₂-BzCh, *N*-(4-Nitrobenzyl)chitosan (*).

Figure 4.9: Substitution control in the synthesis of selected chitosan derivatives bearing either an electron donating or electron withdrawing substituents

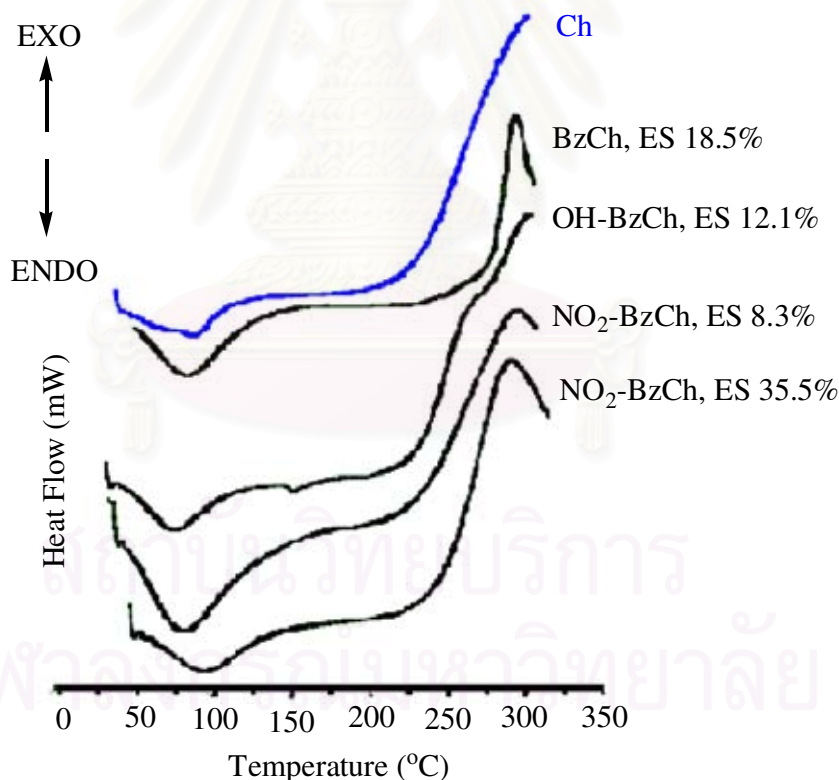
The reaction is driven by the quantitative formation of the Schiff base intermediate. In fact, this interaction which has recently been reported by Fan *et al.* was a method for analyzing amino substituents on polymeric substrates [70]. They also imparted that derivatives with trifluoromethyl aldehydes formed Schiff bases spontaneously, and the resulting imines could be quantified by integration of its unique ¹⁹F resonance.

A study of the halogenated derivatives indicated relative insensitivity of the reaction sequence to subtle electronic effects. The relative influence of the electronic effects could be evaluated by comparing the *meta*- versus *para*-bromo derivatives (Table 4.1). In a series of *para*-halogenated derivatives, the ES sequence is as follows, F > Cl ≈ Br due to the inductive effect. The ES of *meta*-bromo derivative was only slightly greater than that of *para*-bromo derivative due to the resonance effect at *para*-position which made carbonyl carbon less electrophilic.

Chitosan with heterocyclic substituents exhibited different activities. 4-Pyridinecarboxaldehyde behaved as a more electrophilic aldehyde than benzaldehyde, so the higher ES was easily achieved as shown in Table 4.1. In contrast, 2-thiophenecarboxaldehyde exhibited slightly less reactive than benzaldehyde, and the lower ES was obtained.

4.5 Thermal properties of *N*-benzyl chitosans

Native chitosan exhibited an endothermic peak at 88.6°C and an exothermic peak at 301.1°C due to the loss of water and decomposition of the chitosan backbone, respectively [71,72]. When chitosan was dried at 150°C, the endothermic peak at 88.6°C disappeared. This observation as well as its TGA thermogram confirmed that the initial transition could be attributed to water evaporation. Figure 4.10 exhibits the

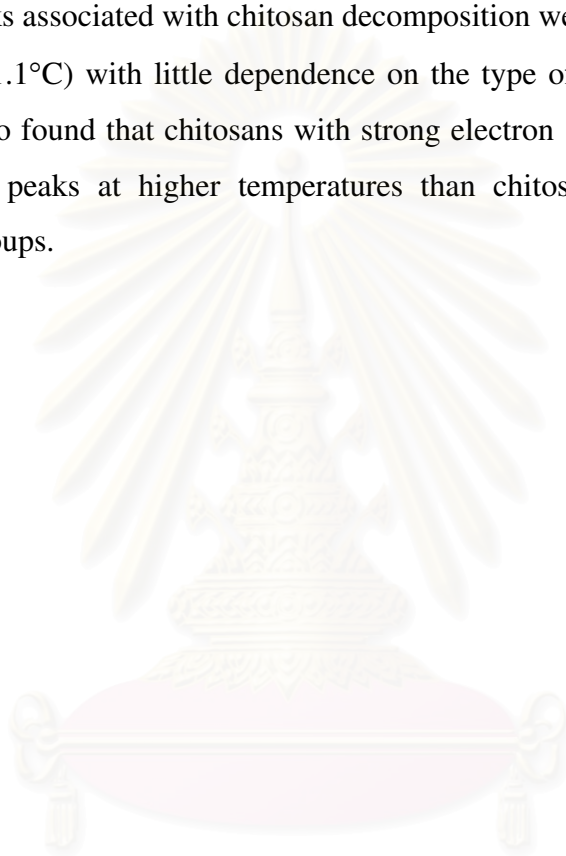


Ch, Chitosan; BzCh, *N*-Benzyl chitosan; OH-BzCh, *N*-(4-Hydroxybenzyl)chitosan; NO₂-BzCh, *N*-(4-Nitrobenzyl)chitosan.

Figure 4.10: DSC thermograms of chitosan and selected *N*-benzyl chitosans

DSC thermograms of chitosan and selected *N*-benzyl chitosans, which were firstly dried at 150°C then allowed to reequilibrate with water by storing them in 100% humidity for one month before recording.

The endothermic peak of selected *N*-benzyl chitosans shifted to a lower temperature than that of chitosan (Table 4.2). This could be attributed to the weaker interactions between water and the *N*-benzyl groups in chitosan side chain. The exothermic peaks associated with chitosan decomposition were slightly lower than that of chitosan (301.1°C) with little dependence on the type of substituents on aromatic ring. It was also found that chitosans with strong electron donating groups exhibited the exothermic peaks at higher temperatures than chitosans with strong electron withdrawing groups.



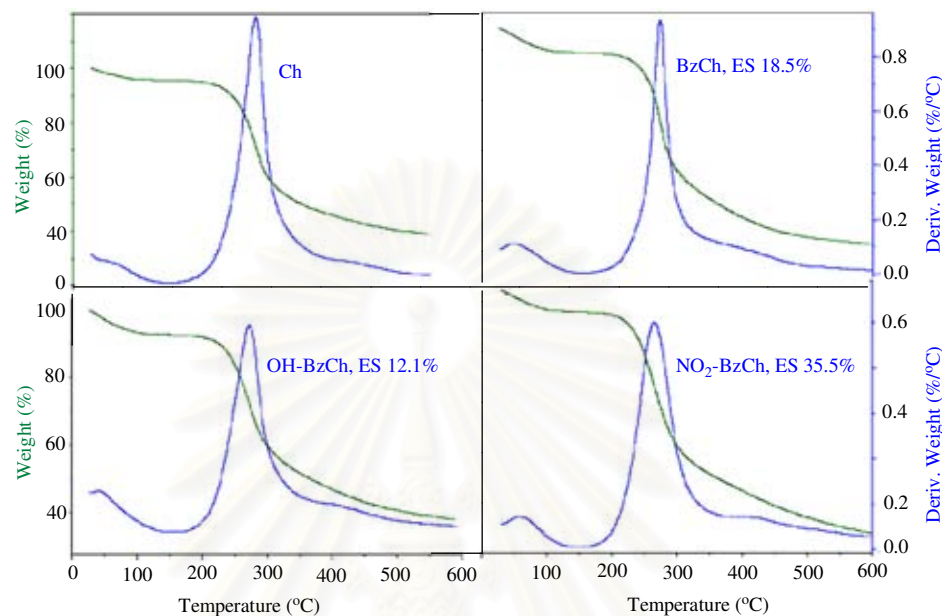
สถาบันวิทยบริการ
จุฬาลงกรณ์มหาวิทยาลัย

Table 4.2: DSC and TGA datas of chitosan and selected chitosan derivatives

Samples	ES (%)	DSC			TGA									
		Degradation _{max}			Thermal degradation in N ₂					Oxidative degradation in Air				
		Endo peak		Exo peak	150°C	(150-400°C)			(150-400°C)			(350-600°C)		
		Temp (°C)	$\Delta H(J/g)$	Temp (°C)	wt loss (%)	Onset	DTG _{max}	wt loss (%)	Onset	DTG _{max}	wt loss (%)	Onset	DTG _{max}	wt loss (%)
Ch	-	87	216.1	301	4.3	250	280	49.8	247	284	55.5	434	490	44.3
BzCh	18.5	78	246.3	289	7.1	253	274	48.5	257	287	41.9	471	523	54.1
OH-BzCh	12.1	70	200.2	263, 299	7.0	240	273	45.7	243	285	49.1	455	510	49.5
N(CH ₃) ₂ -BzCh	42.5	77	191.0	294	3.4	271	298	43.0	257	287	39.2	496	535	58.3
NO ₂ -BzCh	8.3	74	205.4	288	9.2	230	266	41.0	244	282	41.9	484	526	53.2
	24.7	89	113.1	275	3.3	229	263	41.8	240	277	41.8	497	536	59.4
	35.1	80	178.2	276	4.6	233	265	39.5	244	280	39.9	488	530	58.0

Ch, Chitosan; BzCh, *N*-Benzyl chitosan; OH-BzCh, *N*-(4-Hydroxybenzyl)chitosan; N(CH₃)₂-BzCh, *N*-(4-*N,N*-dimethylaminobenzyl)chitosan; NO₂-BzCh, *N*-(4-Nitrobenzyl)chitosan.

Figure 4.11 exhibits the TGA thermograms of chitosan and selected *N*-benzyl chitosans after drying and reequilibration in 100% humidity.



Ch, Chitosan; BzCh, *N*-Benzyl chitosan; OH-BzCh, *N*-(4-Hydroxybenzyl)chitosan; NO₂-BzCh, *N*-(4-Nitrobenzyl)chitosan.

Figure 4.11: TGA thermograms of chitosan and selected chitosan derivatives

The TGA's were performed in either nitrogen or air atmosphere. The decomposition temperatures along with the corresponding weight losses (%) are compiled in Table 4.2. The weight loss at temperature up to 150°C in the nitrogen corresponded to water desorption from polymer backbone [73]. It was found that the water weight loss of the selected *N*-benzyl chitosans was higher than that observed for chitosan. Apparently, the selected *N*-benzyl chitosans with ES's less than 18.5% can absorb more water than chitosan due to the decreased chitosan crystallinity created by *N*-benzylation leading to hydrophobic side chains. At concentration higher than 18.5%, the hydrophobicity of the derivatives reduces the water reabsorption. The TGA's of the selected *N*-benzyl chitosans showed that these derivatives exhibited lower thermal stability than chitosan, i.e. see DTG_{max} data (Table 4.2).

Moreover, the ES of selected *N*-benzyl chitosans did not affect the weight loss (%) in the temperature range of 150-600°C in either nitrogen or air. In fact, under nitrogen, derivatives with a higher extent of substitution actually appeared more stable than the parent chitosan. In air atmosphere, the weight loss (%) between 350-600°C was consistently 54.4±5% regardless of the extent and nature of the substituents. The oxidative degradation occurring above 400°C consumed the remained sample.

4.6 Solubility of *N*-benzyl chitosans

The solubility of the selected *N*-benzyl chitosans with various ES's was determined in several solvents as shown in Table 4.3. The solubility of *N*-benzyl chitosans depended on ES and functional group on the aromatic aldehydes as shown in Table 4.3. In case of OctCh, BzCh, and Me-BzCh with high ES's (ES>10.3%, 18.5%, and 15.6%, respectively), the derivatives would dissolve in DMSO and swell in pyridine and NMP [39]. The enhanced solubility of these samples is due to the increase in hydrophobicity of the substituted chitosan side chain leading to a corresponding decrease in crystallinity. These high ES derivatives no longer dissolved in dilute acetic acid solvent. Introduction of functional groups such as hydroxyl, fluoro, nitro or trifluoromethyl on the benzyl ring did not enhance the solubility of the derivatives in organic solvents. Derivatives with amino substituents, such as *N,N*-dimethylamino and pyridylmethyl, remained soluble in dilute acetic acid throughout the substitution range explored. Introducing of the thiophenyl substituent produced a derivative soluble in DMSO and dilute acetic acid solvent.

Table 4.3: Solubility of chitosan and selected chitosan derivatives in various solvents

Samples	ES (%)	Solubility (10 mg/mL)					
		1% (v/v) AcOH	CHCl ₃	Pyridine	DMF	DMSO	NMP
Ch	-	+	-	-	-	-	-
OctCh	>10.3	-	-	+/-	+/-	+	+/-
	≤10.3	+	-	-	-	-	-
BzCh	>18.5	-	-	+/-	+/-	+	+/-
	≤18.5	+	-	-	-	-	-
Me-BzCh	>15.6	-	-	+/-	+/-	+	+/-
	≤15.6	+	-	-	-	-	-
OH-BzCh	>12.1	-	-	-	-	-	-
	≤12.1	+	-	-	-	-	-
N(CH ₃) ₂ -BzCh	42.2	+	-	-	-	-	-
	17.5	+	-	-	-	-	-
F-BzCh	>25.7	-	-	-	-	-	-
	≤25.7	+	-	-	-	-	-
CF ₃ -BzCh	>35.8	-	-	-	-	-	-
	≤35.8	+	-	-	-	-	-
NO ₂ -BzCh	>35.1	-	-	-	-	-	-
	≤35.1	+	-	-	-	-	-
PyMeCh	30.4	+	-	-	-	-	-
2ThMeCh	13.3	+	-	-	-	+	-

+ Soluble within one hour; +/- Swelling; - Insoluble; > higher than; ≤ equal to or less than.

Ch, Chitosan; OctCh, *N*-n-Octyl chitosan; BzCh, *N*-Benzyl chitosan; Me-BzCh, *N*-(4-Methylbenzyl)chitosan; OH-BzCh, *N*-(4-Hydroxybenzyl)chitosan; N(CH₃)₂-BzCh, *N*-(4-*N,N*-Dimethylaminobenzyl)chitosan; F-BzCh, *N*-(4-Fluorobenzyl)chitosan; NO₂-BzCh, *N*-(4-Nitrobenzyl)chitosan, PyMeCh; *N*-(4-Pyridylmethyl)chitosan, 2ThMeCh; *N*-(2-Thiophenylmethyl)chitosan.

PART B: QUATERNIZATION OF CHITOSAN AND *N*-SUBSTITUTED CHITOSAN DERIVATIVES

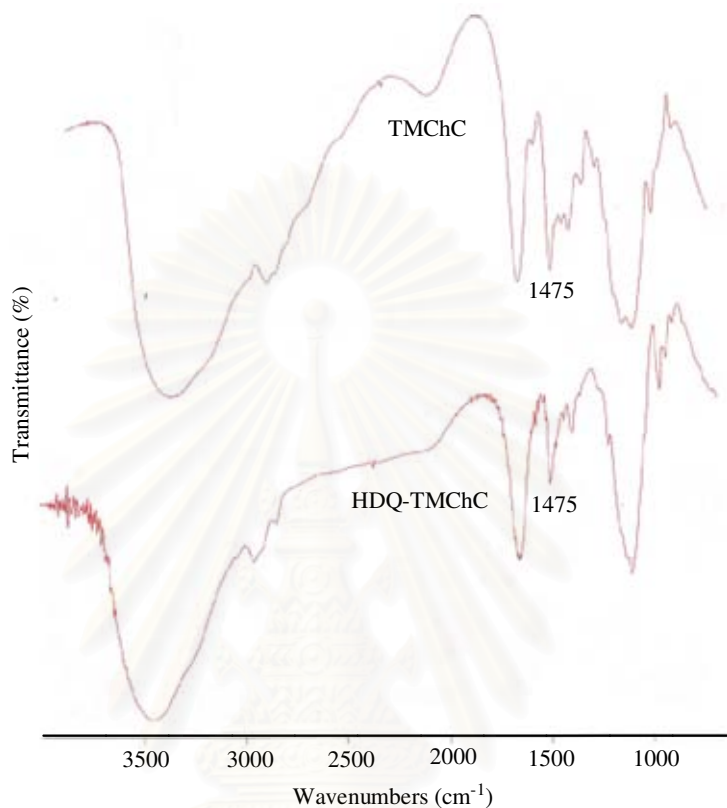
The introduction of permanent positive charges into the chitosan chains can be accomplished in the form of quaternary ammonium salts. The first alternative for preparation of quaternary ammonium salt of chitosan is the common method using iodomethane as the quaternizing agent. The second one involves the reaction of chitosan with a quaternary ammonium epoxide, generated from 3-chloro-2-hydroxypropyl trimethylammonium chloride (Quat-188). In this study, quaternary ammonium salts of chitosan and *N*-substituted chitosans were synthesized using both methods.

4.7 Quaternization of chitosan and *N*-substituted chitosans using iodomethane

4.7.1 *N,N,N*-trimethylammonium chitosan chloride and its high degree of quaternization

The methylation was based on a nucleophilic substitution of the primary amino group on the C-2 position of chitosan with iodomethane in the presence of sodium hydroxide and sodium iodide in *N*-methyl-2-pyrrolidone (NMP) at 50°C. It was reported that chloride counter-ion would enhance the stability of the quaternary ammonium salts of chitosan more than the iodide one [14]. In this work, the iodide counter-ion was thus exchanged with the chloride counter-ion by dissolving *N,N,N*-trimethylammonium chitosan iodide (TMChI) in an aqueous solution of 15% (w/v) sodium chloride and then dialysing with deionized water. Furthermore, the *N,N,N*-trimethylammonium chitosan chloride (TMChC) from the first methylation was subjected to methylation for two more times in order to increase the degree of quaternization. This latter product was called *N,N,N*-trimethylammonium chitosan chloride (TMChC) with a high degree of quaternization (HDQ-TMChC).

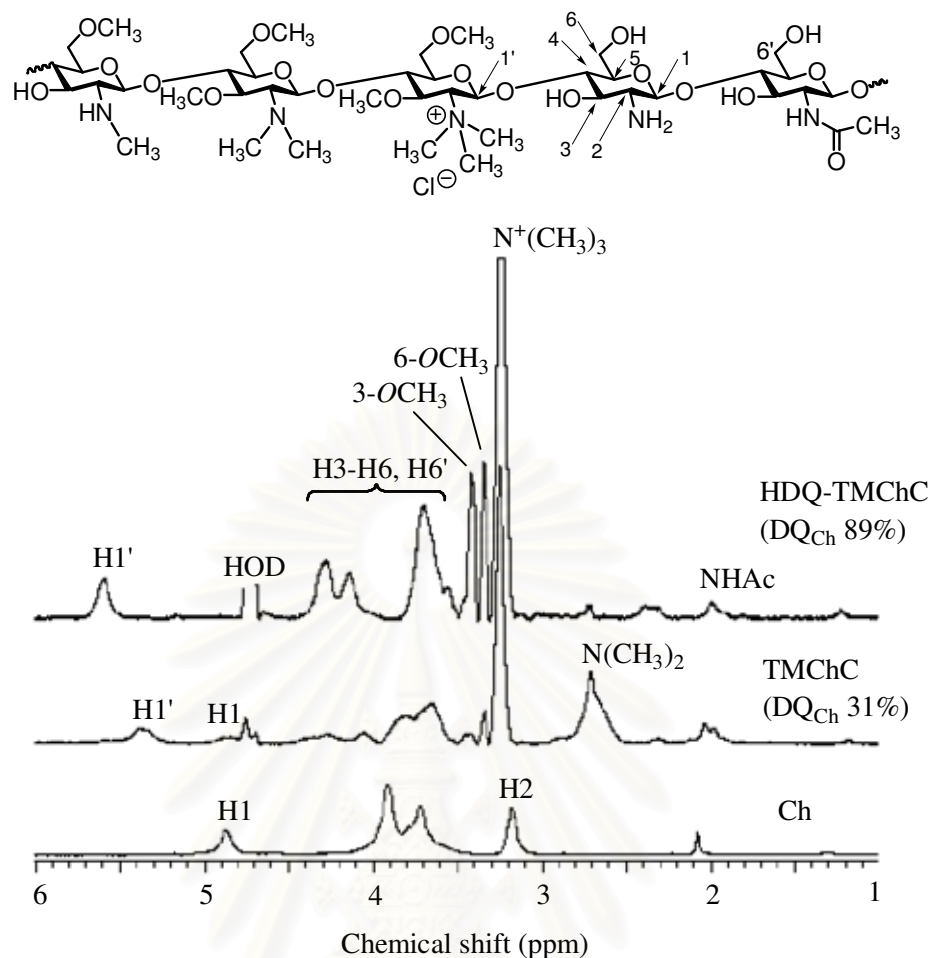
Figure 4.12 exhibit the FT-IR spectra of TMChC and HDQ-TMChC. Both of them were similar to that of chitosan except the absorption band at wavenumber 1475 cm^{-1} which was due to C-H symmetric bending of methyl substituent of the quaternary ammonium groups [28].



TMChC, *N,N,N*-Trimethylammonium chitosan chloride; HDQ-TMChC, High degree of quaternization of TMChC.

Figure 4.12: FT-IR (KBr) spectra of *N,N,N*-trimethylammonium chitosan chloride and its analog having high degree of quaternization

The $^1\text{H-NMR}$ spectra of TMChC and HDQ-TMChC are shown in Figure 4.13. Both spectra had all the signals belonging to chitosan and the additional signals due to methylation. There were two types of methylation, *N*-methylation and *O*-methylation of the GlcN of chitosan which could be differentiated by $^1\text{H-NMR}$ spectroscopy. For *N*-methylation, H1 proton of the GlcN of chitosan is normally deshielded and is assigned as H1' in this work. The chemical shift of H1' depends on DQ_{Ch} . The higher DQ_{Ch} , the lower downfield chemical shift of H1'.



Ch, Chitosan; TMChC, *N,N,N*-Trimethylammonium chitosan chloride; HDQ-TMChC, High degree of quaternization of TMChC.

Figure 4.13: ^1H -NMR spectra of chitosan ($\text{D}_2\text{O}/\text{CF}_3\text{COOD}$) and quaternized chitosan (D_2O) respectively, using iodomethane as quaternizing agent

The signals at δ 5.59 and 5.42 ppm belonged to $\text{H1}'$ protons of the GlcN of HDQ-TMChC and TMChC, respectively. The other signals appeared at δ 3.2, 2.7 and 2.3 ppm were due to *N,N,N*-trimethyl protons, *N,N*-dimethyl protons, and *N*-methyl protons of the different GlcN's of chitosan, respectively. For *O*-methylation, the signals appeared at δ 3.4 and 3.3 ppm due to methoxy protons at 3- and 6-hydroxy groups of the GlcN of chitosan. The similar observation of *N*-methylation and *O*-methylation of chitosan with iodomethane was also reported by Sieval *et al.* [50].

The degree of quaternization was generally determined by using Equation 4.3

$$\text{DQ (mol\%)} = \left[\frac{\frac{\text{N}^+(\text{CH}_3)_3}{9}}{\text{H1}} \right] \times 100 \quad (4.3)$$

In the experimental results, DQ at the primary amino group of chitosan is denoted as DQ_{Ch} . $\text{N}^+(\text{CH}_3)_3$ is the integral area of the *N,N,N*-trimethyl protons at δ 3.2 ppm, and H1 is the integral area of both H1' and H1 protons in the range of δ 5.6-4.9 ppm.

[50]. When chitosan was quaternized with iodomethane by single treatment, TMChC was obtained with *N,N,N*-trimethylation or DQ_{Ch} 31%, *N,N*-dimethylation 23% and a trace of *N*-methylation. However, higher DQ_{Ch} 89% was yielded and only traces of *N,N*-dimethylation and *N*-methylation were obtained after repeated treatments with iodomethane for two times. It clearly demonstrated that DQ_{Ch} of chitosan significantly increased with the number of methylation treatments. The same observations had been reported by Sieval *et al.* and Hamman and Kotze [50,51].

The degrees of 3-*O*- and 6-*O*-methylation were each determined by using Equation 4.4 [53]. Besides methylation at the primary amino group on the C-2 position

$$\text{DOM (mol\%)} = \left[\frac{\frac{\text{OCH}_3}{3}}{\text{H1}} \right] \times 100 \quad (4.4)$$

Where DOM (mol%) is the degree of *O*-methylation, OCH_3 is the integral area of methoxy protons of either 3- or 6-hydroxy groups at δ 3.4 ppm or 3.3 ppm, respectively, and H1 is the combined integral area of the H1' and H1 protons in the range of δ 5.6-4.9 ppm.

of chitosan, *O*-methylation of hydroxy groups at C-3 and C-6 positions was also detected as revealed by its $^1\text{H-NMR}$ spectrum (Figure 4.13). When chitosan was single treated with iodomethane, the degree of *O*-methylation (DOM) was 33%. The higher DOM 177% was obtained, after repeated methylation with iodomethane for two times. In addition, Sieval *et al.* and Polnok *et al.* found that the high DOM from repeated methylation affected the physical properties of quaternized chitosan, i.e., lower

solubility in water and easier degradation, as well as lower yield [50,53]. The similar behaviors of the quaternized chitosans in this work were also observed.

4.7.2 Quaternized *N*-(4-methylbenzyl)chitosan

N-(4-Methylbenzyl)chitosan (Me-BzCh) with ES 11.0% was quaternized with iodomethane by single treatment with iodomethane under the same condition as TMChC. The $^1\text{H-NMR}$ spectrum of quaternized *N*-(4-methylbenzyl)chitosan (QMe-BzCh2) is shown in Figure 4.14. This spectrum is similar to that of Me-BzCh with

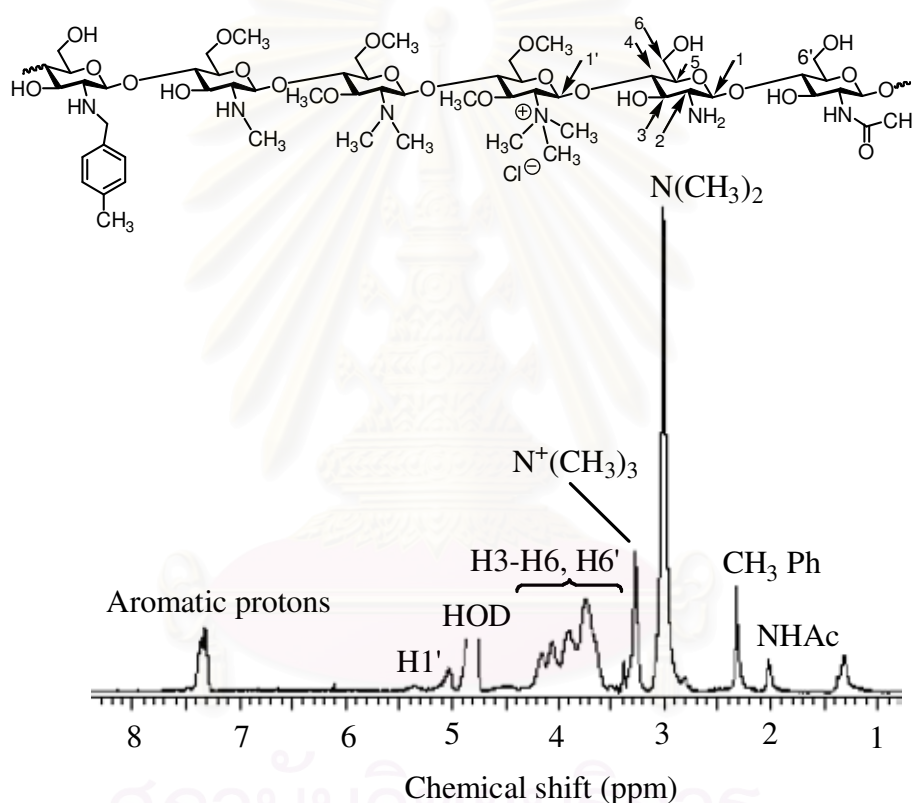


Figure 4.14: $^1\text{H-NMR}$ spectrum of quaternized *N*-(4-methylbenzyl)chitosan with ES 11.0% in $\text{CF}_3\text{COOD}/\text{D}_2\text{O}$ using 15% (w/v) NaOH

some additional signals. The signal at δ 5.59 ppm belonged to H1' proton of the GlcN of QMe-BzCh. The other signals at δ 3.2, 2.7 and 2.3 ppm were due to *N,N,N*-trimethyl protons, *N,N*-dimethyl protons, and *N*-methyl protons of the GlcN of chitosan, respectively. In this case, *O*-methylation was also observed at the GlcN of

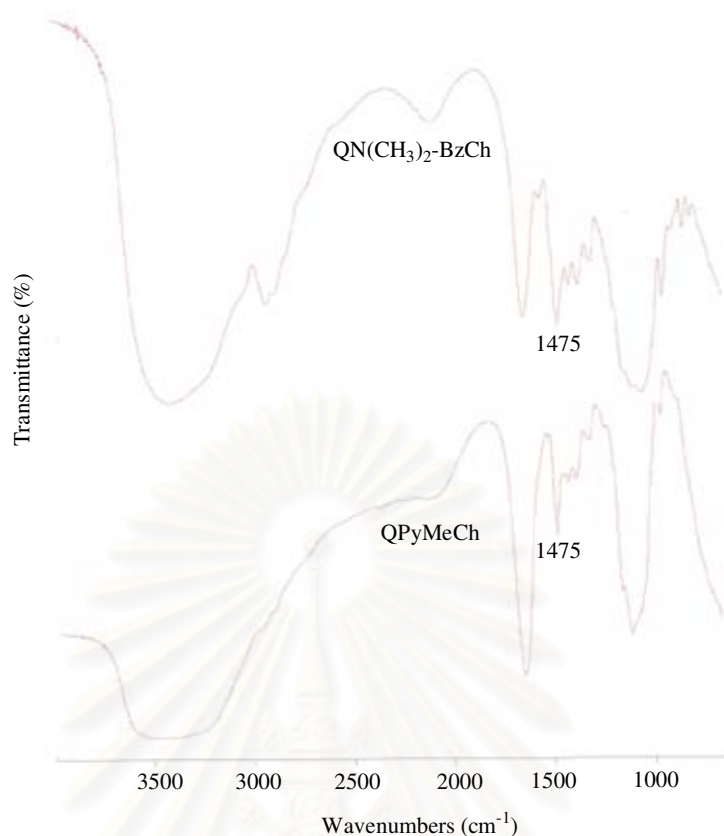
chitosan. The 6-hydroxy group is exposed to methylation more easily than the 3-hydroxy group.

Furthermore, it was found that the quaternized product could not dissolve in water. This was likely that the DQ_{Ch} 11% achieved was too low due to the bulkiness of *N*-methylbenzyl substituent. It is plausible that the 4-methylbenzyl substituent at any GlcN can cause steric hindrance to the methylation at a nearby GlcN unit. In comparison to TMChC, although lower DOM of QMe-BzCh was resulted, the lower DQ_{Ch} obtained which made it insoluble in water.

4.7.3 Quaternized *N*-(4-*N,N*-dimethylaminobenzyl)chitosan and quaternized *N*-(4-pyridylmethyl)chitosan

To enhance the water solubility, the *N*-(4-*N,N*-dimethylaminobenzyl)chitosan ($N(CH_3)_2$ -BzCh) and *N*-(4-pyridylmethyl)chitosan (PyMeCh) were quaternized by single treatment with iodomethane. The formation of the quaternary ammonium salt; *N,N*-dimethylaminobenzyl and *N*-pyridylmethyl substituents, favored dissolution of the chitosan substrate and led to more homogeneous *N*-benzylation which led to increased DQ_{Ch} and decreased DOM. The methylation of $N(CH_3)_2$ -BzCh and PyMeCh by single treatment with iodomethane was conducted under the same conditions as TMChC. In this work, two sodium hydroxide concentrations, 5% (w/v) and 15% (w/v), were used.

Figure 4.15 exhibits the FT-IR spectra of quaternized $N(CH_3)_2$ -BzCh (Q $N(CH_3)_2$ -BzCh) and quaternized PyMeCh (QPyMeCh). Each of them had similar spectrum to the corresponding $N(CH_3)_2$ -BzCh and PyMeCh except for the absorption band at wavenumber 1475 cm^{-1} due to C-H symmetric bending of the methyl substituent of quaternary ammonium groups [28].



QN(CH₃)₂-BzCh, Quaternized *N*-(4-*N,N*-Dimethylaminobenzyl)chitosan; QPyMeCh, Quaternized *N*-(4-Pyridylmethyl)chitosan.

Figure 4.15: FT-IR (KBr) spectra of quaternized *N*-(4-*N,N*-dimethylaminobenzyl)chitosan and quaternized *N*-(4-pyridylmethyl)chitosan

The ¹H-NMR spectra of QN(CH₃)₂-BzCh1 and QPyMeCh2 are shown in Figures 4.16 and 4.17, respectively. Both spectra are similar to that of the corresponding N(CH₃)₂-BzCh1 and PyMeCh2 except the additional signals of H1' proton. The signal at δ 5.40 ppm was belong to H1' proton of the GlcN of quaternized chitosan. The other signals at δ 3.5, 3.2, 2.7 and 2.3 ppm were due to the methyl protons at the aromatic substituent, and *N,N,N*-trimethyl protons, *N,N*-dimethyl protons, and *N*-methyl protons of the GlcN of chitosan, respectively. For *O*-methylation, the signals appeared at δ 3.4 and 3.3 ppm due to methoxy protons at 3- and 6-hydroxy groups of the GlcN of chitosan.

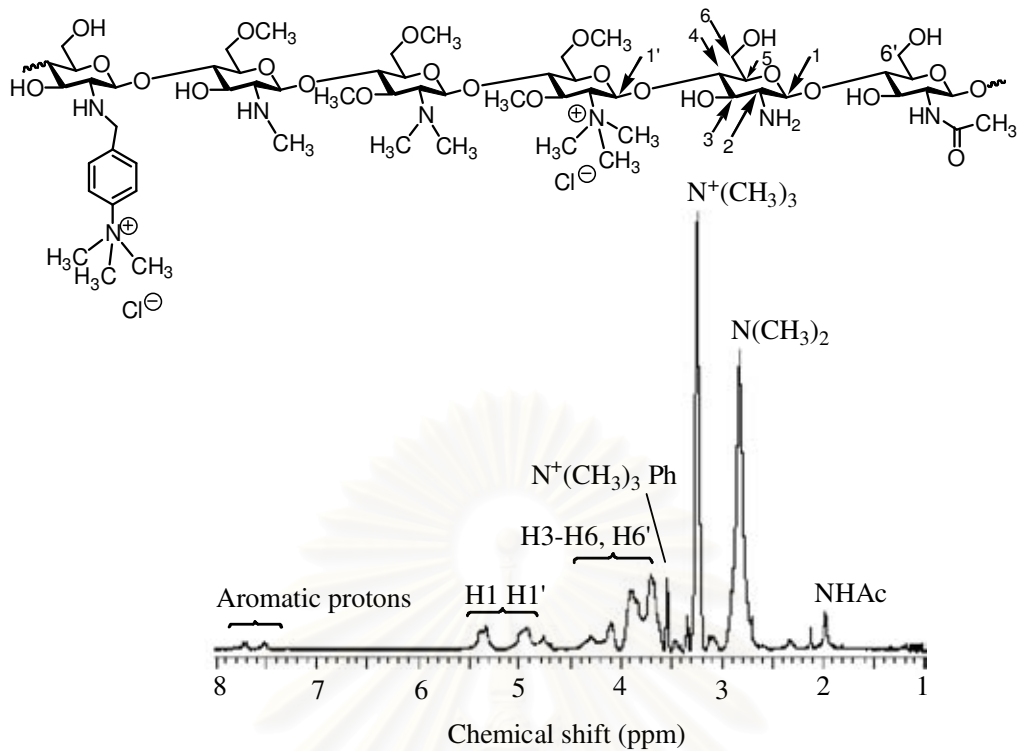


Figure 4.16: ^1H -NMR spectrum of quaternized *N*-(4-*N,N*-dimethylaminobenzyl)chitosan with ES 2.7% in D_2O using 15% (w/v) NaOH

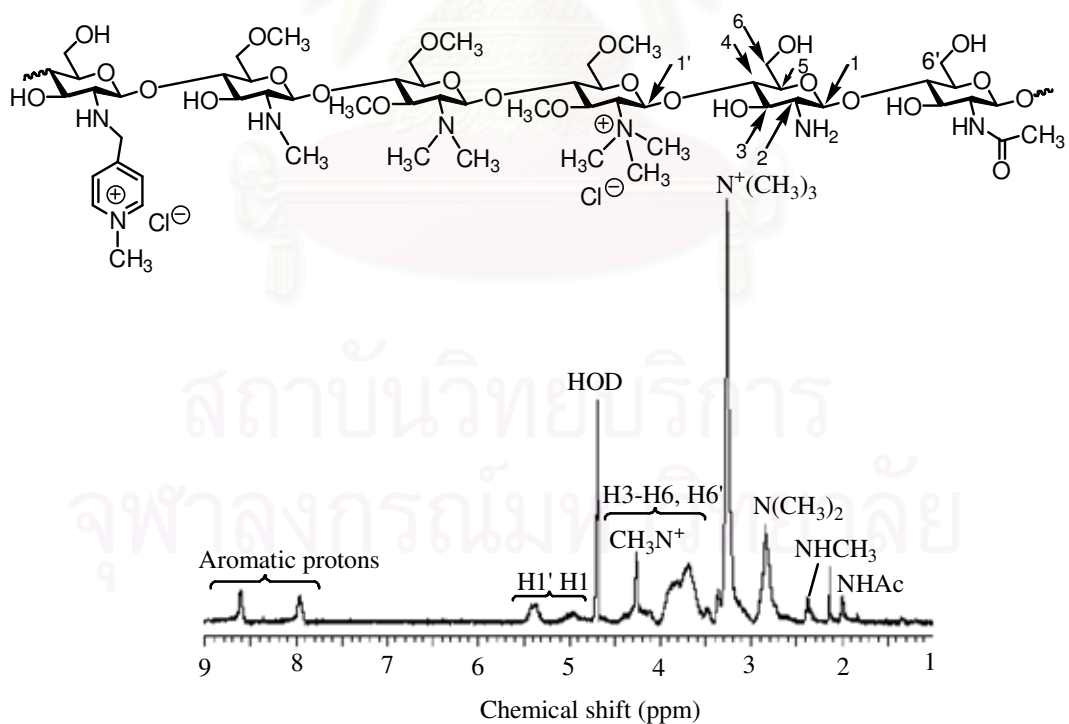


Figure 4.17: ^1H -NMR spectrum of quaternized *N*-(4-pyridylmethyl)chitosan with ES 12.5% in D_2O using 15% (w/v) NaOH

The ^{13}C -NMR spectrum of $\text{QN}(\text{CH}_3)_2\text{-BzCh}_3$ is shown in Figure 4.18. The aromatic carbon signals exhibited at δ 145, 141, 131, and 119 ppm. The other carbon signals were at δ 96.3-58.7, 57.0, 53.8, 41.8, and 36.3 ppm due to C1-C6, *N,N,N*-trimethyl carbons of the aromatic substituent, *N,N*-dimethyl carbons, and *N*-methyl carbons of the GlcN of chitosan, respectively.

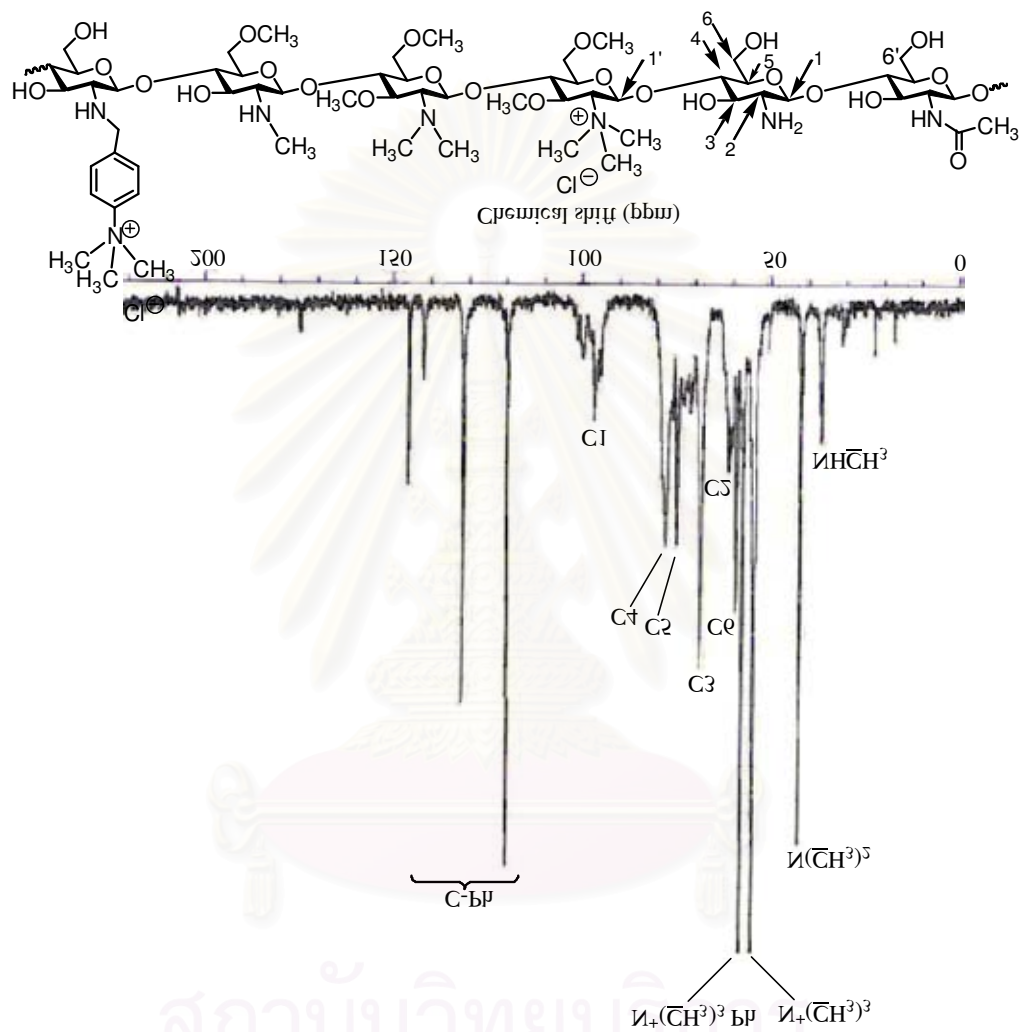


Figure 4.18: ^{13}C -NMR spectrum of quaternized *N*-(4-*N,N*-dimethylaminobenzyl) chitosan with ES 17.5% in D_2O using 5% (w/v) NaOH

4.7.4 Chemoselective methylation of *N*-(4-*N,N*-dimethylaminobenzyl) chitosan and *N*-(4-pyridylmethyl)chitosan

Single treatment methylation with iodomethane of $N(\text{CH}_3)_2\text{-BzCh}$ and PyMeCh with various ES's was studied. The results of chemoselective methylation of both chitosan derivatives are shown in Table 4.4. *N*-methylation leading to

Table 4.4: Quaternization of chitosan and *N*-benzyl chitosans using iodomethane

Samples	ES (%)	NaOH (w/v) (%)	DQ _T (%)		N(CH ₃) ₂ (%)	NHCH ₃ (%)	3- <i>O</i> (%)	6- <i>O</i> (%)	Recovery (%)
			DQ _{Ar} (%)	DQ _{Ch} (%)					
TMChC	-	15	-	31	23	Trace	10	23	82
HDQ-TMChC	-	15	-	89	Trace	Trace	80	97	28
QMe-BzCh1	11.0	5	-	ND	32	10	ND	ND	80
QMe-BzCh2	11.0	15	-	11	61	ND	ND	Trace	76
QN(CH ₃) ₂ -BzCh1	2.7	15	2.7	27	48	Trace	Trace	7	86
QN(CH ₃) ₂ -BzCh2	10.0	5	10.0	12	65	Trace	ND	7	74
QN(CH ₃) ₂ -BzCh3	17.5	5	17.5	16	28	13	ND	7	80
QN(CH ₃) ₂ -BzCh4	17.5	15	17.5	30	20	17	Trace	15	68
QN(CH ₃) ₂ -BzCh5	42.5	5	42.5	5	Trace	7	ND	Trace	78
QN(CH ₃) ₂ -BzCh6	42.5	15	42.5	14	Trace	12	Trace	17	84
QPyMeCh1	12.5	5	12.5	18	45	Trace	ND	Trace	86
QPyMeCh2	12.5	15	12.5	36	22	7	3.3	7	76

ES is the extent of *N*-substitution; DQ_{Ar} is degree of quaternization at aromatic substituents; DQ_{Ch} is degree of quaternization; N(CH₃)₂ is *N,N*-dimethylation; NHCH₃ is *N*-methylation; Total DOM is total degree of *O*-methylation at 3-hydroxy and 6-hydroxy positions of GlcN of chitosan, respectively; Recovery (%) is weight of product (g) / weight of starting reactant (g)×100; ND is non detectable.

quaternization of $N(\text{CH}_3)_2\text{-BzCh}$ and PyMeCh can occur at both the aromatic substituent and primary amino group of GlcN of chitosan. The results clearly exhibited that the total degree of quaternization (DQ_T), $\text{DQ}_T = \text{DQ}_{Ar} + \text{DQ}_{Ch}$, increased with increasing ES of chitosan derivatives. It also indicated that *N,N*-dimethylamino group on the aromatic substituent is more reactive than the primary amino group of chitosan. In other words, all *N,N*-dimethylamino groups was completely quaternized giving

DQ_{Ar} values equal to the corresponding ES's (Table 4.4). This was confirmed by ¹H-NMR spectra shown in Figure 4.19. The signal at δ 3.1 ppm of *N,N*-dimethyl protons

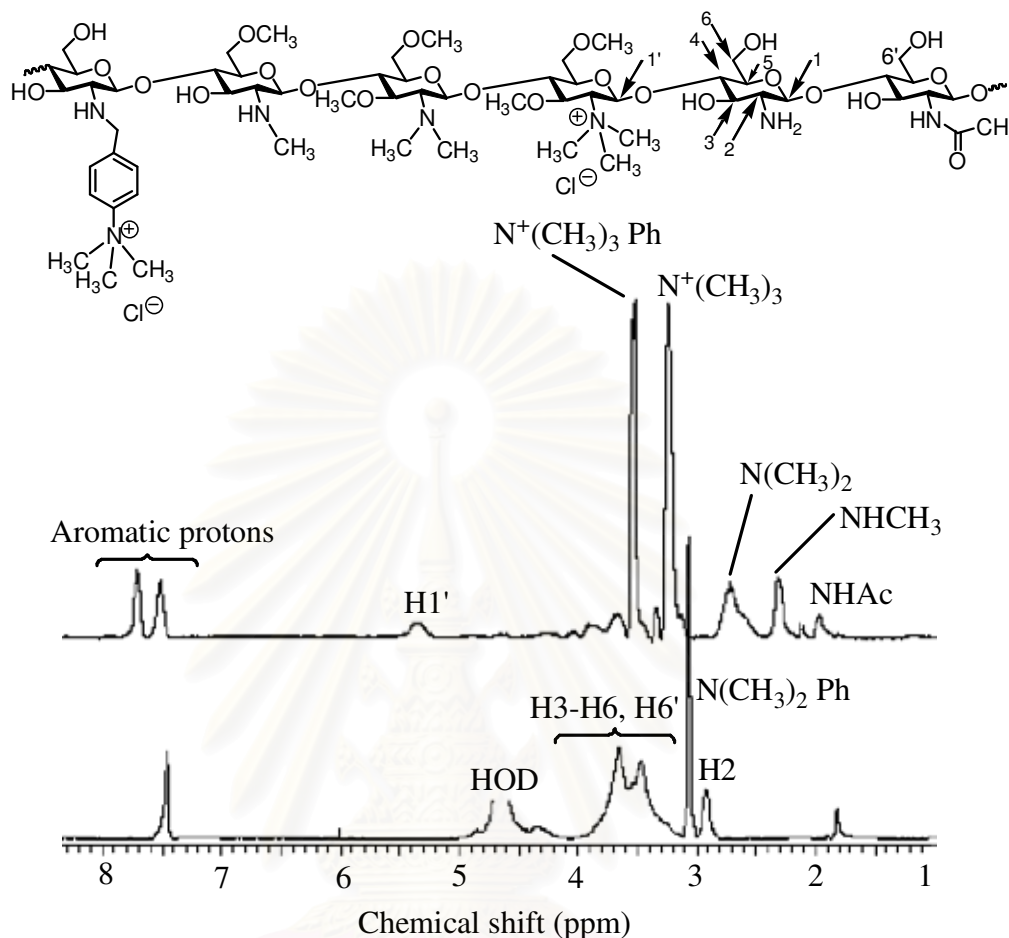


Figure 4.19: ¹H-NMR spectra of *N*-(4-*N,N*-dimethylaminobenzyl)chitosan (D₂O/CF₃COOD) and quaternized *N*-(4-*N,N*-dimethylaminobenzyl)chitosan (D₂O) with ES 17.5% using 15% (w/v) NaOH

was changed to *N,N,N*-trimethyl protons at δ 3.5 ppm on aromatic substituent [74]. However, increasing ES did not enhance DQ_{Ch} (Table 4.4). This could be attributed to the steric effect of the aromatic substituent as well as the lower numbers of the available primary amino groups of GlcN of chitosan reacting with iodomethane. Increasing the sodium hydroxide concentration from 5 to 15 % (w/v) led to the increase of DQ_T (Table 4.4 and Figure 4.20). It can be explained that sodium hydroxide is a role to prevent the protonation of unreacted primary amino group from hydroiodic acid (HI) which was by product as the methylation process by forming sodium salt. Besides quaternization, *N,N*- dimethylation and *N*-methylation at the

primary amino group of GlcN of chitosan were also observed. The *N,N*-dimethylation decreased when higher ES was introduced into the chitosan side chain. In addition, the higher sodium hydroxide concentration was used, the lower *N,N*-dimethylation were also resulted.

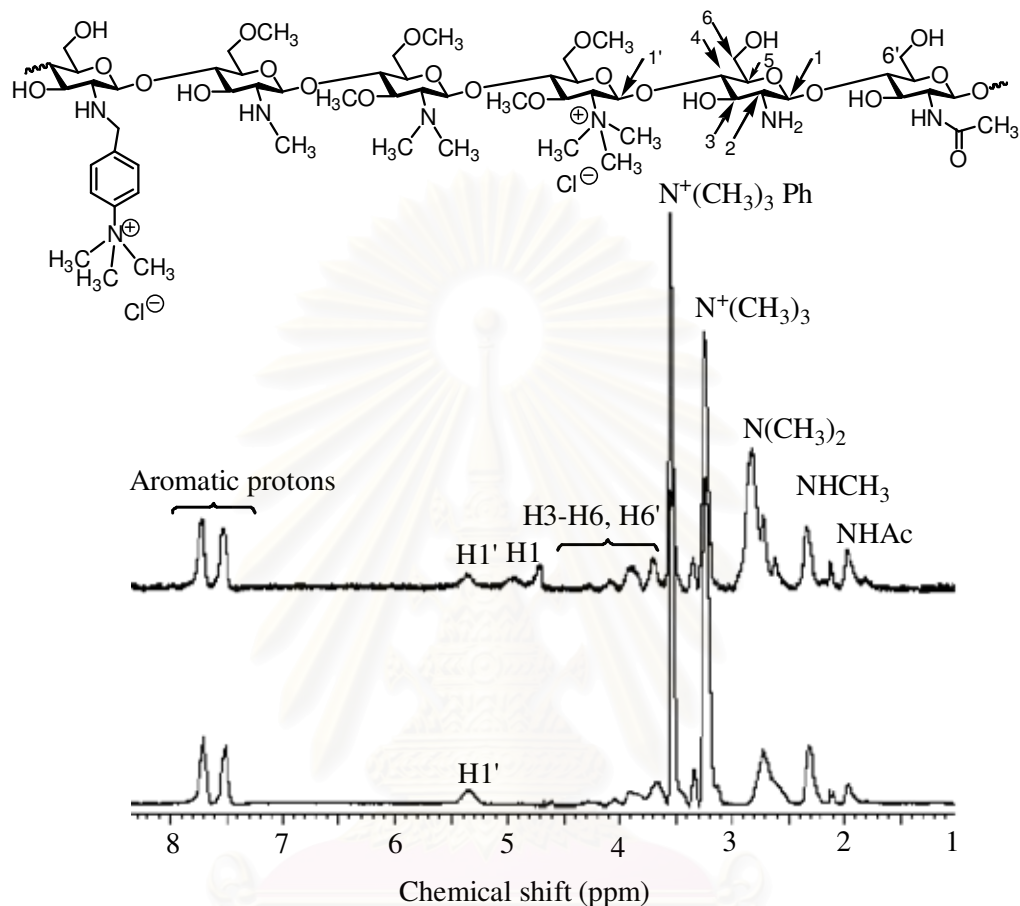


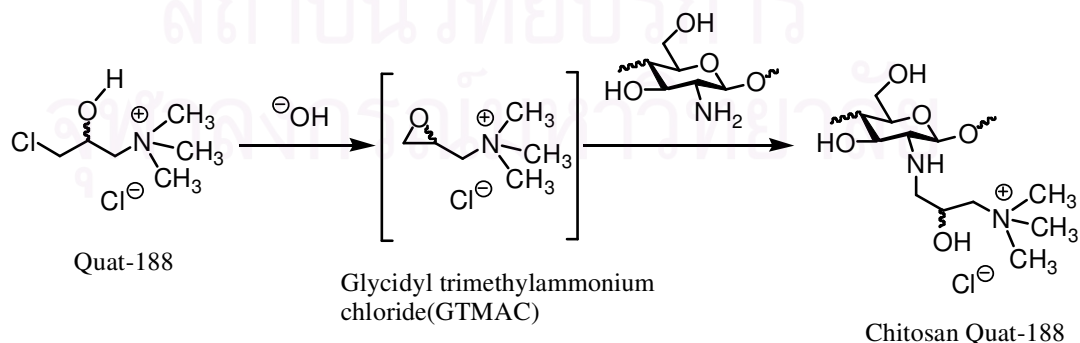
Figure 4.20: ^1H -NMR spectra of quaternized *N*-(4-*N,N*-dimethylaminobenzyl) chitosan (D_2O) with ES 17.5% using 5% and 15% (w/v) NaOH

The results also revealed that 6-*O*-methylation could occur more readily than 3-*O*-methylation (Table 4.4). This could be explained that 6-hydroxy groups could be more structurally exposed to methylation than 3-hydroxy groups due to effect of intramolecular hydrogen bonding of 3-hydroxy position. The ES insignificantly influenced the *O*-methylation while the higher concentration of sodium hydroxide could favor 6-*O*-methylation.

The presence of the aromatic substituents bearing N-atom on chitosan backbone could increase the total degree of quaternization of chitosan by single treatment with iodomethane. The concentration of sodium hydroxide obviously affected the DQ_T , DQ_{Ch} and DOM ; higher *N*-methylation and *O*-methylation of chitosan were observed when higher concentration of sodium hydroxide was used. Iodomethane reacted with either 4-*N,N*-dimethylaminobenzyl or 4-*N*-pyridylmethyl substituents more readily than the primary amino and hydroxyl groups of GlcN of chitosan. The DQ_T is the sum of substitution on the aromatic substituents bearing N-atom and the substitution of the primary amino of chitosan. In conclusion, the chemoselective methylation depended on ES and the concentration of sodium hydroxide used in the reaction.

4.8 Quaternization of chitosan and *N*-substituted chitosans using 3-chloro-2-hydroxypropyl trimethylammonium chloride

The biocidal activity of chitosan can be increased by at least an order of magnitude by treatment with *N*-3-chloro-2-hydroxypropyl trimethylammonium chloride (Quat-188) [26,56]. The treatment inserts a quaternary ammonium function which is effective in solubilizing derivatives with hydrophobic substituents in water at all pH ranges. Quaternization is performed using commercially available Quat-188 in a heterogeneous process under alkaline conditions. Under this condition, Quat-188 readily generates the corresponding epoxide, which reacts with the primary amino groups of chitosan in a nucleophilic substitution pathway (Scheme 4.3) to introduce the quaternary ammonium substituent.



Scheme 4.3: Synthetic pathway of chitosan Quat-188

The quaternization process imparts water solubility to the *N*-benzyl chitosans over a wide pH range. A similar quaternization of chitosan using glycidyl trimethyl ammonium chloride (GTMAC) has been reported [57-62]. However, in this study, commercially available Quat-188 was selected. In this study, the degree of quaternization (DQ_{Ch}) of chitosan Quat-188 (ChQ) was determined by titration with aqueous silver nitrate and applying Equation 4.3 [62,75].

$$DQ_{Ch} (\text{mol}\%) = \left[\frac{\frac{VC}{1000}}{\frac{VC}{1000} + \frac{W_1(DA)}{Mw_1} + \frac{(W_1 DDA - W_2)}{Mw_2}} \right] \times 100 \quad (4.3)$$

Where V and C are the volume and concentration of silver nitrate solution, respectively, DA, and DDA are the degree of acetylation and deacetylation of chitosan, Mw_1 and Mw_2 are the molecular weight of GlcNAc and GlcN units, respectively, W_1 is the weight of the test sample and W_2 is calculated by the following Equation 4.4.

$$W_2 = \frac{VC Mw_3}{1000} \quad (4.4)$$

Where Mw_3 is the molecular weight of the repeating unit of chitosan Quat-188. For DQ_{Ch} of *N*-benzyl chitosan derivatives Quat-188 was calculated by modifying Equation 4.3.

The FT-IR spectrum of the ChQ (Figure 4.21) showed the presence of an absorption band at 1480 cm^{-1} due to C-H symmetric bending of the methyl groups on the quaternary ammonium substituents [15]. The $^1\text{H-NMR}$ spectrum of ChQ (Figure 4.22) exhibited characteristic resonances at δ 4.20, 3.3, 3.2, and 2.9 ppm which are attributed to methine protons (b), methylene protons (c), *N,N,N*-trimethyl protons (d), and methylene protons (a), respectively.

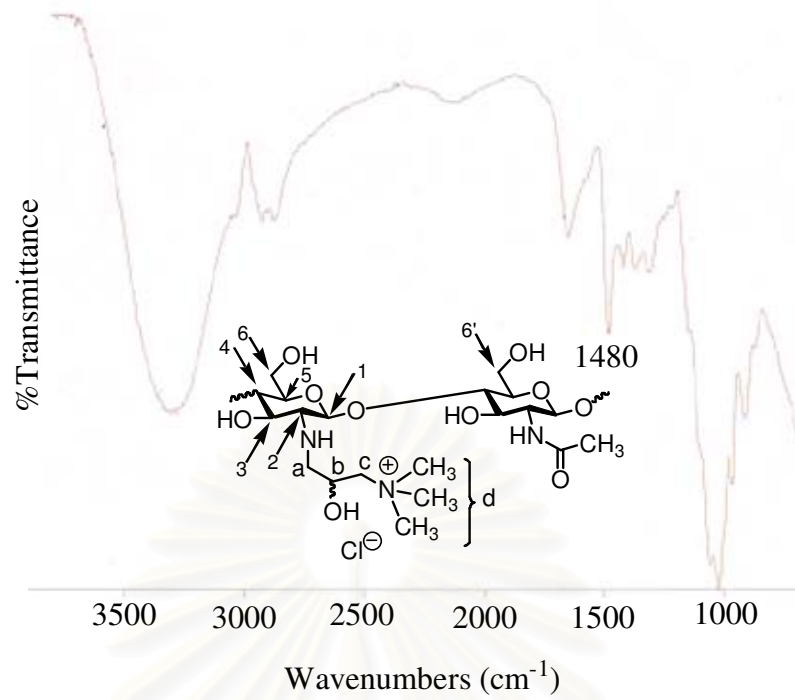


Figure 4.21: FT-IR (KBr) spectrum of chitosan Quat-188

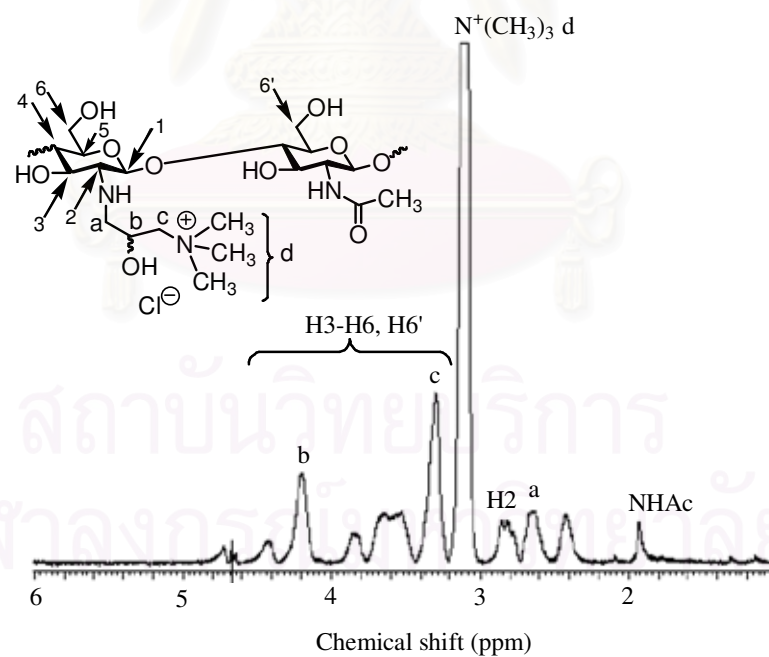


Figure 4.22: $^1\text{H-NMR}$ spectrum of chitosan Quat-188 in D_2O

The ^{13}C -NMR spectrum of ChQ (Figure 4.23) contained the signals at δ 68.9, 65.0, 64.5, 54.0, and 51.6 ppm due to methylene carbons (c), methine carbons (b), *N,N,N*-trimethyl carbons (d), and methylene carbons (a), respectively. This was consistent with the spectra reported by Loubaki *et al.* [15].

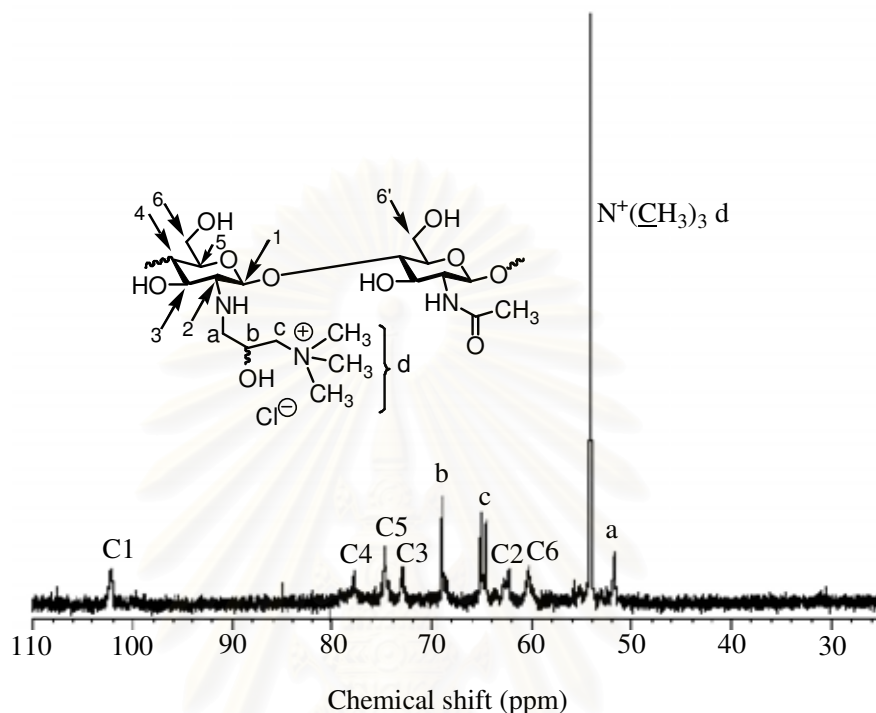


Figure 4.23: ^{13}C -NMR spectrum of chitosan Quat-188 in D_2O

In this work, the DQ_{Ch} of ChQ can be calculated as well from the ^1H -NMR spectrum using the ratio of the integral area of methine protons (b) at δ 4.2 ppm relative to the integral area of 1/3*N*-acetyl proton of GlcNAc δ 1.9 ppm as shown in Equation 4.5

$$\text{DQ}_{\text{Ch}} (\text{mol}\%) = \left[\frac{\text{Integral area (b)}}{\text{Integral area (b)} + \frac{1}{3}(\text{NAc})} \right] \times 100 \quad (4.5)$$

Where NAc is integral area of GlcNAc protons.

The FT-IR spectra of OctCh and all *N*-benzyl chitosan derivatives Quat-188 were similar to those of OctCh and all *N*-benzyl chitosan derivatives except the absorption band at wavenumber 1480 cm^{-1} due to C-H symmetric bending of the quaternary ammonium groups.

Figure 4.24 and Figure 4.25 exhibit the $^1\text{H-NMR}$ spectrum of OctCh Quat-188 and $^1\text{H-NMR}$ spectra of selected *N*-benzyl chitosan Quat-188, respectively. They were similar to those of the OctCh and selected *N*-benzyl chitosan except the additional signals at δ 4.20, 3.3, 3.3, and 2.9 ppm which belonged to methine protons (b), methylene protons (c), *N,N,N*-trimethyl protons, and methylene protons (a), respectively.

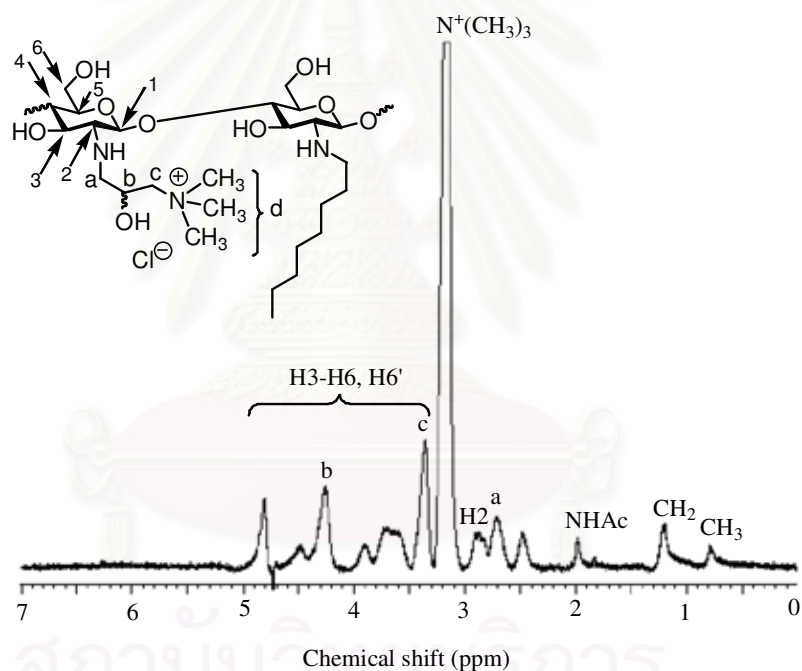
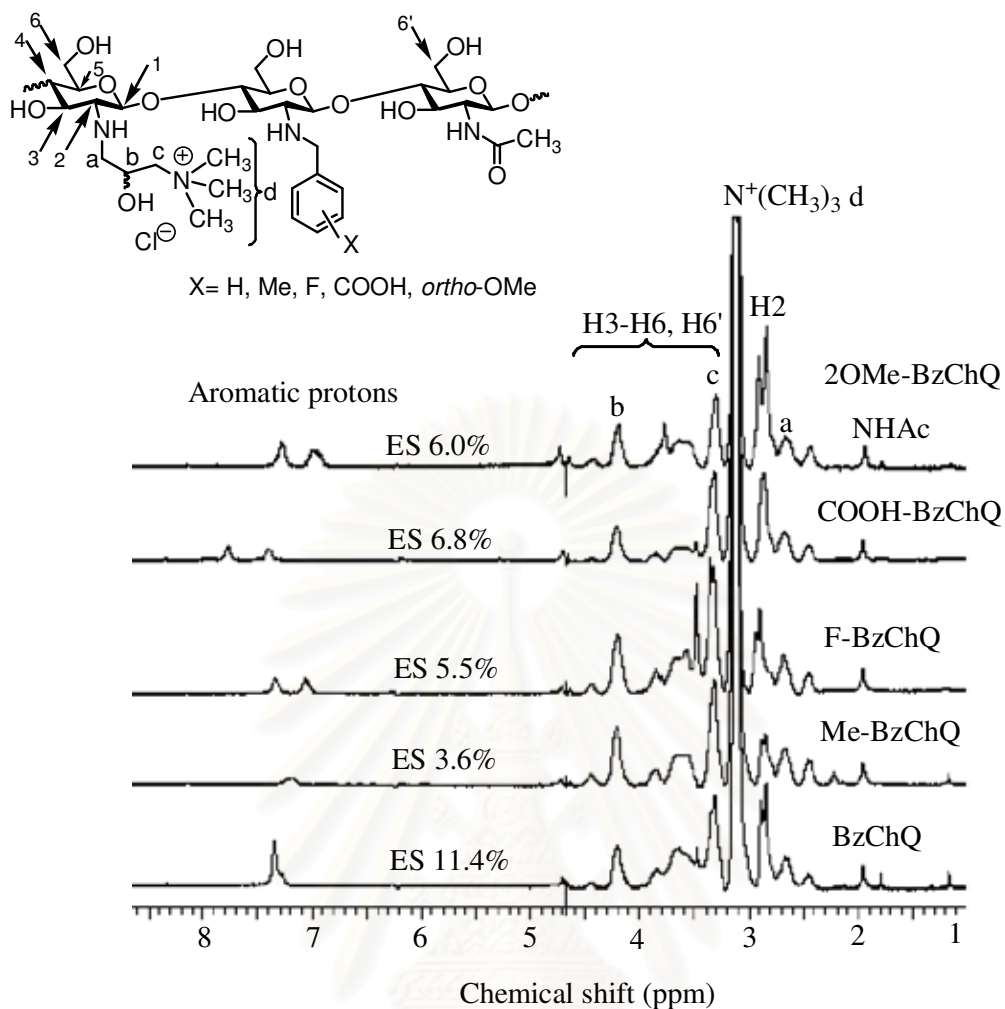


Figure 4.24: $^1\text{H-NMR}$ spectrum of *N*-n-octyl chitosan Quat-188 with ES 4.7% in D_2O



BzChQ, *N*-Benzyl chitosan Quat-188; Me-BzChQ, *N*-(4-Methylbenzyl)chitosan Quat-188; F-BzChQ, *N*-(4-Fluorobenzyl)chitosan Quat-188; COOH-BzChQ, *N*-(4-Carboxybenzyl) chitosan Quat-188; 2OMe-BzChQ, *N*-(2-Methoxybenzyl)chitosan Quat-188.

Figure 4.25: ^1H -NMR spectra of selected *N*-benzyl chitosans Quat-188 in D_2O

Figure 4.26 and Figure 4.27 exhibit the ^{13}C -NMR spectra of BzChQ and 2ThMeChQ, respectively. It was similar to that of ChQ except the signals at δ 130 ppm which belonged to aromatic carbons.

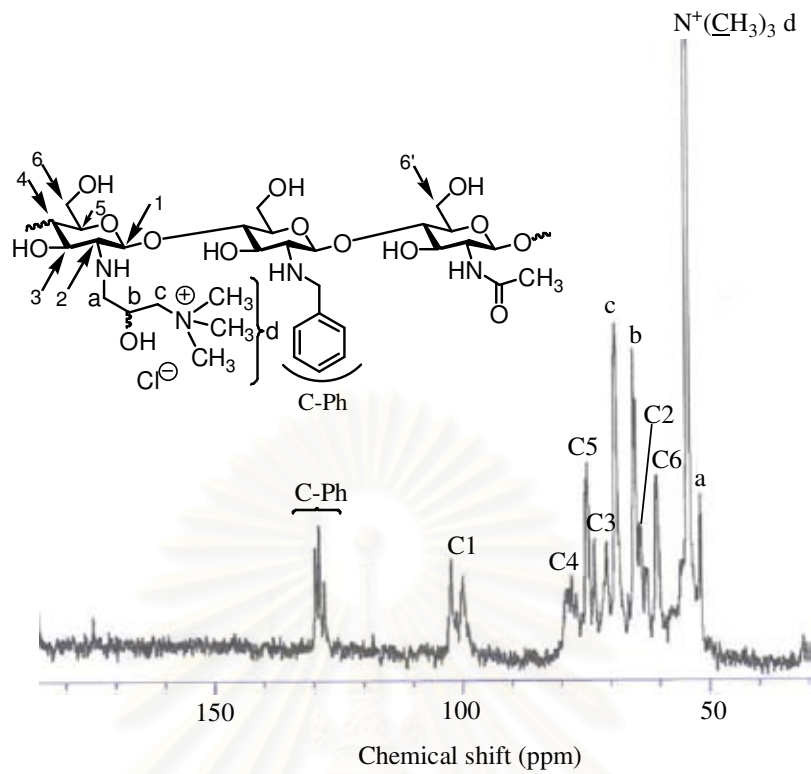


Figure 4.26: ^{13}C -NMR spectrum of *N*-benzyl chitosan Quat-188 with ES 11.4% in D_2O

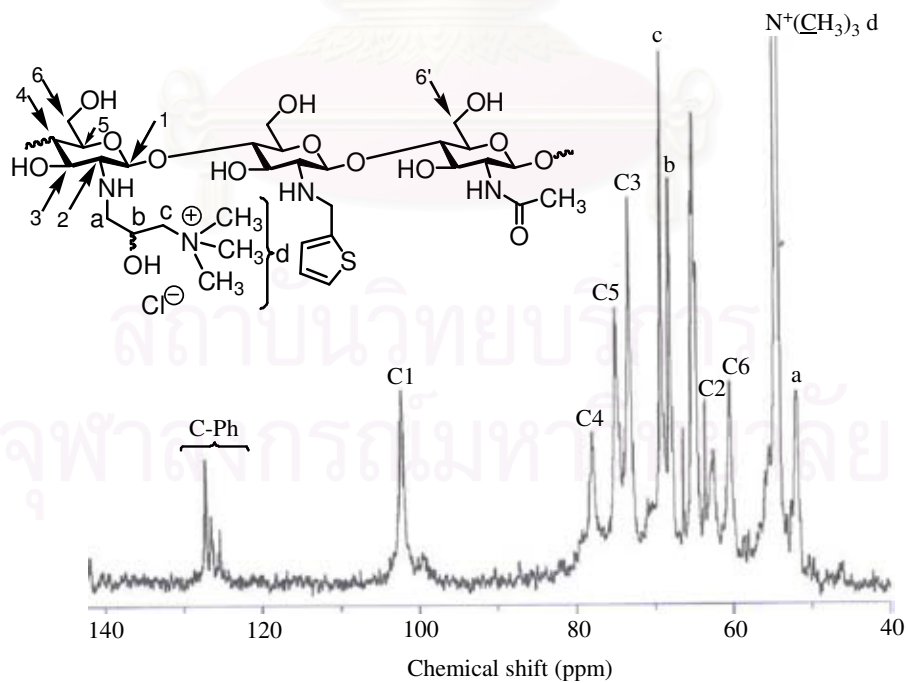


Figure 4.27: ^{13}C -NMR spectrum of *N*-(2-thiophenylmethyl)chitosan Quat-188 with ES 9.6% in D_2O

In Table 4.5, when ES decreased, DQ_{Ch} increased obviously due to more free amino groups of GlcN of chitosan reacting with Quat-188. The water solubility of quaternized chitosan using Quat-188 was better than that of quaternized chitosan using iodomethane. The DQ_{Ch} more than 58.4% were readily water soluble.

Table 4.5: Quaternization of chitosan and *N*-benzyl chitosans using Quat-188

Samples	ES(%)	DQ _{Ch} (%)		Solubility in water (10 mg/mL)	Yield (%)
		¹ H-NMR	Titration		
ChQ	-	93.0	91.2	++	57.9
	-	83.0	78.6	++	63.8
OctChQ	10.3	78.4	66.5	+	74.5
	4.7	83.3	75.1	++	66.7
	1.8	93.0	82.3	++	58.9
BzChQ	18.5	68.2	60.0	++	54.7
	11.4	79.7	75.1	++	74.9
	3.6	89.5	86.4	++	67.8.
	2.3	92.8	86.7	++	81.4
Me-BzChQ	15.6	73.0	68.5	++	81.4
	11.0	86.9	79.5	++	60.3
	3.4	91.2	86.7	++	74.7
	1.7	92.8	88.4	++	65.3
OH-BzChQ	6.4	86.4	84.2	+	75.9
	3.1	90.4	86.7	++	78.7
2OMe-BzChQ	6.0	71.6	67.7	++	86.7
4OMe-BzChQ	8.0	60.3	68.4	++	83.3
34OMe-BzChQ	7.8	69.8	65.4	++	78.9
N(CH ₃) ₂ -BzChQ	5.9	57.6	58.4	+	76.3
	2.7	92.8	84.4	++	80.6
F-BzChQ	25.7	57.6	69.3	++	90.2
	17.5	66.4	60.2	++	87.7
	5.5	84.5	84.9	++	84.4
	2.5	92.8	86.7	++	70.4

Table 4.5: Quaternization of chitosan and *N*-benzyl chitosans using Quat-188 (cont.)

Samples	ES(%)	DQ _{Ch} (%)		Water solubility (10 mg/mL)	Yield (%)
		¹ H-NMR	Titration		
Cl-BzChQ	10.0	86.4	78.3	++	85.4
3Br-BzChQ	12.5	78.4	60.0	++	79.6
4Br-BzChQ	11.2	77.3	64.2	++	82.8
CF ₃ -BzChQ	35.8	57.6	54.7	+	75.4
	6.7	89.4	75.6	++	85.3
	4.6	90.4	82.3	++	64.5
NO ₂ -BzChQ	35.1	57.6	51.4	+	60.7
	24.7	67.8	60.6	++	59.4
	8.3	86.2	78.3	++	83.4
	3.3	90.4	84.2	++	64.5
COOH-BzChQ	12.5	78.9	79.8	++	82.2
	6.8	84.5	82.3	++	76.9
PyMeChQ	30.4	60.2	54.2	++	78.4
	20.3	73.0	64.5	++	58.6
	5.2	87.6	80.5	++	67.5
	3.0	91.2	86.4	++	73.8
2ThMeChQ	13.3	-	-	-	-
	9.6	72.4	70.8	++	73.6
	3.2	84.9	74.0	++	68.4

++ readily soluble; + totally soluble in one minute; - non insoluble

Yield (%) = ([weight of *N*-benzyl chitosan derivatives Quat-188 (g) × FW of *N*-benzyl chitosan derivatives] / [0.5 (g) × calculated FW of *N*-benzyl chitosan derivatives Quat-188]) ×100.

4.9 Reduction in molecular weight of chitosan during derivatization

The molecular weight of chitosan is one of the important factors affecting the antibacterial activity. Chitosan is more effective in inhibiting growth of bacteria than chitosan oligomers [76], and the molecular weight of chitooligosaccharides is critical for microorganism inhibition; it should be higher than 10,000 [77]. The antibacterial activity against *E.coli* of quaternized chitosan with molecular weight 214,000, molecular weight of starting chitosan, was higher than that of the chitosan reported by Jia *et al.* [29]. The molecular weight of chitosan before and after derivatization had been studied for antibacterial activity [34,78]. No other literature references report the effect of chemical modification on the molecular weight of the corresponding derivatives.

Recently, a new type of gel permeation chromatography (GPC) column, ViscoGEL Poly-CAT™, that can be used under dilute acidic condition was developed [79]. Using these columns with multiple detections, i.e., differential reflective index, multi-angles light-scattering and viscometry, enabled us to ascertain the change in molecular weight resulting for each step of the benzylation process. Different samples were passed through the equipment to get the molar mass distribution (Figure 4.28) from which the function radius of gyration (R_g) is obtained directly (Figure 4.29). First, the increment of refractive index (dn/dc) was determined. The dn/dc was later used to calculate the exact value of molecular weight by GPC coupled with a multi-angles laser light-scattering detector shown in Table 4.6. Light-scattering was also used to measure the weight-average molecular weight (M_w) (Table 4.6) of chitosan and its derivatives samples. Every sample measurement was repeated three times.

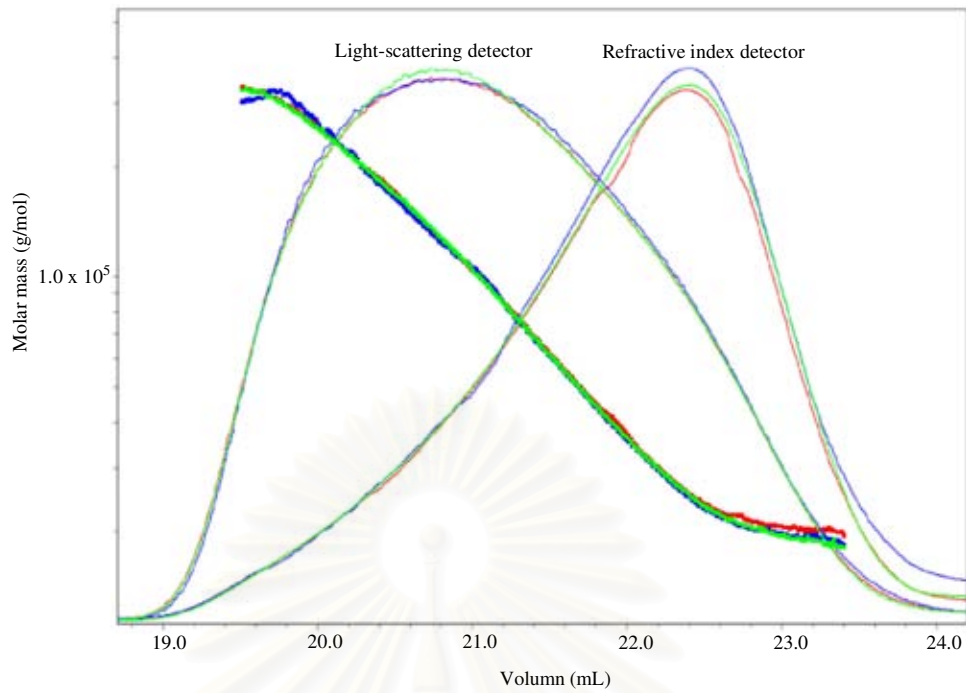


Figure 4.28: Examples of differential distribution of molar mass obtained by GPC on a quaternized *N*-(4-*N,N*-dimethylaminobenzyl)chitosan with ES 17.5% using iodomethane when 5% (w/v) NaOH was used

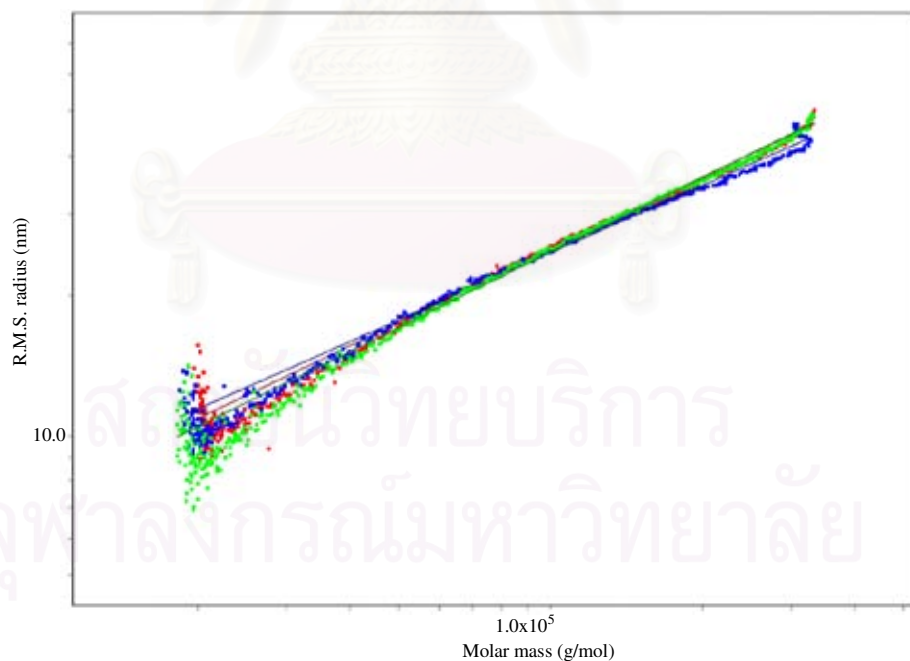


Figure 4.29: Radius of gyration (RMS) expressed in nm plotted as a function of the molar mass (g/mol) on a quaternized *N*-(4-*N,N*-dimethylaminobenzyl)chitosan with ES 17.5% using iodomethane when 5% (w/v) NaOH was used

Table 4.6: Determination of the increment of refractive index, the molecular weight and the radius of gyration from chitosan and its derivatives

Chitosan derivatives	ES (%)	DQ _{Ch} (%) [*]	dn/dc	M _n kDa	M _w kDa	M _w /M _n	R _g	η (mL/g)
Ch	-	-	0.165	87	276	3.2	56.4	434.5
BzCh	3.6	-	0.149	65	144	2.2	60.0	167.7
2OMe-BzCh	6.0	-	0.149	81	130	1.7	20.5-	146.5
NO ₂ -BzCh	8.3	-	0.149	42	124	2.9	28.8	173.9
TMChC	-	31.1	0.128	71	162	2.3	28.4	121.7
QN(CH ₃) ₂ -BzCh	17.5	18.9 ¹	0.151	35	62	1.8	27.9	90.1
ChQ	-	91.2	0.134	44	70	1.6	10.9	41.9
BzChQ	3.6	87.5	0.150	17	26	1.5	24.3	26.7
Me-BzChQ	15.6	76.6	0.165	11	29	2.6	5.1	39.6
NO ₂ -BzChQ	3.3	87.5	0.140	20	65	3.2	5.7	28.7
NO ₂ -BzChQ	8.3	83.9	0.146	17	26	1.5	6.7	23.3
PyMeChQ	5.2	87.5	0.149	24	46	1.9	16.7	32.6
2ThMeChQ	3.2	85.7	0.155	16	34	2.1	24.5	20.0

^{*}DQ_{Ch} was determined by titrating with silver nitrate

From Table 4.6, it was found that treatment with benzaldehyde and Borch reduction caused the molecular weight to decrease as observed from Ch and BzCh. The reduction in molecular weight and narrowing of the M_w/M_n were consistent with a random cleavage with backbone under these reaction conditions. The indicated molecular weight of chitosan in *N*-benzylation step was slightly decreased. In contrast, the quaternization of the BzCh with Quat-188 was accompanied by numerous backbone cleavages and a concomitant reduction in the molecular weight of the quaternized product. The molecular weight of BzChQ with an ES 3.6% was decreased compared to that of Ch [80].

Surprisingly, these reactions which were conducted under basic conditions led to substantial degradation of the chitosan backbone. No effort was made to exclude oxygen from these reactions, so an oxidative degradation process was proposed. These results demonstrated that estimating molecular weights of chitosan products based upon the initial molecular weight of the starting chitosan can be misleading. The low value of the R_g indicated that the quaternized derivatives might be able to diffuse through bacterial cell walls, and thus they were more effective biocides.



สถาบันวิทยบริการ
จุฬาลงกรณ์มหาวิทยาลัย

PART C: ANTIBACTERIAL ACTIVITY OF QUATERNIZED CHITOSAN AND N-SUBSTITUTED CHITOSANS

The antimicrobial activity of chitosan has been observed against a wide variety of microorganisms, including fungi, algae, and bacteria. However, the antimicrobial action is greatly influenced by many factors, such as the source of chitosan, concentration, DDA, molecular weight, type of microorganism, pH of growth medium and environmental conditions. MIC of chitosan for Gram-positive and Gram-negative bacteria vary widely from 10-1000 $\mu\text{g}/\text{mL}$ depending on the factors above [5]. Generally, Gram-positive cell walls are much thicker and far less structured than Gram-negative ones. However, the outer membrane of Gram-negative bacteria has lipopolysaccharide (LPS) that contains endotoxin as a toxic substance. Quaternary ammonium derivatives of chitosan show enhanced antibacterial activity compared to the native chitosan. Quaternization also generates a permanent positive charge on the polymer backbone which renders water solubility to such derivatives under neutral pH conditions.

Antibacterial activities of quaternized chitosans and its derivatives were evaluated using MIC values against *S.aureus* (Gram-positive) and *E.coli* (Gram-negative) bacteria at pH 7.0. Higher MIC values indicated lower antibacterial activities (Tables 4.7 and 4.8). The MIC data show that the ES had a considerable influence on the antibacterial activity against the bacterium. When ES increased, antibacterial activity decreased. This was because of the decreasing number of available free amines for quaternization, meaning less cationic charge density placed on the chitosan backbone. All quaternized chitosan derivatives in this study showed very low MIC values which were in the range of 8-64 $\mu\text{g}/\text{mL}$ against both bacteria, compared to other quaternized chitosans which had much higher MIC values ranged from 500-2048 $\mu\text{g}/\text{mL}$ in the same neutral medium [34,78]. The MIC results of water soluble quaternized chitosan derivatives obtained by using iodomethane and Quat-188 were also compared.

4.10 Antibacterial activity of quaternized chitosan and *N*-substituted chitosans using iodomethane

The antibacterial activity of quaternized chitosan derivatives compared to that of quaternized chitosan is shown in Table 4.7.

Table 4.7: Antibacterial activity of quaternized of chitosan and *N*-benzyl chitosans using iodomethane

Samples	ES (%)	Water solubility	DQ _T (%)		MIC (μg/mL)	
			DQ _{Ar}	DQ _{Ch}	<i>S.aureus</i>	<i>E.coli</i>
TMChC	-	++	-	31	32	128
HDQ-TMChC	-	+	-	88	64	128
QN(CH ₃) ₂ -BzCh1	2.7	++	3	27	32	128
QN(CH ₃) ₂ -BzCh2	10.0	++	10	12	64	128
QN(CH ₃) ₂ -BzCh3	17.5	++	17	16	32	64
QN(CH ₃) ₂ -BzCh4	17.5	++	17	30	32	64
QN(CH ₃) ₂ -BzCh5	42.5	+	42	5	64	128
QN(CH ₃) ₂ -BzCh6	42.5	+	42	14	32	128
QPyMeCh1	12.5	++	12	18	128	128
QPyMeCh2	12.5	++	12	36	64	128

++ clearly solution

+ slightly turbidity

*DQ_{Ch} (%) was determined by ¹H-NMR.

The higher degree of quaternization (DQ_{Ch}) exhibited enhanced antibacterial activity due to electrostatic interactions between the positively charged of quaternary ammonium group of chitosan macromolecule and negatively charged bacterial cell wall which is accordingly disrupted and disintegrated [31]. HDQ-TMChC, however, has higher QD_{Ch} than TMChC but its antibacterial activity against *S.aureus* was lower. It was probably due to its low solubility in water [50].

Introduction of the *N,N*-dimethylaminobenzyl and *N*-pyridylmethyl substituents into chitosan backbone did not contribute the antibacterial activity. Although total degrees of quaternization (DQ_T) were rather higher, the antibacterial activity did not dramatically increased. It was noted that the antibacterial activity of quaternized chitosan and its derivatives were more active against *S.aureus* (Gram-positive) than *E.coli* (Gram-negative) bacteria due to the different component of bacterial cell wall.

4.11 Antibacterial activity of quaternized chitosan and *N*-substituted chitosans using Quat-188

Antibacterial activity of quaternized chitosans and its derivatives were evaluated using minimum inhibitory concentration (MIC) procedure against *S.aureus* (Gram-positive) and *E.coli* (Gram-negative) bacteria at pH 7.0, where a higher MIC value indicates lower antibacterial activity. As shown in Table 4.8, the MIC data show that the ES has a considerable influence on the antibacterial activity against the bacterium. When ES increases, antibacterial activity decreases. This is attributed to the decreasing number of available amines for quaternization, which means less cationic charge density can be placed on the chitosan backbone. All quaternized chitosan derivatives in this study showed very low MIC values, which was in the range of 8-64 µg/mL against both bacteria, compared to other quaternized chitosans, which had much higher MIC values ranging from 500-2048 µg/mL against *S.aureus* and *E. coli* bacteria in the same neutral medium [35,78]. However, the MIC value is influenced by intrinsic factors and the environmental conditions [5]. In comparison to *N*-n-octyl chitosan at the same degree of quaternization, the presence of benzyl substituents in chitosan obviously enhanced antibacterial activity against *S.aureus* bacteria. At the same level of quaternization, all quaternized *N*-benzyl chitosan derivatives exhibited better antibacterial activity than quaternized chitosan, although few of them might be evaluated to have at least comparable antibacterial activity to quaternized chitosan. On the other hand, either electron donating or electron withdrawing substituents decreased the antibacterial activity against *S.aureus* bacteria relative to a corresponding content of benzyl substituents in chitosan. However, their antibacterial activity is better than quaternized chitosan at the proximate level of

degree of quaternization. Surprisingly, *N*-(2-Thiophenylmethyl) chitosan Quat-188 with ES 3.2% exhibited higher antibacterial activity than quaternized chitosan against both *S.aureus* and *E. coli* bacteria.

The mechanism of antibacterial activity of chitosan and their derivatives is still not resolved. However, it is proposed that the positive charge density of quaternized chitosan absorbed onto the negatively charged cell surface of bacteria leads to the leakage of proteinaceous and other intracellular constituents [5-11]. An additional effect deriving from the hydrophobic-hydrophobic interactions between the benzyl substituent and the hydrophobic interior of the bacterial cell wall is proposed from our results. The similar result was reported by Kim and co-workers, who reported that alkyl substituent with increased chain length on the quaternary ammonium chitosan salt displayed higher antibacterial activity as well [28]. These results clearly demonstrated that hydrophobicity and cationic charge of the introduced substituent strongly affect the antibacterial activity of quaternized chitosan derivatives. On the other hand, if ES higher than 30%, a reduction of the antibacterial activity resulted. The quaternized *N*-benzyl chitosan derivatives were not as effective against *E.coli* bacteria as against *S.aureus* bacteria. The antibacterial activity of chitosan towards Gram-negative bacteria should be considered in terms of its chemical and structural properties [81]. These chitosan derivatives may not be able to penetrate the outer membrane (OM) of Gram-negative bacteria, since this membrane functions as an efficient outer permeability barrier against macromolecules. Furthermore, neither electron donating nor electron withdrawing groups on quaternized *N*-benzyl substituents nor their positions on the benzene ring significantly affects the antibacterial activity against either bacteria.

จุฬาลงกรณ์มหาวิทยาลัย

Table 4.8: Antibacterial activity of quaternized of chitosan and *N*-benzyl chitosans using Quat-188

Samples	ES (%)	DQ (%) ^a	DQ (%) ^b	MIC (MIC _{DQ}) ^c , µg/mL	
				<i>S. aureus</i>	<i>E. coli</i>
ChQ	-	93.0	91.2	64 (57)	64 (57)
	-	83.0	78.6	16 (16)	32 (31)
OctChQ	10.3	78.4	66.5	32 (23)	32 (23)
	4.7	83.3	75.1	16 (13)	32 (26)
	1.8	93.0	82.3	16 (14)	32 (27)
BzChQ	18.5	68.2	60.0	32 (22)	32 (22)
	11.4	79.7	75.1	8 (7)	32 (26)
	3.6	89.5	86.4	8 (8)	32 (29)
	2.3	92.8	86.7	8 (8)	32 (29)
CH ₃ -BzChQ	15.6	73.0	68.5	16 (13)	32 (26)
	11.0	86.9	79.5	16 (15)	32 (28)
	3.4	91.2	86.7	16 (15)	32 (30)
	1.7	92.8	88.4	16 (16)	32 (31)
HO-BzChQ	6.4	86.4	84.2	64 (56)	32 (29)
	3.1	90.4	86.7	16 (15)	32 (29)
2CH ₃ O-BzChQ	6.0	71.6	67.7	32 (23)	32 (23)
4CH ₃ O-BzChQ	8.0	60.3	68.4	32 (23)	32 (23)
3,4CH ₃ O-BzChQ	7.8	69.8	65.4	32 (22)	32 (22)
N(CH ₃) ₂ -BzCh	5.9	57.6	58.4	64(40)	64(40)
	2.7	92.8	84.4	16(15)	32(29)
F-BzChQ	25.7	57.6	69.3	32 (24)	32 (24)
	17.5	66.4	60.2	16 (11)	32 (21)
	5.5	84.5	84.9	16 (15)	32 (29)
	2.5	92.8	86.7	16 (16)	32 (29)

Table 4.8: Antibacterial activity of quaternized of chitosan and *N*-benzyl chitosans using Quat-188 (cont.)

Samples	ES (%)	DQ (%) ^a	DQ (%) ^b	MIC (MIC _{DQ}) ^c , µg/mL	
				<i>S. aureus</i>	<i>E. coli</i>
Cl-BzChQ	10.0	86.4	78.3	16 (14)	32 (27)
3Br-BzChQ	12.5	78.4	60.0	32 (21)	32 (21)
4Br-BzChQ	11.2	77.3	64.2	32 (22)	32 (22)
F ₃ C-BzChQ	35.5	57.6	54.7	32 (18)	32 (18)
	6.7	89.4	75.6	16 (13)	32 (26)
	4.6	90.4	82.3	16 (14)	32 (27)
O ₂ N-BzChQ	35.1	57.6	51.4	64 (35)	64 (35)
	24.7	67.8	60.6	32 (21)	64 (41)
	8.3	86.2	78.3	16 (14)	32 (27)
	3.3	90.4	84.2	16 (15)	32 (29)
COOH-BzChQ	12.5	78.9	79.8	16 (14)	32 (27)
	6.8	84.5	82.3	16 (15)	32 (28)
PyMeChQ	30.4	60.2	54.2	64 (37)	64 (37)
	20.3	73.0	64.5	32 (22)	32 (22)
	5.2	87.6	80.5	16 (14)	32 (27)
	3.0	91.2	86.4	8 (8)	32 (29)
2ThMeChQ	9.6	72.4	70.8	16 (12)	32 (24)
	3.2	84.9	74.0	8 (7)	16 (13)

^aDQ was determined by ¹H-NMR

^bDQ was determined by titrating with silver nitrate

^cMIC_{DQ} corrected for the actual concentration of quaternary ammonium groups

CHAPTER V

CONCLUSION

N-substituted chitosans were successfully synthesized by the reductive alkylation of chitosan with various aromatic aldehydes that contained either electron donating or electron withdrawing groups under mild acidic conditions. The chemical structure and physical properties of *N*-benzyl chitosans were characterized by FTIR, ¹H-, ¹³C-NMR, TGA and DSC. The ES can be determined by ¹H-NMR spectroscopy. The ES's of *N*-benzyl chitosans controlled by the electrophilicity of the carbonyl group. The electron withdrawing substituents on the benzene ring facilitated the intermediate Schiff base formation and ultimately high ES was achieved. The solubility of *N*-benzyl chitosans depended on ES and functional group on the aromatic aldehyde. *N*-Octyl, *N*-benzyl and *N*-methylbenzyl substituents with higher ES than 18.5% would dissolve in DMSO and swelled in pyridine and NMP. Introduction of functional groups such as hydroxyl, fluoro, nitro or trifluoromethyl on the benzene ring did not enhance the solubility of the derivatives in organic solvents. Introduction of the aromatic substituents is an effective method for altering the hydrophobic character of chitosan.

Quaternary ammonium salts of chitosan and *N*-substituted chitosans were synthesized using two methods. One was the common method using iodomethane, and the other was by introducing the inherent quaternary ammonium salt using 3-chloro-2-hydroxypropyltrimethylammonium chloride (Quat-188) as the quaternizing agent.

The higher degree of quaternization (DQ_{Ch}) was resulted, particularly after sequential treatments with iodomethane as well as an increase in the *O*-methylation. The presence of the aromatic substituents bearing N-atom could increase the total degree of quaternization (DQ_T) of chitosan. The concentration of sodium hydroxide controlled the chemoselectivity of the methylation. 4-*N,N*-dimethylaminobenzyl and *N*-methylpyridyl substituents reacted with iodomethane by single treatment more readily than the primary amino and hydroxyl groups of GlcN of chitosan.

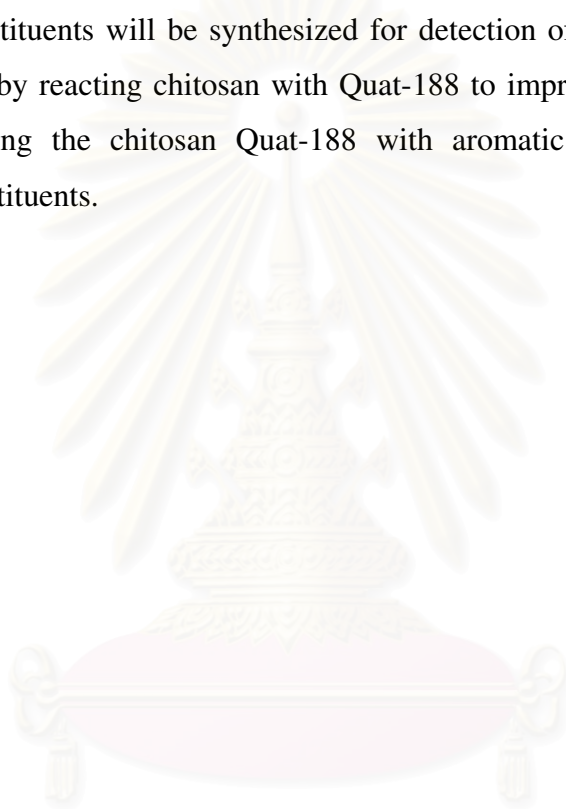
O-alkylation was not observed for quaternization of chitosan using Quat-188. Moreover, the DQ_{Ch} using Quat-188 was always higher than using iodomethane as quaternizing agent at the same level of ES.

The molecular weight of chitosan after derivatization was determined by gel permeation chromatography coupled with multiple detections, i.e., differential reflective index, multi-angles light-scattering and viscosimeter detectors. The molecular weight of chitosan was much more decreased in the quaternization step than the *N*-benzylation step. The extent of degradation depended on the reaction conditions and the number of reaction step.

Antibacterial activity of quaternized chitosan and its derivatives were evaluated using minimum inhibitory concentration (MIC) value against *S.aureus* (Gram-positive) and *E.coli* (Gram-negative) bacteria at pH 7.0. The ES had a considerable influence on the antibacterial activity against the bacteria. When ES increased, the antibacterial activity decreased. The quaternization of $N(CH_3)_2$ -BzCh and PyMeCh with iodomethane by single treatment, introducing of the *N,N*-dimethylaminobenzyl and *N*-pyridylmethyl substituents into chitosan backbone, did not alter the antibacterial activity. Although they possessed higher total degrees of quaternization (DQ_T), the antibacterial activity did not dramatically increased. In contrast, chitosan and its derivatives Quat-188 exhibited very high antibacterial activity against *S.aureus* and *E. coli* bacteria. All quaternized derivatives of chitosan showed high antibacterial activity, but derivatives with ES's higher than 20% exhibited low antibacterial activity due to the paucity of residual amines available for quaternization. However, hydrophobic-hydrophobic interactions between the benzyl and thiophenylmethyl substituents with the hydrophobic interior of the bacterial cell wall appeared to enhance the biocidal activity, especially against *S. aureus* bacteria. The results imply that *N*-benzyl chitosans Quat-188 derivatives will be useful as a potential new antibacterial agents.

FURTHRE DIRECTION

In this work, the molecular weight of chitosan was the one of the factor that affected the antibacterial activity. However, the molecular weight of chitosan reduced after derivatization. Therefore, the effect of molecular weight of chitosan derivatives on the antibacterial activity shall be studied by varing the molecular weight of the staring chitosan. The mechanism of degradation of chitosan backbone during quaternization will be studied. Moreover, water soluble chitosan containing fluorescent substituents will be synthesized for detection of a cell in order to follow the machanism by reacting chitosan with Quat-188 to improve its solubility in water and then reacting the chitosan Quat-188 with aromatic aldehydes that contains fluorescent substituents.



สถาบันวิทยบริการ
จุฬาลงกรณ์มหาวิทยาลัย

REFERENCES

- [1]. May, O. W. Polymeric Antimicrobial Agents. *In Disinfection, Sterilization and Preservation*, Fourth ed.; Block, S. S., Ed.; Philadelphia: Lea & Febiger Pub, **1991**: 322-333.
- [2]. Merianos, J. J. Surface-Active Agents: Quaternary Ammonium Compounds. *In Disinfection, Sterilization and Preservation*, Fourth ed.; Block, S. S., Ed.; Philadelphia: Lea & Febiger Pub, **1991**: 225-255.
- [3]. Thorsteinsson, T.; Masson M.; Kristinsson, K.G.; Hjalmarsdottir, M. A.; Hilmarsson, H.; Loftsson, T. Soft Antimicrobial Agents: Synthesis and Activity of Labile Environmentally Friendly Long Chain Quaternary Ammonium Compounds, *Journal of Medical Chemistry*, **2003**, 46, 4173-4181.
- [4]. Muzzarelli, R.A.A. *Chitin*, Oxford, Pergamon Press, **1997**.
- [5]. Rabea, E.I.; Badawy, M.E-T.; Stevens, C.V.; Smaghe, G.; Steurbaut, W. Chitosan as Antimicrobial Agent: Applications and Mode of Action, *Biomacromolecules (Review)*, **2003**, 4(6), 1457-1465.
- [6]. Franklin, T. J.; Snow, G.A. *Biochemistry of Antimicrobial Action*, Chapman and Hall, London: **1981**.
- [7]. Muzzarelli, R.; Tarsi, R.; Filippini, O.; Giovanetti, E.; Biagini, G.; Varaldo, P.E. Antimicrobial Properties of *N*-carboxybutyl Chitosan, *Antimicrobial Agents and Chemotherapy*, **1990**, 34(10), 2019-2023.
- [8]. Helander, I. M.; Nurmiabo-Lassila, E-L.; Ahvenainen, R.; Rhoades, J.; Roller, S. Chitosan Disrupts the Barrier Properties of Out Membrane of Geam-negative Beacteria, *International Journal of Food Microbiology*, **2001**, 71, 235-244.
- [9]. Liu, H.; Du, Y.; Wang, X.; Sun, L. Chitosan Kills Bacteria through Cell Membrane Damage, *International Journal of Food Microbiology*, **2004**, 95, 147-155.

- [10]. Je, J. Y.; Kim, S.K. Chitosan Derivatives Killed Bacteria by Disrupting the Outer and Inter Membrane, *Journal of Agricultural and Food Chemistry*, **2006**, 54(18), 5529-6633.
- [11]. Chung, Y. C.; Su, Y. P.; Chen, C. C.; Jia, G. Relationship between Antibacterial Activity of Chitosan and Surface Characteristics of Cell Wall, *Acta Pharmacologica Sinica*, **2004**, 25(7), 932-936.
- [12]. Kumar R, M. N. V.; Muzzarelli, R.A.A.; Muzzarelli, C.; Sashiwa, H.; Domb, A. J. Chitosan Chemistry and Pharmaceutical Perspectives, *Chemical Reviews*, **2004**, 104, 6017-6084.
- [13]. Sashiwa, H.; Aiba, S-I. Chemically Modified Chitin and Chitosan as Biomaterials, *Progress in Polymer Science*, **2004**, 29(9), 887-908.
- [14]. Domard, A.; Rinaudo, M.; Terrassin, C. New Method for the Quaternization of Chitosan, *International Journal of Biological Macromolecules*, **1986**, 8, 105-107.
- [15]. Loubaki, E.; Ourevitch, M.; Sicsic, S. Chemical Modification of Chitosan by Glycidyl Trimethylammonium Chloride. Characterization of Modified Chitosan by ^{13}C -and ^1H -NMR Spectroscopy, *European Polymer Journal*, **1991**, 27, 311-317.
- [16]. <http://www.hull.ac.uk/php/chsanb/LMWeb/BacterialMembranes.pdf>.
- [17]. Chen, C. Z.; Beck-Tan, N. C.; Dhurjati, P.; Dyk, T. K. V.; LaRossa, R. A.; Cooper, S. L. Quaternary Ammonium Functionalized Poly(propylene imine) Dendrimers as Effective Antimicrobials: Structure-Activity Studies, *Biomacromolecules*, **2000**, 1, 473-480.
- [18]. Franklin, T. J.; Snow, G.A. Biochemistry and Molecular Biology of Antimicrobial Drug Action, fifth ed.; Kluwer Academic Publishers: Dordrecht, The Netherlands, **1998**: 107-118.
- [19]. <http://www.Bact.wisc.edu/Microtextbook/index.php?module>
- [20]. Kumar, R. M. N. V. A Review of Chitin and Chitosan Applications, *Reactive & Functional Polymers*, **2000**, 46, 1-27.

- [21]. Senel, S.; McClure, S. J. Potential Application of Chitosan in Veterinary Medicine, *Advanced Drug Delivery Reviews*, **2004**, 56(10), 1467-1480.
- [22]. Prashanth, K. V. H.; Tharanathan, R. N. Chitin/Chitosan Modifications and their Unlimited Application Potential-an Overview, *Trends in Food Science & Technology*, **2006**, 1-15
- [23]. Rinaudo, M. Chitin and Chitosan: Properties and Applications, *Progress in Polymer Science*, **2006**, 31, 603-632.
- [24]. Chee-Shan, C.; Wan-Yu, L.; Y.; Guo-Jan.; T. Antibacterial Effects of *N*-sulfonated and *N*-sulfo benzoyl Chitosan and Application to Oyster Preservation, *Journal of Food Protection*, **1998**, 61(9), 1124-1128.
- [25]. Sudarshan, N. R.; Hoover, D. G.; Knorr, D. Antibacterial Action of Chitosan, *Food Biotechnology*, **1992**, 6(3), 257-272.
- [26]. Daly, W. H.; Manuszak-Guerrini, M. A. Biocidal Chitosan Derivatives for Cosmetics and pharmaceuticals. U.S. Patent 6,306,835, October 23, **2001**.
- [27]. Macossy, J. Ph.D. Dissertation, Louisiana State University, Baton Rouge, LA, **1995**. 46-48, 110-114.
- [28]. Kim, C. H.; Choi, J. W.; Chun, H. J.; Choi, K. S. Synthesis of Chitosan Derivatives with Quaternary Ammonium Salt and their Antibacterial Activity, *Polymer Bulletin*, **1997**, 38, 387-393.
- [29]. Jia, Z.; Shen, D.; Xu, W. Synthesis and Antibacterial Activities of Quaternary Ammonium Salt of Chitosan, *Carbohydrate Research*, **2001**, 333, 1-6.
- [30]. Kim, C. H.; Kim, S. Y.; Choi, K. S. Synthesis and Antibacterial Activity of Water-soluble Chitin Derivatives, *Polymer for Advanced Technologies*, **1996**, 8, 319-325.
- [31]. Li, Z.; Liu, X. F.; Zhuang, X.; Guan, Y.; Yao, K. Manufacture and Properties of Chitosan / *N,O*-carboxymethylated Chitosan Viscose Rayon Antibacterial Fibers, *Journal Applied Polymer Science*, **2002**, 84, 2049-2059.
- [32]. Xie, W.; Xu, P. X.; Wang, W.; Liu, Q. Preparation of Water-soluble Chitosan Derivatives and their Antibacterial Activity, *Journal Applied Polymer Science*, **2002**, 85(7), 1357-1361.

- [33]. Pospieszny, H. Antiviral Activity of Chitosan, *Crop Protection*, **1997**, 16(2), 105-106.
- [34]. Tanigawa, T.; Tanaka, Y.; Shashiwa, H.; Saimoto, H.; Shigemasa, Y. Advances in Chitin and Chitosan, Brione, C. J.; Sandford, P. A.; Zikakis, J. P.; Eds, London, New York: Elsevier Applied Science Publishers Ltd, **1992**: 156-161.
- [35]. Holappa, J.; Hjalmsdottir, M.; Masson, M.; Runarsson, O.; Asplund, T.; Soininen, P.; Nevalainen, T.; Jarvinen, T. Antimicrobial Activity of Chitosan *N*-betainates, *Carbohydrate Polymers*, **2006**, 65(1), 114-118.
- [36]. Liu, W. G.; Zhang, X.; Sun, S. J.; Sun G. J.; Yao, K. D. *N*-Acylyated Chitosan as a Potential Nonviral Vector for Gene Transfection, *Bioconjugate Chemistry*, **2003**, 14(4), 782-789.
- [37]. Desbrieres, J.; Martinez, C.; Rinaudo, M. Hydrophobic Derivatives of Chitosan: Characterization and Rheological Behaviour, *Biological Macromolecules*, **1996**, 19, 21-28.
- [38]. Sashiwa, H.; Shigemasa, Y. Chemical Modification of Chitin and Chitosan 2: Preparation and Water Soluble Property of *N*-acylated or *N*-alkylated partially Deacetylated Chitins, *Carbohydrate Polymer*, **1999**, 39, 127-138.
- [39]. Keisuke, K.; Satoko, M.; Yasuhiro, N.; Manabu, H. *N*-Alkylation of Chitin and some Characteristics of the Novel Derivatives, *Polymer Bulletin*, **2002**, 48, 159-166.
- [40]. Uragami, T.; Kato, S.; Miyata, T. Structure of *N*-alkyl Chitosan Membranes on Water-permselectivity for aqueous Ethanol Solutions, *Journal of Membrane Science* **1997**, 124, 203-211.
- [41]. Desbrieres, J. Autoassociative Natural Polymer Derivatives: The Alkyl Chitosans, Rheological Behaviour and Temperature Stability, *Polymer*, **2004**, 45, 3285-3295.
- [42]. Baba, Y.; Hirakawa, H.; Yoshizuka, K.; Inoue, K.; Kawano, Y. Adsorption Equilibrium of Silver (I) and Copper (II) Ions on *N*-(2-hydroxybenzyl)chitosan Derivatives, *Analytical Sciences*, **1994**, 10(4), 601-605.

- [43]. Baba, Y.; Kawano, Y.; Hirakawa, H. Highly Selective Adsorption Resin. I. Preparation of Chitosan Derivatives Containing 2-pyridylmethyl, 2-thienylmethyl, and 3-(methylthio)propyl groups and their Selective Adsorption of Precious Metals, *Bulletin of Chemical Society of Japan*, **1996**, 69, 1255-1260.
- [44]. Crini, G.; Torri, G.; Guerrini, M.; Morcellet, M.; Weltrowski, M.; Martel, B. NMR Characterization of *N*-benzyl Sulfonated Derivatives of Chitosan, *Carbohydrate Polymers*, **1997**, 33(2-3), 145-151.
- [45]. Rabea, E. I.; Badawy, M. E. I.; Steurbaut, W.; Rogge, T. M.; Stevens, C. V.; Smagghe, G. Synthesis and Biological Activity of New Chitosan Derivatives Against Pest Insects and Fungi, *Communications in Agricultural and Applied Biological Sciences, Gent University*, **2004**, 69, 789-792.
- [46]. Rabea, E. I.; El Badawy, M.; Rogge, T. M.; Stevens, C. V.; Hofte, M.; Steurbaut, W.; Smagghe, G. Insecticidal and Fungicidal Activity of New Synthesized Chitosan Derivatives, *Pest Management Science*, **2005**, 61, 951-960.
- [47]. Muzzarelli, R. A. A.; Tanfani, F. The *N*-Permethylation of Chitosan and the Preparation of *N*-trimethyl Chitosan Iodide, *Carbohydrate Polymer*, **1985**, 5, 297-307.
- [48]. Domard, A.; Gey, C.; Rinaudo, M.; Terrassin, C. ¹³C and ¹H-NMR Spectroscopy of Chitosan and *N*-trimethyl Chloride Derivatives, *International Journal of Biological Macromolecules*, **1987**, 9, 233-327.
- [49]. Dung, P. L.; Milas, M.; Rinaudo, M.; Desbrieres, J. Water Soluble Derivatives Obtained by Controlled Chemical Modifications of Chitosan, *Carbohydrate Polymers*, **1994**, 24, 209-214.
- [50]. Sieval, A. B.; Thanou, M.; Kotze, A. F.; Verhoef, J. C.; Brussee, J.; Junginger, H. E. Preparation and NMR Characterization of Highly Substituted *N*-trimethyl Chitosan Chloride, *Carbohydrate Polymers*, **1998**, 36, 157-165.

- [51]. Hamman, J. H.; Kotze, A. F. Effect of the Type of Base and Number of Reaction Steps on the Degree of Quaternization and Molecular Weight of *N*-trimethyl Chitosan Chloride, *Drug Development and Industrial Pharmacy*, **2001**, 27(5), 373-380.
- [52]. Elisabete, C.; Douglas, D. B.; Sergio, P. C.-F. Methylation of Chitosan with Iodomethane: Effect of Reaction Conditions on Chemoselectivity and Degree of Substitution, *Macromolecular BioScience*, **2003**, 3, 571-576.
- [53]. Polnok, A.; Borchard, G.; Verhoef, J. C.; Sarisuta, N.; Junginger, H. E. Influence of Methylation Process on the Degree of Quaternization of *N*-trimethyl Chitosan Chloride, *European Journal of Pharmaceutics and Biopharmaceutics*, **2004**, 57(1), 77-83.
- [54]. Avadi, M. R.; Sadeghi, A. M. M.; Tahzibi, A.; Bayati, Kh.; Pouladzadeh, M.; Zohuriaan-Mehr, M. J.; Rafiee-Tehrani, M. Diethylmethyl Chitosan as an Antimicrobial agent: Synthesis, Aharacterization and Antibacterial Effects, *European Polymer Journal*, **2004**, 40(7), 1355-1361.
- [55]. Lang, G.; Wendel, H.; Konrad, E. Cosmetic Agent Based on Chitosan Derivatives and Preparation of these Derivatives. US. Patent, 4,921,949, **1990**.
- [56]. Daly, W. H.; Manuszak-Guerrini, M. A. Use of Polysaccharide Derivatives as Anti-Infectives Substances, *Polymeric Materials Science & Engineering*, **1998**, 79, 220-221.
- [57]. Num, C. W.; Kim, Y. H.; Ko, S.W. Modification of Polyacrylonitrile (PAN) Fiber by Blending with *N*-(2-Hydroxy)propyl-3-trimethylammonium Chitosan Chloride, *Journal of Applied Polymer Science*, **1999**, 74, 2258-2265.
- [58]. Seong, H. S.; Whang, H. S.; Ko, S. W. Synthesis of a Quaternary Ammonium Derivative of Chito-oligosaccharide as Antimicrobial Agent for Cellulosic Fibers, *Journal of Applied Polymer Science*, **2000**, 76, 2009-2015.
- [59]. Kim Y. H.; Nam, W. C.; Choi, J. W.; Jang, J. Durable Antimicrobial Treatment of Cotton Fabrics using *N*-(2-Hydroxy)propyl-3-trimethylammonium Chitosan Chloride and Polycarboxylic Acids, *Journal of Applied Polymer Science*, **2003**, 88, 1567-1572.

- [60]. Kim, J. Y.; Lee, J. K.; Lee, T. S.; Park, W. H. Synthesis of Chito-oligosaccharide Derivative with Quaternary Ammonium group and its Antimicrobial Activity against *Streptococcus mutans*, *International Journal of Biological Macromolecules*, **2003**, 32, 23-27.
- [61]. Lim, S. H.; Hudson, S. M. Synthesis and Antimicrobial Activity of a Water-soluble Chitosan Derivative with a Fiber-reactive Group, *Carbohydrate Research*, **2004**, 339, 313-319.
- [62]. Li, H.; Yumin, Du, Y.; Wu, X.; Zhan H. Effect of Molecular Weight and Degree of Substitution of Quaternary Chitosan on its Adsorption and Flocculation Properties for Potential Retention-aids in Alkaline Papermaking, *Colloids and Surfaces*, **2004**, 242, 1-8.
- [63]. Thatte, M. Doctoral Dissertation, Louisiana state University, Baton Rouge, LA, **2004**.
- [64]. Borch, R. F.; Bernstein, M. D.; Durst, H. D. Reduction of Aldehydes with Sodium Cyanoborohydride, *Journal of American Chemical Society* **1971**, 93, 2897-2904.
- [65]. Brugnerotto, J.; Lizardi, J.; Goycoolea, F. M.; Arguelles-Monal, W.; Desbrieres, J.; Rinaudo, M. An Infrared Investigation in Relation with Chitin and Chitosan Characterization, *Polymer*, **2001**, 42(8), 3569-3580.
- [66]. Fernandez-Megia, E.; Novoa-Carballal, R.; Quinoa, E.; Riguera, R. Optimal Conditions for the Determination of the Degree of Acetylation of Chitosan by ¹H-NMR, *Carbohydrate Polymers*, **2005**, 61(2), 155-161.
- [67]. Lavertu, M.; Xia, Z.; Serreqi, A. N.; Berrada, M.; Rodrigues, A.; Wang, D.; Buschmann, M. D.; Gupta, A. A Validated ¹H-NMR Method for the Determination of the Degree of deacetylation of Chitosan, *Journal of Pharmaceutical and Biomedical Analysis*, **2003**, 32, 1149-1158.
- [68]. Rodrigues, CA.; Laranjeira, MCM.; T.de Favere, V.; Stadler, E. Interaction of Cu (II) on *N*-(2-pyridylmethyl) and *N*-(4-pyridylmethyl) Chitosan, *Polymer* **1998**, 39, 5121-5126.
- [69]. Ramos, V. M.; Rodriguez, N. M.; Rodriguez, M. S.; Heras, A.; Agullo, E. Modified Chitosan Carrying Phosphonic and Alkyl groups, *Carbohydrate Polymers* **2003**, 51(4), 425-429.

- [70]. Fan, L. H.; Du, Y. M.; Zhang, B. Z.; Yang, J. H.; Cai, J.; Zhang, L. N.; Zhou, J. P. Preparation and Properties of Alginate/Water-soluble Chitin Blend fibers, *Journal of Macromolecular Science, Part A: Pure and Applied Chemistry* **2005**, A42, 723-732.
- [71]. Kittur, F. S.; Harish Prashanth, K. V.; Udaya Sankar, K.; Tharanathan, R. N. Characterization of Chitin, Chitosan and their Carboxymethyl Derivatives by differential Scanning Calorimetry, *Carbohydrate Polymers*, **2002**, 49(2), 185-193.
- [72]. Mucha, M.; Pawlak, A. Thermal Analysis of Chitosan and its Blends, *Thermochimica Acta*, **2005**, 427(2), 69-76.
- [73]. Santos, J. E.; Dockal, E. R.; Cavalheiro, E. T. G. Thermal Behavior of Schiff Base from Chitosan, *Journal of Thermal Analysis and Calorimetry*, **2005**, 79, 243-248.
- [74]. Poucher, C. J.; Campbell, J. R. The Aldrich Library of NMR Spectra, Volume V, Aldrich Chemical Company, Inc., Milwaukee, Wisconsin: USA. **1974**: 121.
- [75]. Wu, J.; Zhi-Guo, S.; Guang-Hui, M. A Thermo- and pH-Sensitive Hydrogel Composed of Quaternized Chitosan/Glycerophosphate, *International Journal of Pharmaceutics*, **2006**, 315(1), 1-11.
- [76]. No, K. H.; Park, N. Y.; Lee, S. H.; Meyers, S. P. Antibacterial Activity of Chitosans and Chitosan oligomers with different Molecular Weights, *International Journal of Food Microbiology*, **2002**, 74, 65-72.
- [77]. Jeon, Y. J.; Kim, S. K. Production of Chitoooligosaccharides using an Ultrafiltration Membrane Reactor and their Antibacterial Activity, *Carbohydrate Polymers*, **2000**, 41(2), 133-144.
- [78]. Hu, Y.; Du, Y.; Yang, J.; Kennedy, J. F.; Wang, X.; Wang, L. Synthesis, Characterization and Antibacterial Activity of Guanidinylated Chitosan, *Carbohydrate Polymers*, **2007**, 67(1), 66-72.
- [79]. Sajomsang, W.; Daly, W. H.; Wong, W. S.; Soleymannezhad, A. Novel Triple Detector GPC/SEC Method for characterization of *N*-Benzyl Chitosan Quat-188 Derivatives, *World Polymer Congress 41st International Symposium on Macromolecules*, **2006**, Rio de Janeiro, Brazil.

- [80]. Sajomsang, W.; Tangpasusuthadol, V.; Tantayanon, S.; Daly, W. H. Degradation of Chitosan During Synthesis of *N*-benzyl Chitosan and *N*-benzyl Chitosan Quat-188, *2nd Mathematics and Physical Sciences Graduate Congress*, **2006**, National University of Singapore, Singapore.
- [81]. Kenawy, E. R.; Abdel-Hay, F. I.; El-Shanshoury, A. El-R.; El-Newehy, M. H. Biologically Active Polymers: Synthesis and Antimicrobial Activity of Modified Glycidyl Methacrylate Polymers having a quaternary Ammonium and Phosphonium Groups, *Journal of Controlled Release*, **1998**, 50, 145-152.



สถาบันวิทยบริการ
จุฬาลงกรณ์มหาวิทยาลัย



APPENDIX A

สถาบันวิทยบริการ
จุฬาลงกรณ์มหาวิทยาลัย

APPENDIX A

FT-IR SPECTRA

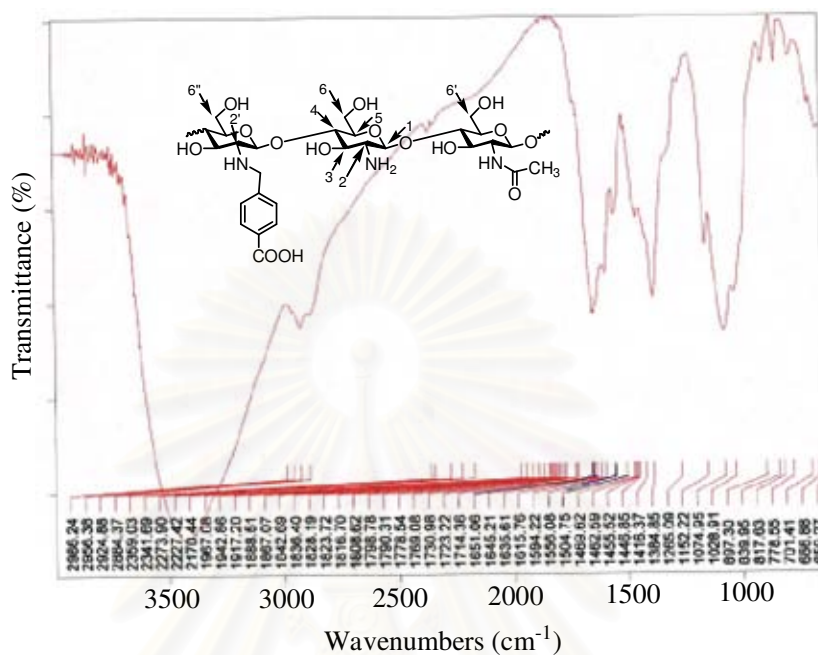


Figure A1: FT-IR spectra of *N*-(4-carboxybenzyl)chitosan with ES 12.5%

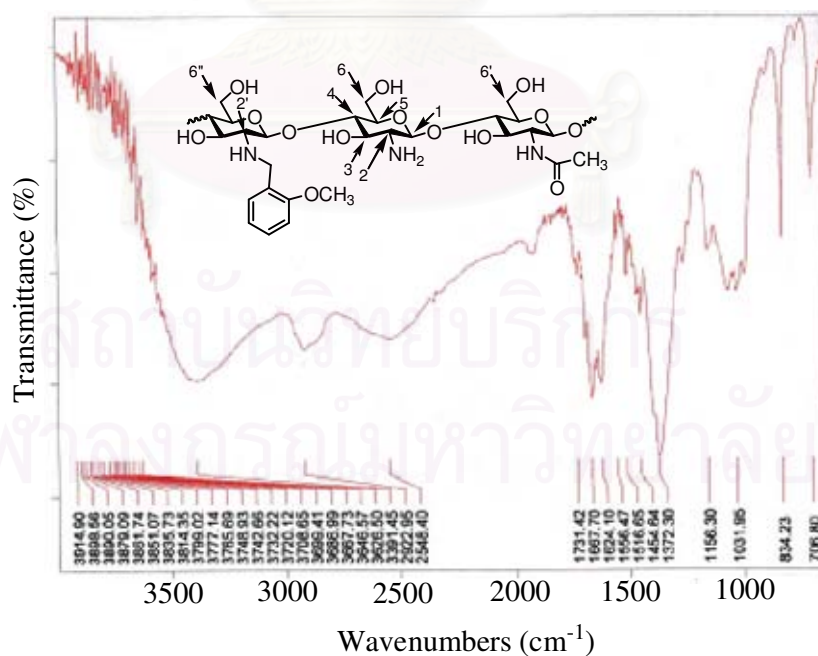


Figure A2: FT-IR spectra of *N*-(2-methoxybenzyl)chitosan with ES 6.0%

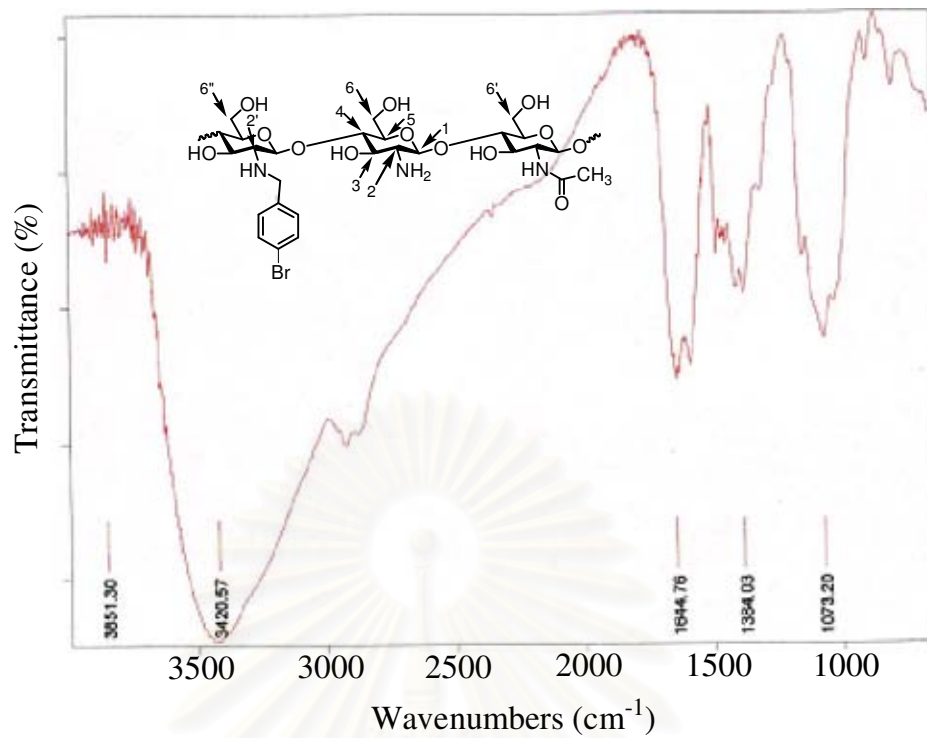


Figure A3: FT-IR spectra of *N*-(4-bromobenzyl)chitosan with ES 11.2%

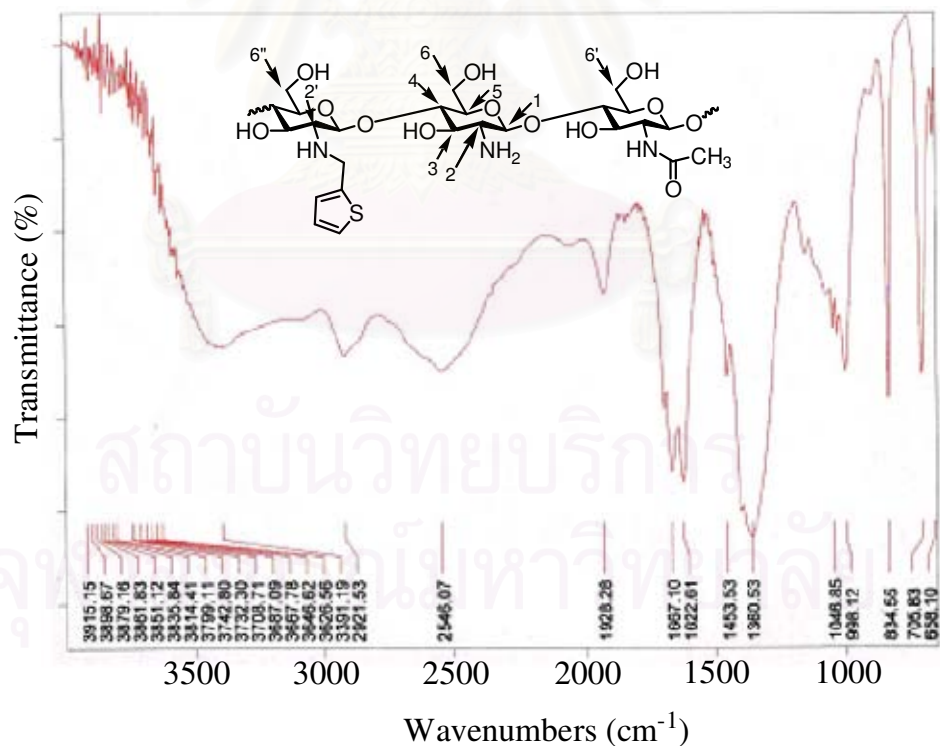


Figure A4: FT-IR spectra of *N*-(2-thiophenylbenzyl)chitosan with ES 13.3%

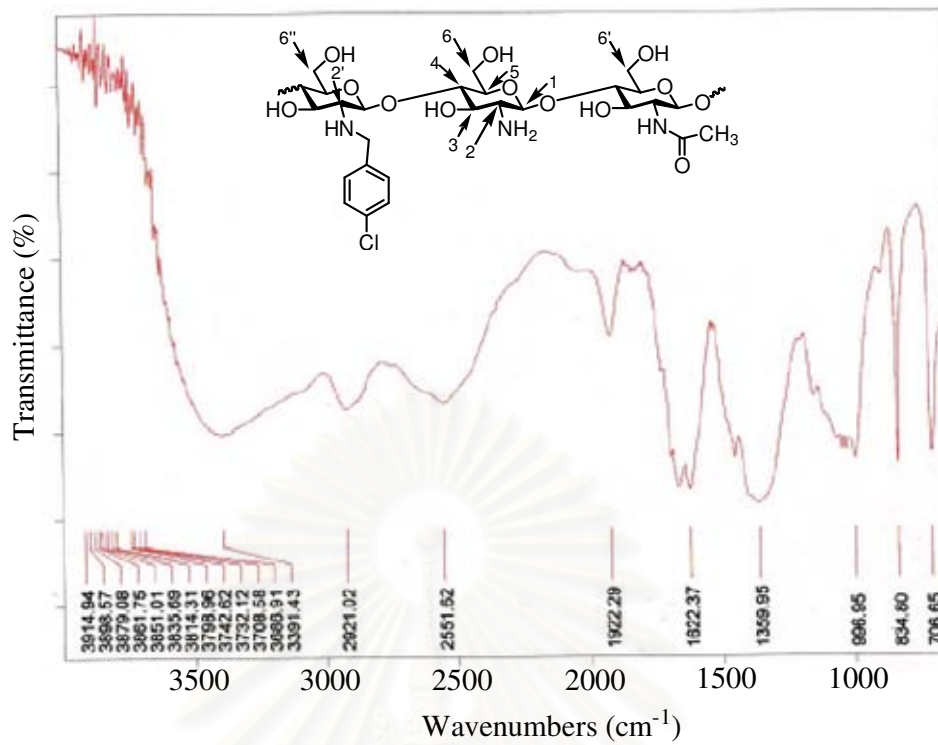


Figure A5: FT-IR spectra of *N*-(4-chlorobenzyl)chitosan with ES 10.0%

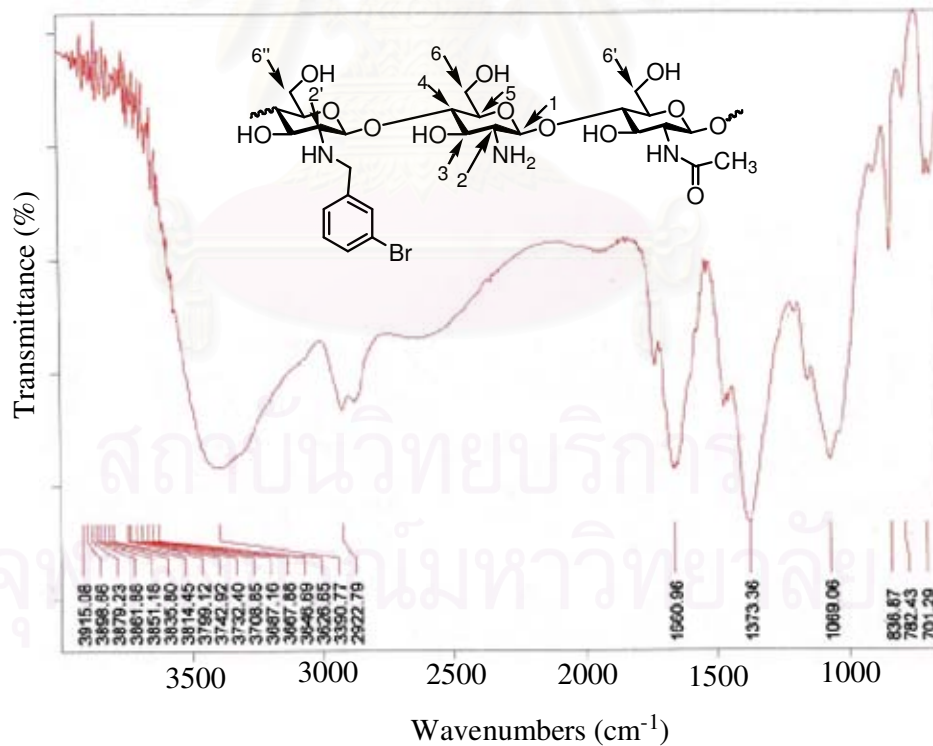


Figure A6: FT-IR spectra of *N*-(3-bromobenzyl)chitosan with ES 12.5%

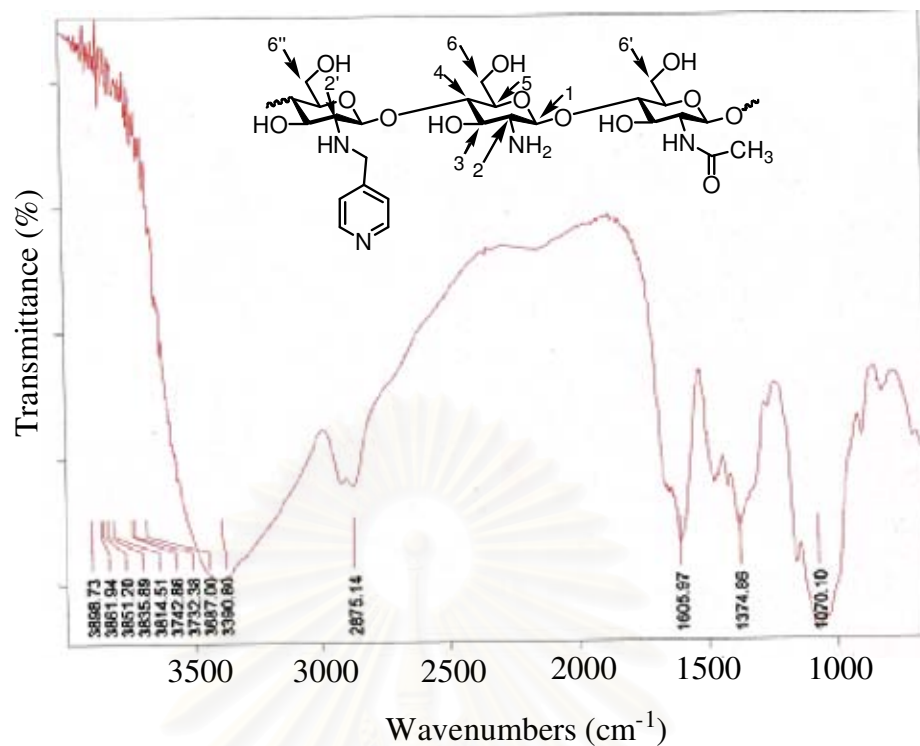


Figure A7: FT-IR spectra of *N*-(4-pyridylmethyl)chitosan with ES 5.2%

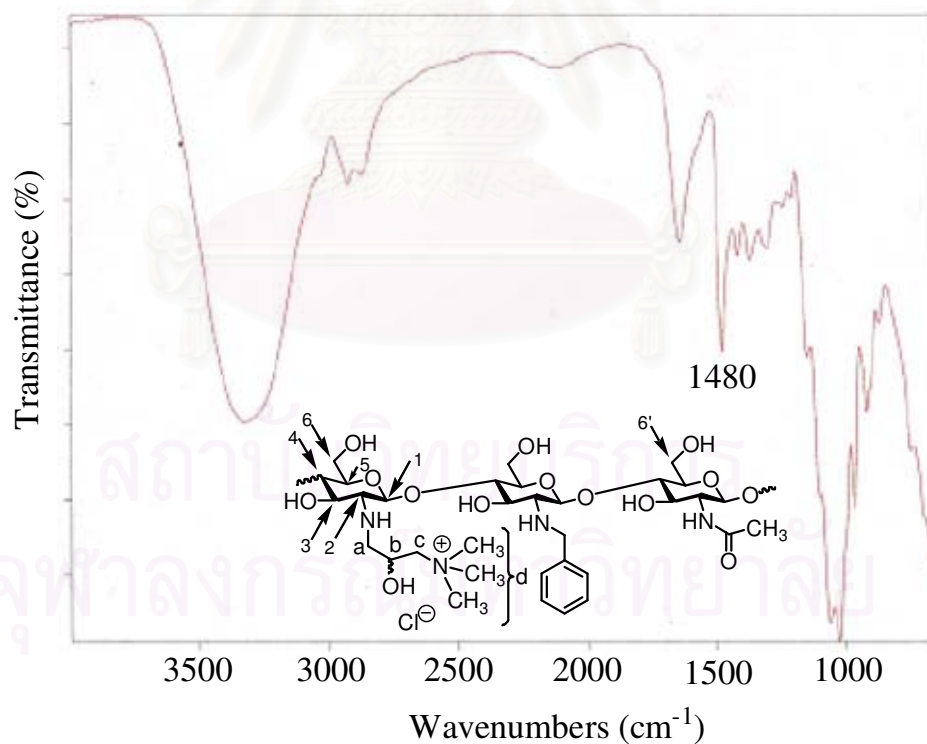


Figure A8: FT-IR spectra of *N*-benzyl chitosan Quat-188 with ES 3.6%

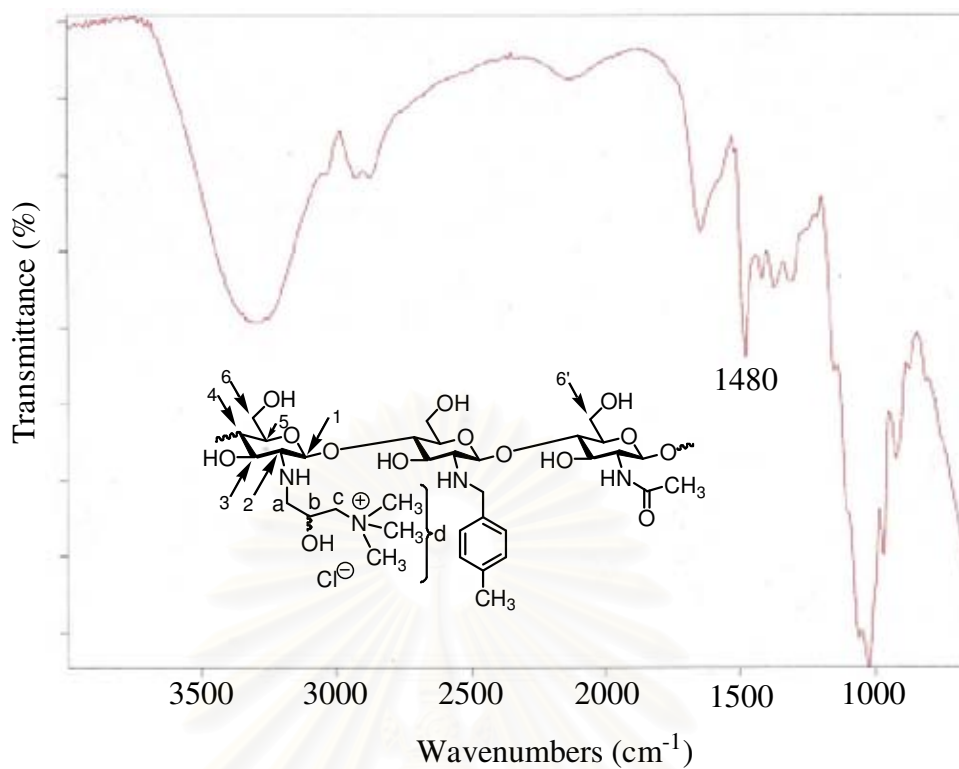


Figure A9: FT-IR spectra of *N*-(4-methylbenzyl)chitosan Quat-188 with ES 3.4%

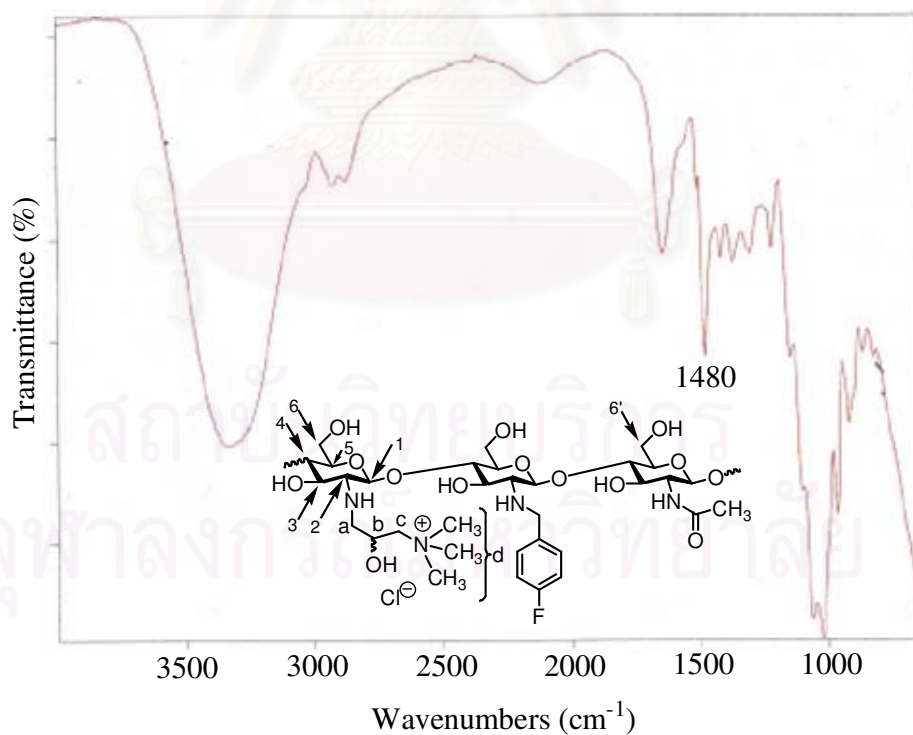


Figure A10: FT-IR spectra of *N*-(4-fluorobenzyl)chitosan Quat-188 with ES 5.5%

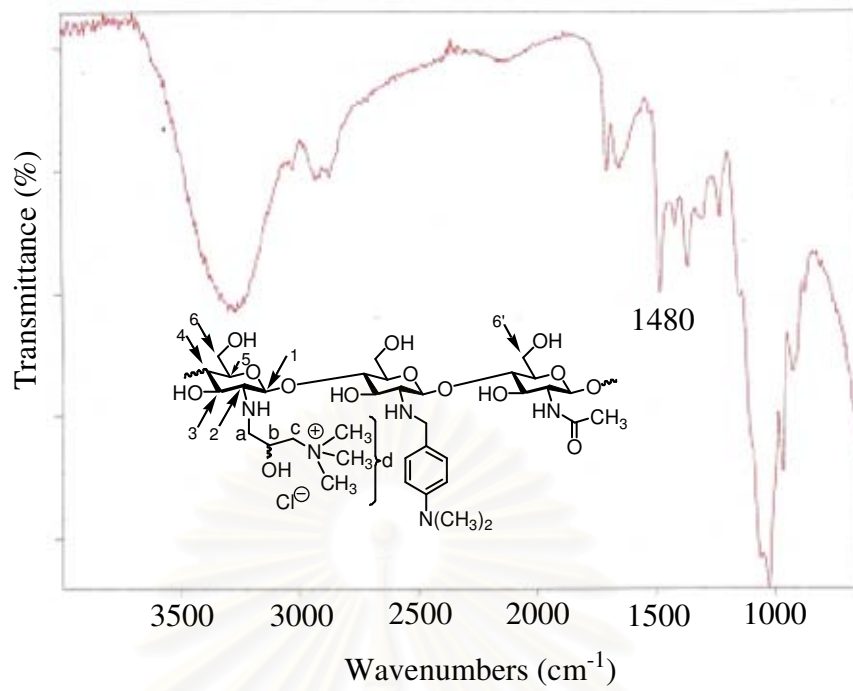
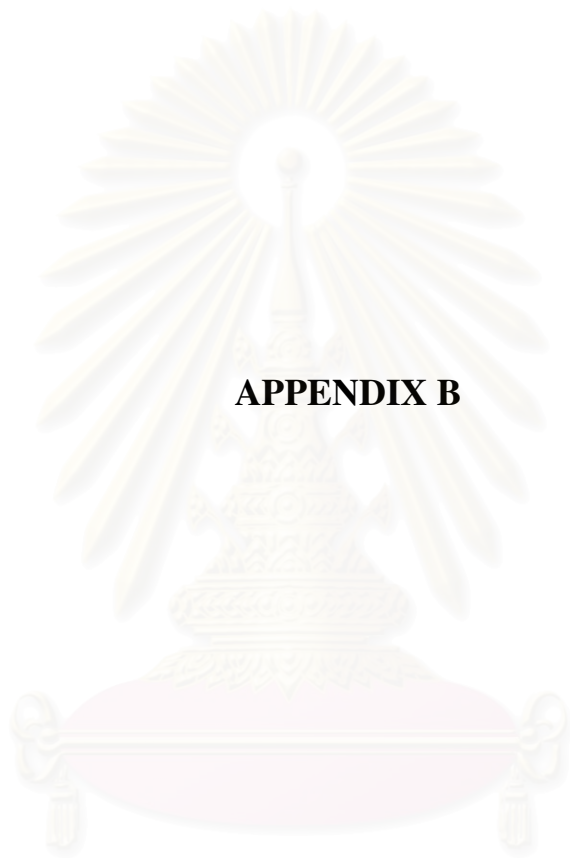


Figure A11: FT-IR spectra of *N*-(4-*N,N*-dimethylaminobenzyl)chitosan Quat-188 with ES 17.5%

สถาบันวิทยบริการ
จุฬาลงกรณ์มหาวิทยาลัย



APPENDIX B

สถาบันวิทยบริการ
จุฬาลงกรณ์มหาวิทยาลัย

APPENDIX B

$^1\text{H-NMR}$ SPECTRA

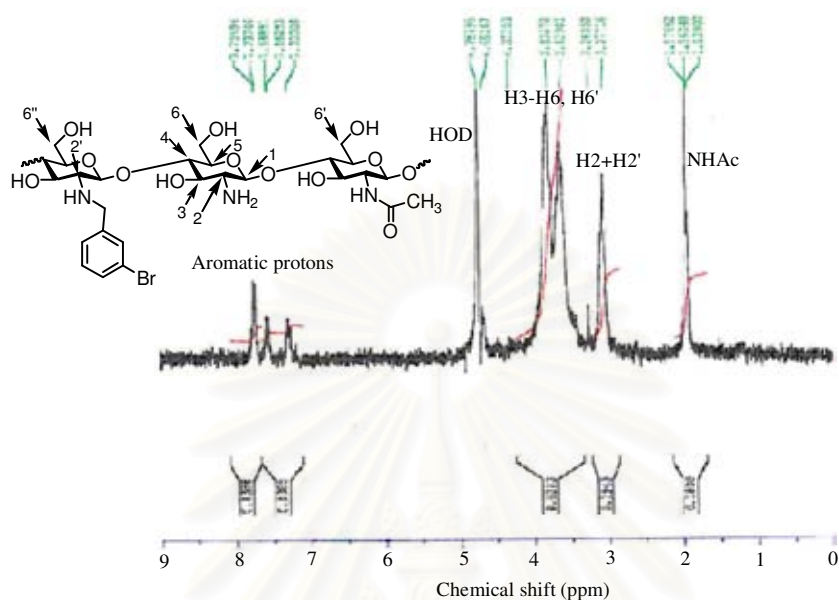


Figure B1: $^1\text{H-NMR}$ spectrum of *N*-(3-bromobenzyl)chitosan Quat-188 with ES 12.5% in $\text{D}_2\text{O}/\text{CF}_3\text{COOD}$

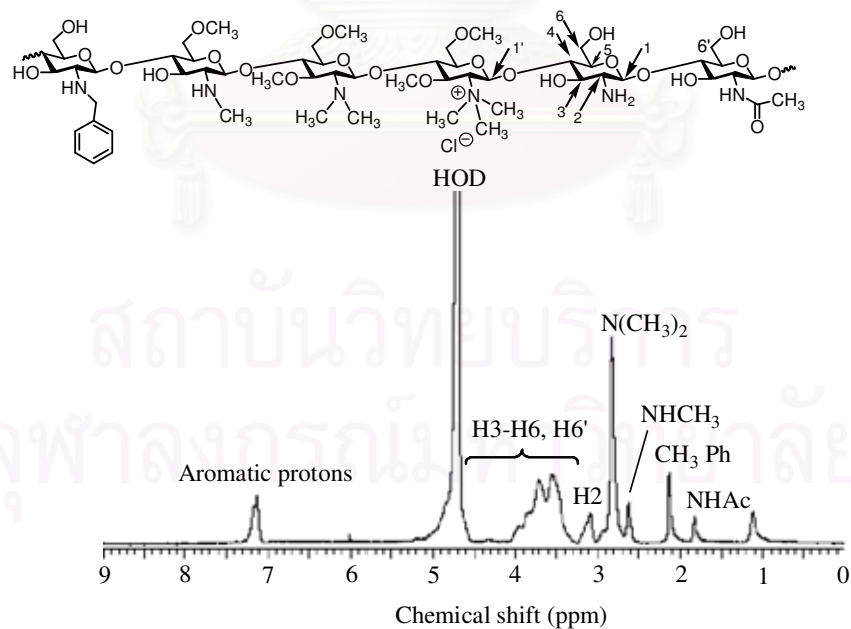


Figure B2: $^1\text{H-NMR}$ spectrum of quaternized *N*-(4-methylbenzyl)chitosan with ES 11.0% in $\text{CF}_3\text{COOD}/\text{D}_2\text{O}$ when 5% (w/v) NaOH was used

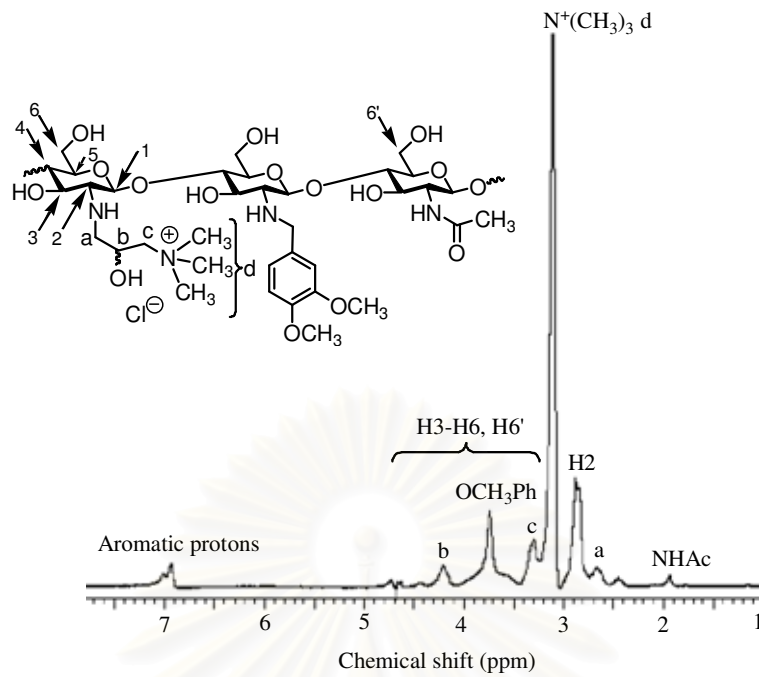


Figure B3: $^1\text{H-NMR}$ spectrum of *N*-(34-dimethoxybenzyl)chitosan Quat-188 with ES 7.8.0% in D_2O

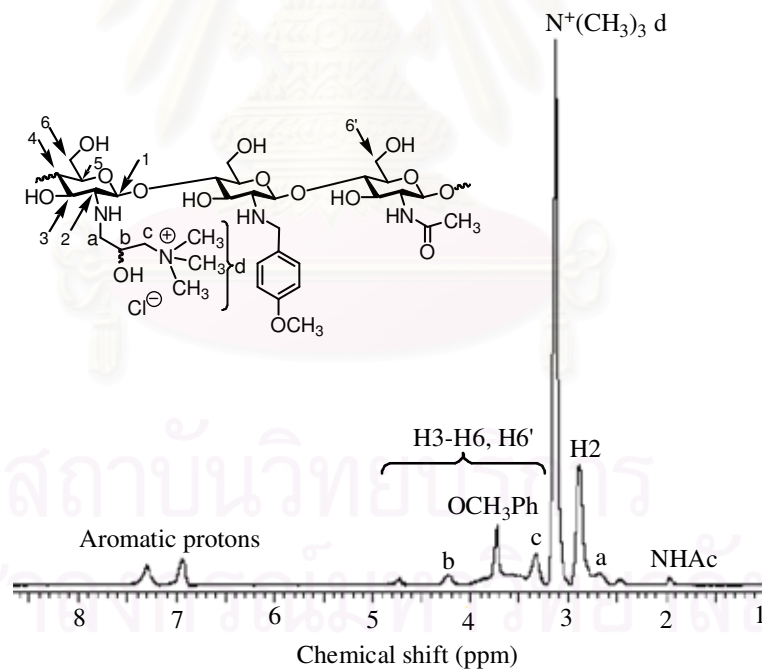


Figure B4: $^1\text{H-NMR}$ spectrum of *N*-(4-dimethoxybenzyl)chitosan Quat-188 with ES 8.0% in D_2O

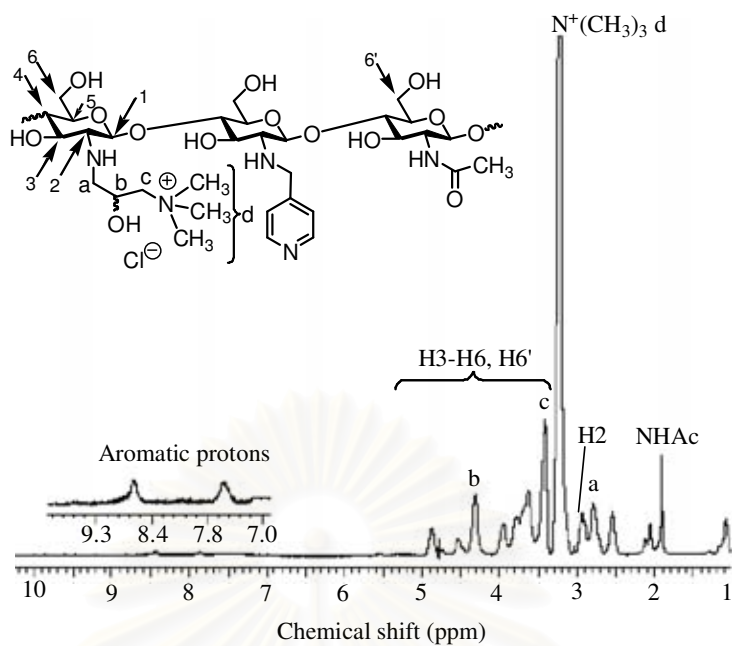


Figure B5: $^1\text{H-NMR}$ spectrum of *N*-(4-dimethoxybenzyl)chitosan Quat-188 with ES 5.2% in D_2O

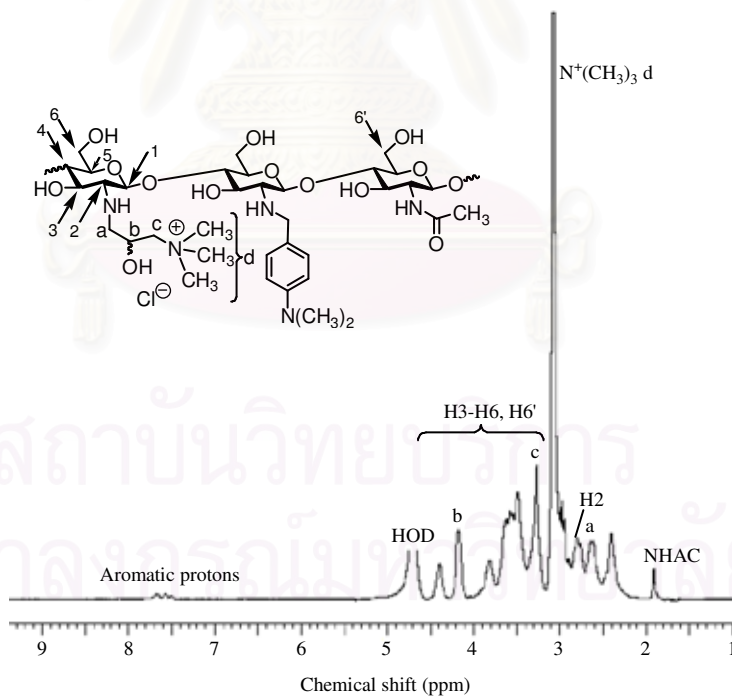


Figure B6: $^1\text{H-NMR}$ spectrum of *N*-(4-*N,N*-dimethylaminobenzyl)chitosan Quat-188 with ES 5.9% in D_2O

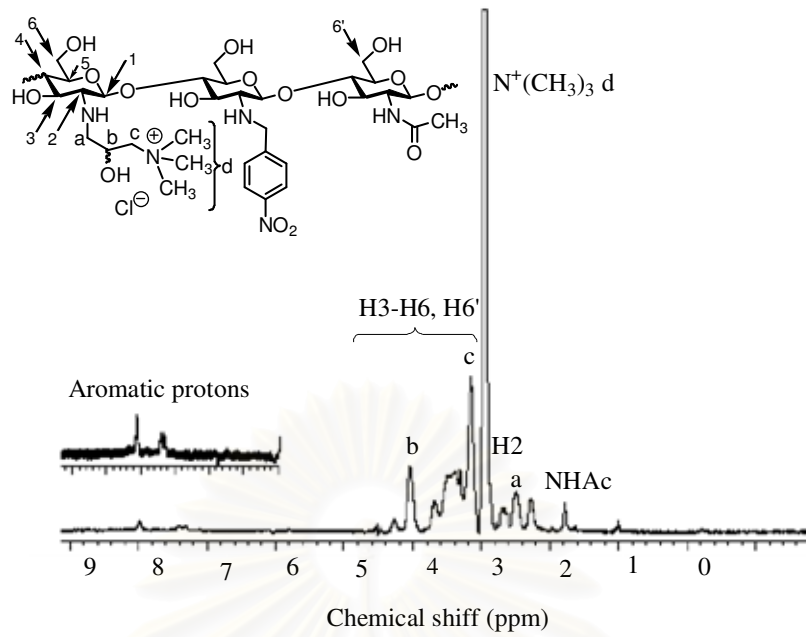


Figure B7: $^1\text{H-NMR}$ spectrum of *N*-(4-nitrobenzyl)chitosan Quat-188 with ES 3.3% in D_2O

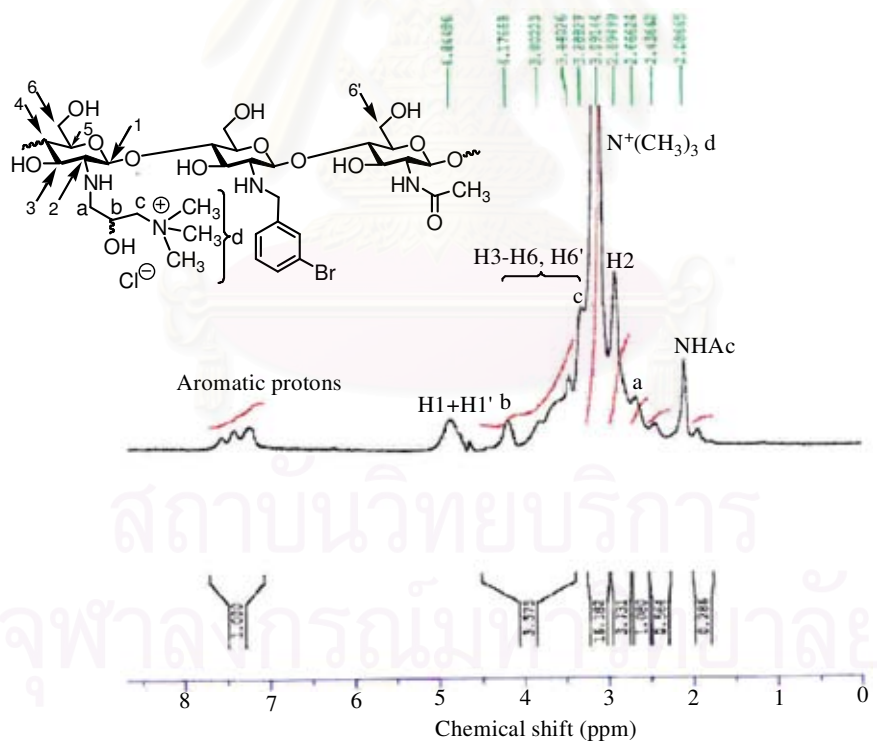
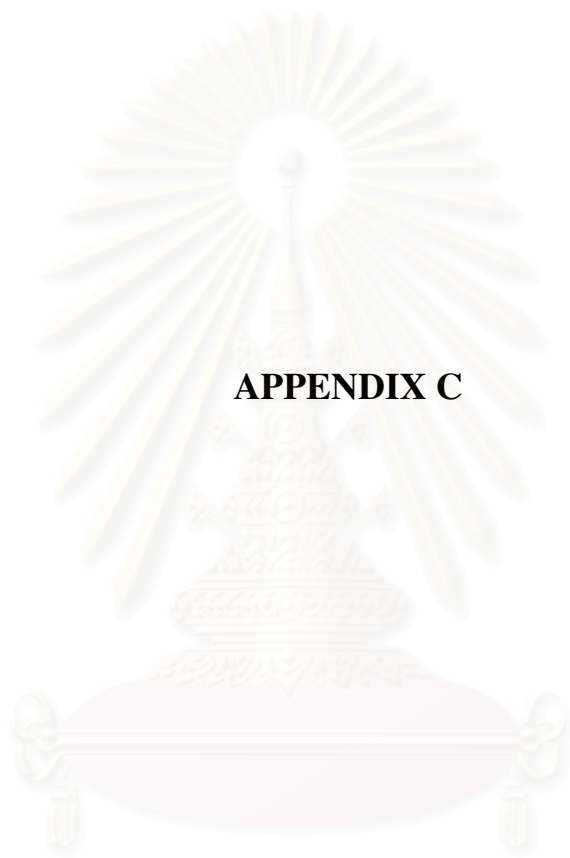


Figure B8: $^1\text{H-NMR}$ spectrum of *N*-(3-bromobenzyl)chitosan Quat-188 with ES 12.5% in D_2O



APPENDIX C

สถาบันวิทยบริการ
จุฬาลงกรณ์มหาวิทยาลัย

APPENDIX C

GPC CHROMATOGRAMS

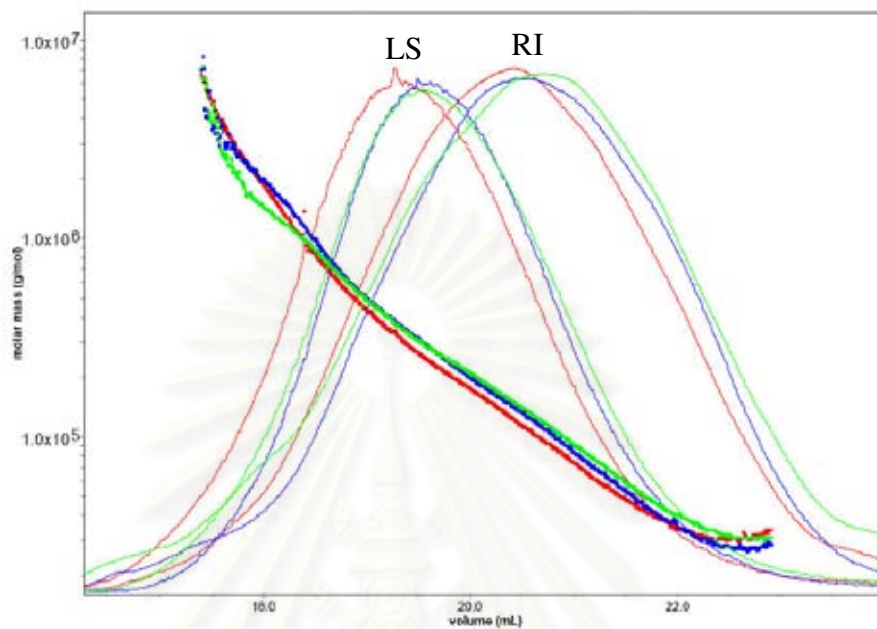


Figure C1: Molar mass distribution of chitosan

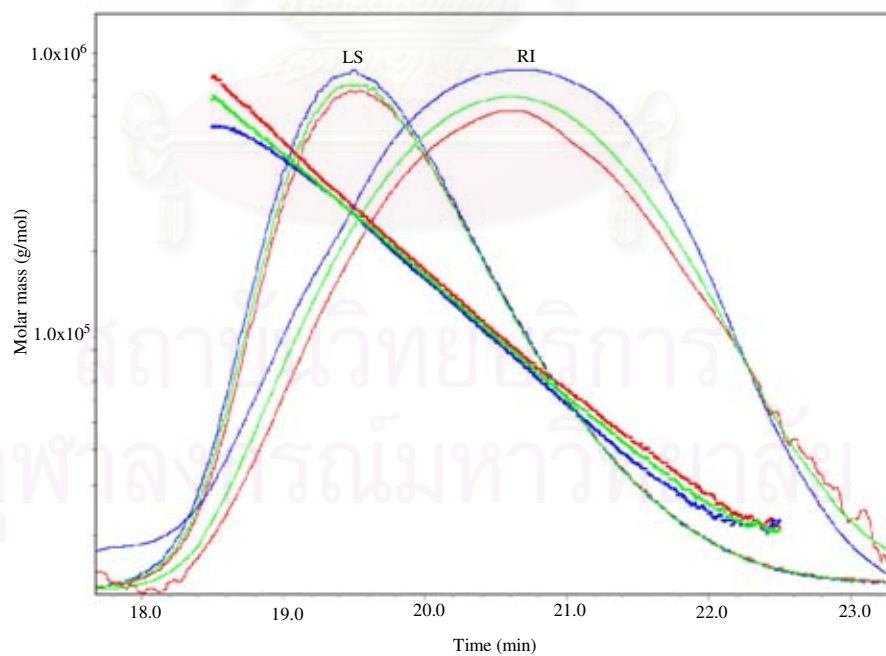


Figure C2: Molar mass distribution of *N*-benzyl chitosan with ES 3.6%

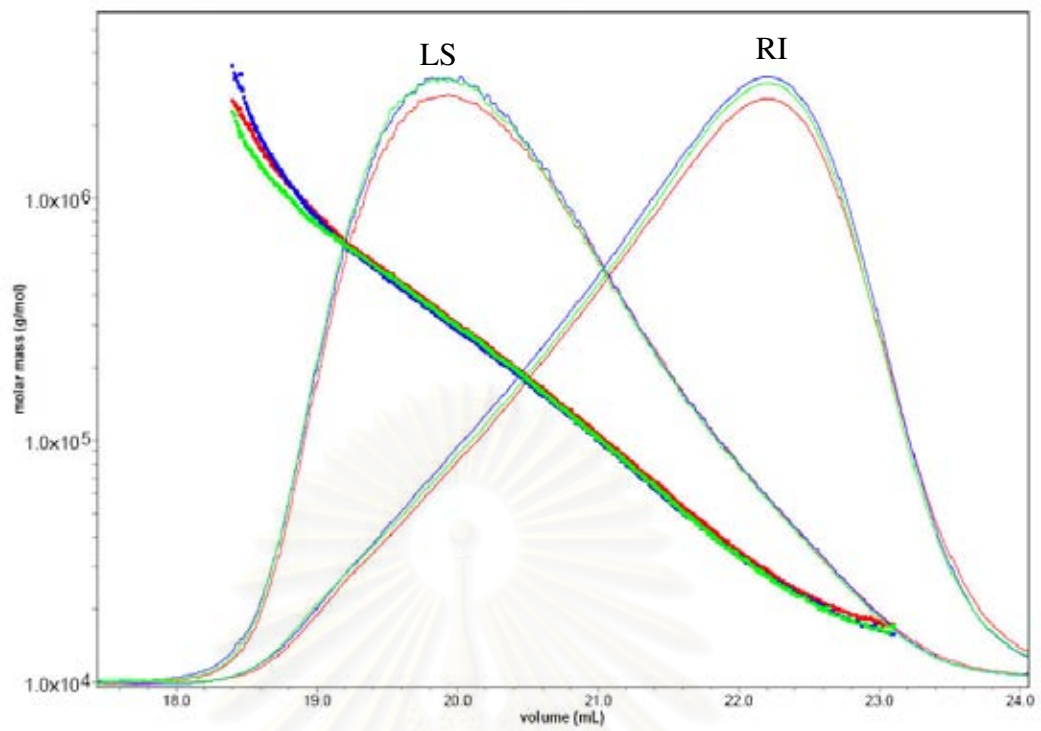


Figure C3: Molar mass distribution of *N*-(4-nitrobenzyl)chitosan with ES 8.3%

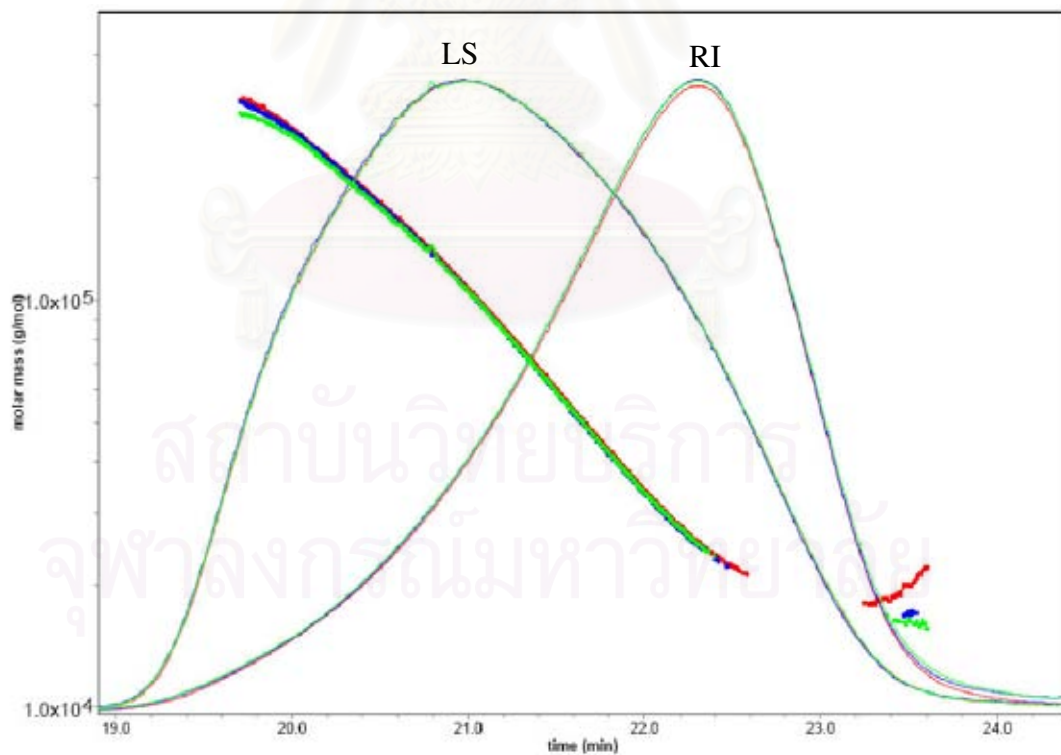


Figure C4: Molar mass distribution of chitosan Quat-188

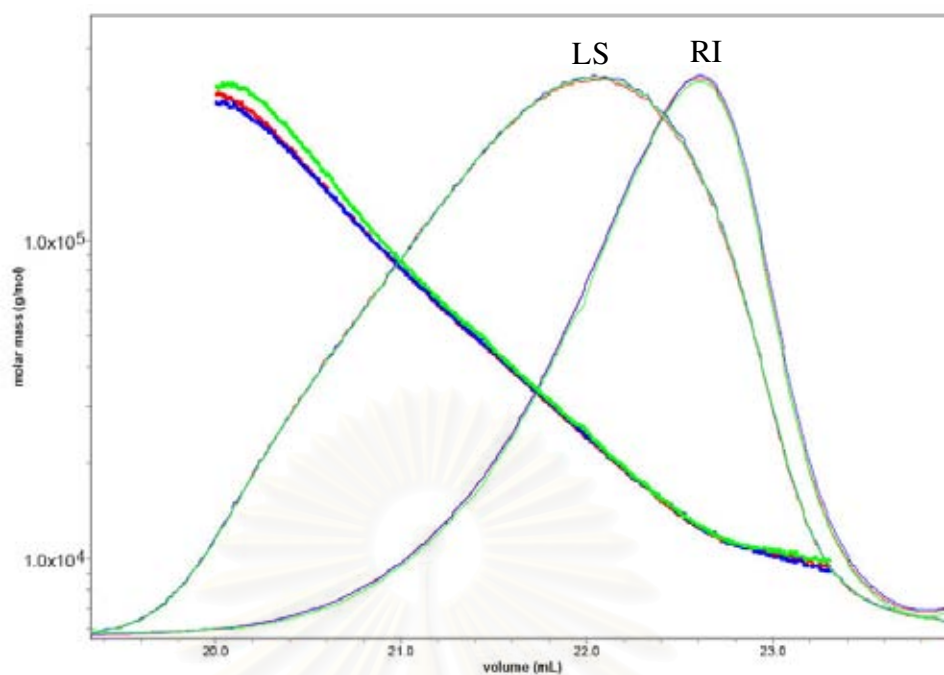


Figure C5: Molar mass distribution of *N*-benzyl chitosan Quat-188 with ES 3.6%

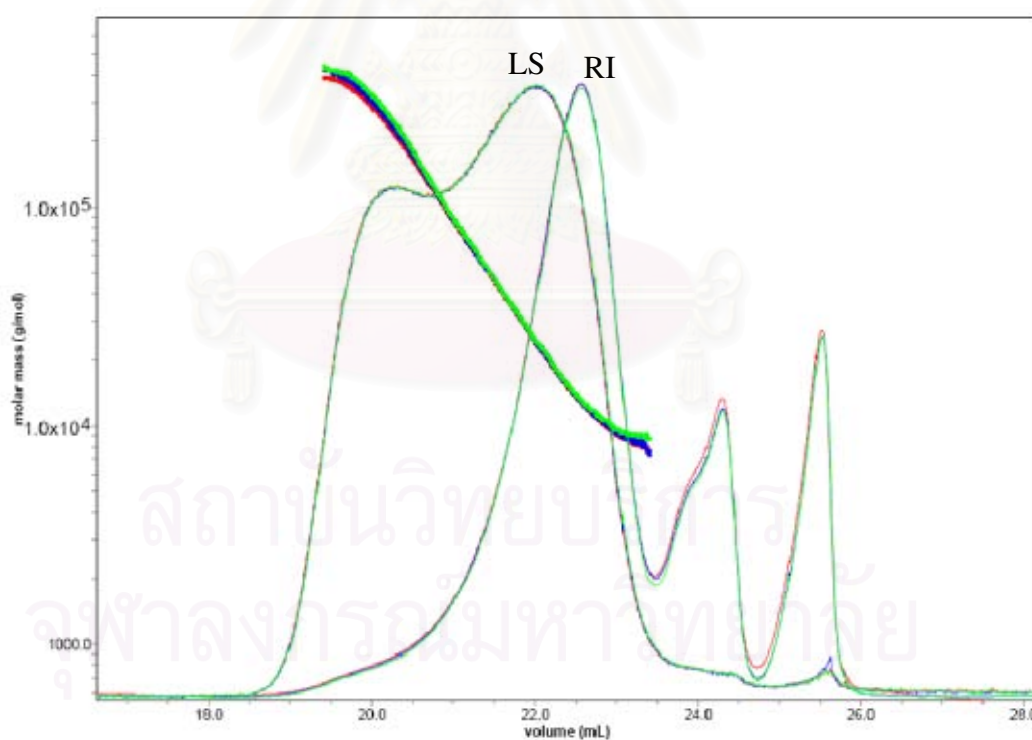


Figure C6: Molar mass distribution of *N*-(4-thiophenylmethyl)chitosan Quat-188 with ES 3.2%

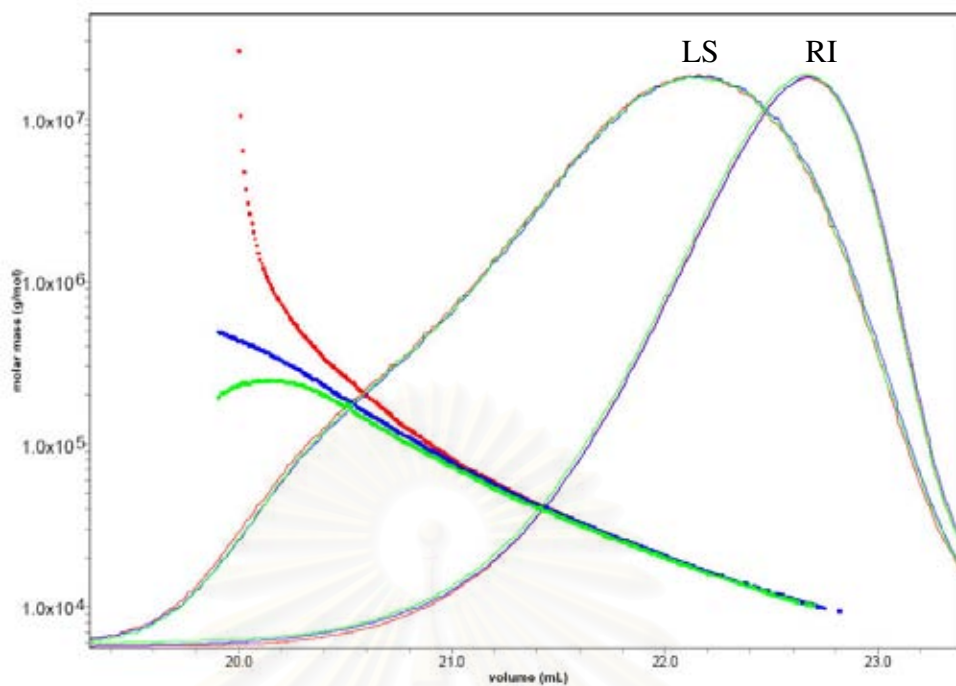


Figure C7: Molar mass distribution of *N*-(4-nitrobenzyl)chitosan Quat-188 with ES 8.3%

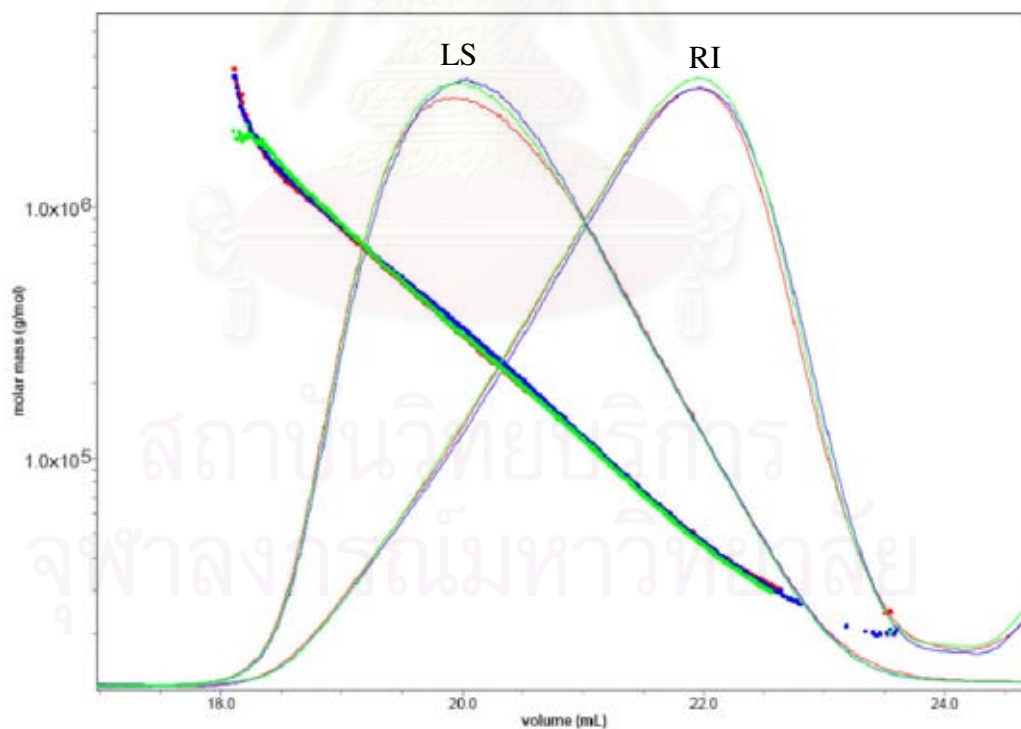


Figure C8: Molar mass distribution of *N,N,N*-trimethylammonium chitosan chloride with DQ_{Ch} 31.1%

VITAE

Name: Mr. Warayuth Sajomsang

Date of Birth: October 06, 1975

Education: In 1994-1999, Bachelor's Degree of Science (Chemistry), Department of Chemistry, Institutute Rajabhat Kanchanaburi, Kanchanaburi, Thailand.

In 1999-2002, Master's Degree of Science (Organic Chemistry), Department of Chemistry, Chiang Mai University, Chiang Mai, Thailand.

Scholarships: In 1996-1997, Student Exchange Promotion Program A.I.E.J Department of chemistry, Osaka Kyoiku University, Osaka, Japan.

In 2003-2005, The financial support from the Thailand Research Fund (TRF) through the Royal Golden Jubilee (RGJ).

Publication:

1. Sajomsang W, Tantayanon S, Tangpasuthadol V, Thatte M, Daly WH. Synthesis and antibacterial activity of quaternary ammonium derivatives of *N*-benzylated chitosans, *Biomacromolecules*, 2007, Submitted.
2. Sajomsang W, Tantayanon S, Tangpasuthadol V, Daly WH, Synthesis and chemoselectivity of novel methylated *N*-benzyl chitosan derivatives with iodomethane, *Polym. Prepr. (Am. Chem. Soc., Div. Polym. Chem.)* 2006; 47(2): 121-122.
3. Sajomsang W, Tantayanon S, Tangpasuthadol V, Thatte M, Daly WH. Synthesis and characterization *N*-benzyl chitosan derivatives, *Polym. Prepr. (Am. Chem. Soc., Div. Polym. Chem.)* 2006; 47(1): 294-295.
4. Vongchan P, Sajomsang W, Kasinrerak W, Subyen D, Kongtawelert P. Anticoagulant activities of the chitosan polysulfate synthesized from marine crab shell by semi-heterogenous conditions, *Science Asia*, 2003; 29: 115.
5. Vongchan P, Sajomsang W, Subyen D, Kongtawelert P. Anticoagulant activity of sulfated chitosan, *Carbohydrate Research*, 2002; 337; 1239.

Presentation:

1. Sajomsang W, Tangpasusuthadol V, Tantayanon S, Daly WH, *Degradation of chitosan during synthesis of N-benzyl chitosan and N-benzyl chitosan Quat-188*, 2nd Mathematics and Physical Sciences Graduate Congress, National University of Singapore, Singapore, December 12-14, 2006.
2. Sajomsang W, Tantayanon S, Tangpasuthadol V, Thatte M, Daly WH, *Synthesis and characterization N-benzyl chitosan derivatives*, 231st ACS National Meeting, Atlanta, GA, USA, March 26-30, 2006.
3. Sajomsang W, Tangpasusuthadol V, Tantayanon S, Daly WH, *Synthesis and characterization of quaternary ammonium derivatives of chitosan for controlling its water soluble*, 6th Asia-Pacific Chitin and Chitosan Symposium, Prince Georg's Park, National University of Singapore, Singapore, May 23-26, 2004.



สถาบันวิทยบริการ
จุฬาลงกรณ์มหาวิทยาลัย